Get AD#

AC Josephson Effect Determination of e/h: A Standard of Electrochemical Potential Based on Macroscopic Quantum Phase Coherence in Superconductors*

T. F. Finnegan,† A. Denenstein and D. N. Langenberg

Department of Physics and Laboratory for Research on the Structure of Matter, University of Pennsylvania

Philadelphia, Pennsylvania 19104

DISCLAIMER NOTICE

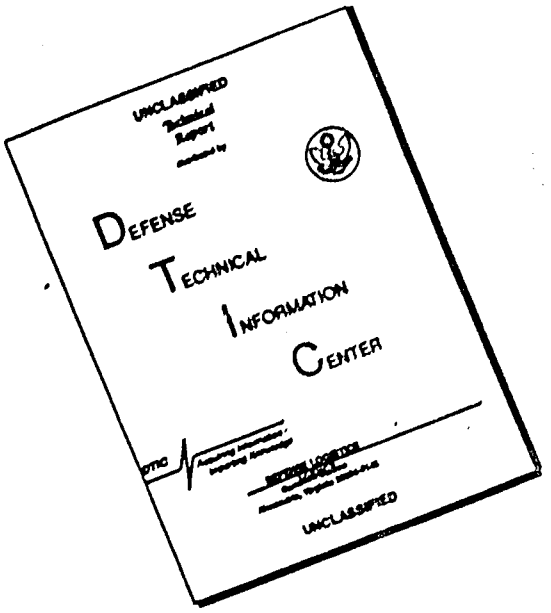

THIS DOCUMENT IS BEST QUALITY AVAILABLE. THE COPY FURNISHED TO DTIC CONTAINED A SIGNIFICANT NUMBER OF PAGES WHICH DO NOT REPRODUCE LEGIBLY.

ABSTRACT

An ac Josephson effect determination of e/h with significantly improved accuracy is reported. The precision of the measurement is determined by uncertainties associated with the comparison of a Josephson device voltage with the emf of an electrochemical standard cell voltage reference and is about 3 parts in 10^8. This precision was made possible by use of Josephson devices at voltages above 10 mV and design and construction of two special voltage comparator instruments. The fabrication and operation of the Josephson devices and the design and performance of the voltage comparators are discussed. The $3/10^8$ precision represents the precision with which a drift-free and readily reproducible Josephson voltage standard can be realized in practice using the techniques developed for these experiments. The accuracy of the final result is about 12 parts in 10^8 and is determined primarily by uncertainties associated with the stability of the local electrochemical voltage standard and with establishment of the relationship between the local volt and the volt maintained by the U. S. National Bureau of Standards. Significant improvements in the maintenance of the local voltage standard which contributed to reduction of the final uncertainty to this value are discussed. During the course of the experiments, the Josephson frequency-voltage relation was shown experimentally to be independent of magnetic field, temperature, and Josephson device bias voltage or induced step number to within the accuracy of the final result. The final experimental result and its one standard deviation uncertainty is $2e/h = 483.593\ 718 \pm 0.000\ 060$ MHz/μV_{NBS69} (0.12 ppm) referred to the volt as maintained by the U. S. National Bureau of Standards after January 1, 1969. This result is in excellent agreement with the earlier less accurate result of

Parker, Langenberg, Denenstein and Taylor, which played an important role in the 1969 adjustment of the fundamental physical constants by Taylor, Parker, and Langenberg. It is in reasonable agreement with values recently reported by several other groups. The significantly improved accuracy of the present result makes possible a small improvement in the accuracy of the derived value of the fine structure constant and clears the way for a larger improvement through more accurate determination of the proton gyromagnetic ratio.

I. INTRODUCTION

In recent years, determinations of e/h based on the ac Josephson effect in weakly coupled superconducting systems have begun to play a significant role in improving our overall knowledge of the fundamental physical constants.[1] Much of the interest in such experiments results from the fact that in combination with determinations of certain other fundamental constants they yield an accurate value of the fine structure constant which can be used to assess unambiguously the status of the agreement between the predictions of quantum electrodynamic theory and experiment. These e/h determinations have also demonstrated the potential of Josephson devices as "atomic" voltage standards with important advantages over present electrochemical standards. In this paper we report an ac Josephson effect determination of e/h with significantly improved accuracy and discuss its implications for our knowledge of the fundamental constants and for the practical realization of a voltage standard based on the ac Josephson effect.

The present experiments, like the earlier ones, depend on the fact that if an electrochemical potential difference $\Delta\mu$ is maintained across a Josephson junction, the junction carries an oscillating supercurrent with fundamental frequency $\nu_J = 2\Delta\mu/h$.[2] If $\Delta\mu$ is identified with eV, where V is the electrostatic potential difference (voltage) across the junction, $\nu_J = 2eV/h$. This is the Josephson frequency-voltage relation, and the effect is the ac Josephson effect. A measurement of the frequency-voltage ratio determines e/h. This can be done by measuring the frequency of the radiation emitted by a biased Josephson junction or by using the microwave-induced steps first observed by Shapiro.[3]

The first accurate determination of e/h using the ac Josephson effect was reported by Parker, Taylor and Langenberg.[4,5] The final result[6] of this determination has a stated one-standard-deviation (1σ) uncertainty of 2.4 parts per million (ppm). This work motivated a new readjustment of the fundamental physical constants and a re-examination of the status of quantum electrodynamic theory and experiment by Taylor, Parker and Langenberg.[7] It also provided the basis for a discussion of the potential application of the ac Josephson effect as a maintenance voltage standard by Taylor, Parker, Langenberg and Denenstein.[8] During the development of the improved voltage measurement techniques used in the present measurement, a previously overlooked source of possible systematic error in the work of Parker et al. was discovered. In order to determine whether the earlier work was in fact in error, the data were re-analyzed and additional measurements were made by Denenstein et al.[9] It was concluded that no significant error actually occurred in the earlier experiments, and a slightly revised value of e/h with an uncertainty of 2.2 ppm was reported. Earlier, Petley and Morris had reported preliminary results of a determination of e/h.[10] Their final result[11] and the revised value of Denenstein et al. are almost identical, both in value and in uncertainty. A value of e/h based on the initial results of the present work has been reported by Finnegan, Denenstein, and Langenberg.[12] It has an assigned uncertainty of 0.46 ppm and is in good agreement with the earlier values. Recently, Harvey, Macfarlane, and Frenkel[13], and Petley and Gallop[14], and Kose, Melchert, Fack, and Schrader[15] have reported high accuracy determinations of e/h. The value reported by Harvey et al. has an assigned uncertainty of 0.2 ppm, that of Petley and Gallop, 0.8 ppm, and that of Kose et al., 0.4 ppm. A detailed comparison of

these results and the result reported here is made in Section IX.

Before proceeding to discuss our experiments, we consider several basic points which are essential to any critical assessment of a Josephson effect determination of e/h. The first concerns possible limits on the precise validity of the Josephson frequency-voltage relation. Questions about the exactness of the "2" and the "e" and about the identification of $\Delta\mu$ with eV have given rise to considerable discussion, published and unpublished.[16] The nature of the superconducting state may be discussed in terms of what Yang has called off diagonal long range order (ODLRO).[17] Within the context of such a discussion the factor 2 follows naturally from the fundamental two-particle (electron pair) nature of the superconducting ODLRO. The existence of ODLRO together with the requirements of gauge invariance and single valuedness of the superconducting wave function has been shown to lead to fluxoid quantization in units of hc/2e.[17,18] Using similar arguments plus the additional requirement of reversibility, Bloch has given a derivation of the Josephson frequency-voltage relation.[19] Even if this result is not accepted as establishing the exactness of the frequency-voltage relation beyond all doubt, it is difficult to escape the conclusion that the "2" is correct. In any case, the factor 2 is almost irrelevant since, as Parker et al. have noted, any integer will suffice for purposes of determining e/h, although the theoretical and experimental arguments for the integer being 2 are very compelling.[6]

With regard to the "e", Nordtvedt has argued that the electron charge in a metal should differ from the free electron value by a material-dependent fractional amount of order 10^{-10}.[20] The difference arises because the Pauli

principle prevents virtual excitation of positron-electron pairs to occupied states in the Fermi sea in a metal, whereas these states are available in vacuo. Counter arguments have been advanced by Langenberg and Schrieffer[21] and by Hartle, Scalapino and Sugar.[22] Langenberg and Schrieffer suggest that in a finite sample (Nordtvedt's calculation was for an infinite medium) Nordvedt's charge renormalization is compensated by a surface renormalization charge so that the transfer of one electron to or from a metal is always accompanied by the transfer of exactly one free electron charge. Hartle et al. reach the same conclusion, showing by explicit calculation that the eigenvalue of the total charge operator on any complete set of proton and electron states is always an integer times the free electron charge. Both sets of authors claim that the question of possible renormalization of e is in any event not directly relevant to Josephson effect determinations of e/h for reasons related to the role of the electrochemical potential in such determinations.

The identification of the electrochemical potential difference $\Delta\mu$ with eV is central to the determination of e/h.[23] In principle there may be contributions to $\Delta\mu$ other than eV; the two are not necessarily identical. Stephen and Scully and Lee[24] have studied the radiating Josephson junction theoretically and predict that the coupling of the junction to the radiation field should cause the radiation frequency to differ from 2eV/h by about 1 part in 10^8. However, McCumber has shown that the electrochemical potential is also modified by the coupling in such a way that $\nu_J = 2\Delta\mu/h$ remains exact.[25] Parker et al.[6] emphasized that because the "voltage" measurements made in an e/h determination are really comparisons of electrochemical potential, there should be no need

for concern about the effect of nonelectrostatic contributions to the electrochemical potential or electron charge corrections associated with the details of the electronic states inside the junction. This point has subsequently been restated and amplified by various authors,[25,16,21,22] but its importance warrants its repetition here: At no point in an ac Josephson effect determination of e/h do the electron charge e or the electrostatic potential V enter separately in a real operational sense! The "voltage measurement" actually is a direct comparison of the electrochemical potential difference across a Josephson junction device with the electrochemical potential of a standard cell. This is done by connecting both devices in a closed conducting circuit which is adjusted for zero current flow, so that $\oint \nabla\mu \cdot d\vec{r} = 0$, where the integral is taken around the circuit. The electrochemical potential of the standard cell is then set equal to e times the "emf" of the cell. This emf has an assigned value in terms of some as-maintained volt (see below) which is determined through a chain of electrochemical potential comparisons terminating at the group of standard cells which defines this as-maintained volt. This process connects the original standard cell emf to the entire system of self-consistent precision electrical standards (the use and maintenance of which is also in actual practice based on electrochemical potential comparisons), and thence to the fundamental definitions of the electrical units. The nature of the factor e is determined by the identification of the charge carrying entity in all of these electrochemical potential comparisons. In all of them, the electrochemical potential is implicitly defined with respect to transfer of electrons, so that e is in effect defined to be the free electron charge. Operationally, e and V never enter except as the product eV, and then only when eV is related

to some standard cell electrochemical potential. Clearly, questions about the meaning of e must be considered in the context of its role in the whole electrical measurement system, not its significance in any specific part of a "voltage" measuring circuit used in an e/h determination, including the Josephson junction. This is why the question of a possible material-dependent charge renormalization in metals is not necessarily relevant to the Josephson effect determination of e/h.[20-22]

Even though there appear to be no really convincing theoretical indications of limitations on the accuracy of the Josephson frequency-voltage relation, experimental tests of the relation's validity are essential in establishing confidence in the use of the ac Josephson effect to determine e/h. In the course of their experiments, Parker et al. found the frequency-voltage ratio to be independent of (1) the junction material (Sn, Pb, Nb, Ta, Nb_3Sn), (2) type of Josephson junction (tunnel junctions and point contacts), (3) temperature ($0.3 \leq T/T_c \leq 0.9$), (4) magnetic field (0 to 10 G), (5) step number ($20 \lesssim n \lesssim 70$), (6) microwave frequency (10 GHz and 70 GHz) and power, and (7) whether the ratio was measured using microwave-induced (Shapiro) steps or radiation emission, all at about the 2 ppm level.[6] Clarke has compared the electrochemical potentials of steps in super-normal-super proximity-effect junctions of several materials, irradiated by the same rf source.[26] He found that the step potentials for Pb, Sn, and In junctions were identical to within 1 part in 10^8. In their experiments, Petley and Morris[10,11] worked near 36 GHz and used solder-drop junctions rather than tunnel junctions or point contacts, and were thus able to investigate several different Pb-Sn-Cd alloys. The internal agreement of their results and

the external agreement with the result of Parker et al. further confirms independence of material and frequency at a level of about 2 ppm. Finnegan et al. have extended the frequency range to 891 GHz in a differential experiment in which the potential of a high-order step induced by 9.48 GHz radiation in a Pb-Pb oxide-Pb tunnel junction was compared directly with the potential of a step induced by HCN laser radiation in a Nb_3Sn-Nb_3Sn point contact.[27] The result indicated that the frequency-voltage ratio was the same within/1.5 ppm/ the uncertainty of the experiment.

/In the present work we have reinvestigated the temperature, magnetic field, and step-number or bias-voltage dependence and confirmed independence to within several parts in 10^8. Taken together, these results indicate that the frequency-voltage ratio is indeed independent of a wide variety of experimental parameters at a level of a few parts in 10^8. In combination with the theoretical ideas discussed above, they strongly support the assumption that the frequency-voltage relation can be used as the basis for a determination of e/h at the level of accuracy claimed in the present work. We have based our work on this assumption. It is important, however, that it be subjected to continuing theoretical and experimental tests. One question which requires further investigation is that of the possible importance of dynamic or non-thermal-equilibrium effects. A Josephson junction being irradiated by a strong rf field can hardly be considered to be in thermal equilibrium. Josephson noted very early that local departures from equilibrium could modify the phase-time relation,[2] and Scalapino has discussed this point.[15] The work of Stephen,[23] Scully and Lee,[24] and McCumber[25] concerned one example of a non-equilibrium effect. It is fair to say, however, that a complete understanding of non-equilibrium effects is not yet available.

A second basic point which requires discussion here is the nature of the voltage measurement[28] and its effect on the uncertainty in an e/h determination. The basic measurements in any ac Josephson effect determination of e/h are of frequency and voltage. The voltage measurement is by far the more difficult and entirely determines the accuracy. The voltage is measured by potentiometric comparison with the potential of an electrochemical standard cell. This cell potential is in turn compared, usually by means of several intermediate standard cell comparisons, with the potentials of the group of standard cells which defines some national or international as-maintained volt. In the case of the present work, this is the United States National Bureau of Standards (NBS) as-maintained volt as redefined effective January 1, 1969, symbolized V_{NBS69}. All Josephson e/h values are expressed in terms of some such as-maintained volt, not the absolute volt, and their uncertainties do not include the uncertainty in the relation between the as-maintained and the absolute volt. (This is presently about 2.6 ppm for V_{NBS69}.[7]) In comparing different e/h values, care must be taken to convert all of them to a common voltage scale, taking into account relative drifts of the national scales as reflected for example in the triennial international comparisons at the Bureau International des Poids et Mesures (BIPM).

Our goal in the present work was an order of magnitude increase in accuracy over that achieved by Parker et al. Our motivation was two-fold. First, we wished to reduce the uncertainty contributed by e/h to our overall knowledge of the fundamental physical constants. Perhaps the most significant result of such a reduction relates to the fine structure constant, which can be written in terms of a particular set of experimentally measured quantities as[7]

$$\alpha^{-1} = \left[\frac{1}{4R_\infty} \frac{c\Omega_{ABS}}{\Omega_{NBS}} \frac{\mu'_p}{\mu_B} \frac{2e/h}{\gamma'_p}\right]^{\frac{1}{2}} . \qquad (1)$$

R_∞ is the Rydberg constant, c is the velocity of light, $\Omega_{ABS}/\Omega_{NBS}$ is the ratio of the absolute ohm to an as-maintained ohm (here NBS), μ'_p/μ_B is the proton magnetic moment in Bohr magnetons, and γ'_p is the proton gyromagnetic ratio as determined in a "low-field" experiment.[7] The primes indicate determinations in spherical samples of water, and it is assumed that 2e/h and γ'_p are determined in terms of the same system of as-maintained electrical units as $\Omega_{ABS}/\Omega_{NBS}$ (here NBS). Eq. 1 has several important features. It contains no quantities which must be derived from experiments using theories with significant quantum electrodynamic corrections. It therefore yields a value of α which can be used to test quantum electrodynamic theory against experiment unambiguously.[7] 2e/h and γ'_p appear in such a way that the rather large uncertainty in the relation between the absolute volt or ampere and the as-maintained volt or ampere is almost completely eliminated. R_∞, $c\Omega_{ABS}/\Omega_{NBS}$, and μ'_p/μ_B have experimental uncertainties less than 1 ppm, so that the uncertainty of α is controlled by the uncertainties of 2e/h and γ'_p. With the 2e/h value of Parker et al., Eq. 1 largely determined the final value of α in the 1969 adjustment of the fundamental constants.[7] A large reduction in the uncertainty of 2e/h would immediately yield a more accurate value of α, and would provide an opportunity to achieve even higher accuracy by improving the determination of γ'_p. The continuing advance of quantum electrodynamic theory and related experiments makes this a highly desirable goal.

Our second motivation was to establish the Josephson junction as a practical

primary voltage (electrochemical potential) standard. The accuracy of the measurements of Parker et al. (and also of Petley and Morris) was limited by the modified commercial voltage measurement instrumentation used in these experiments. Since, as we shall see, the uncertainties associated with electrochemical standard cells are of the order of a few parts in 10^7, attainment of an order of magnitude increase in accuracy in e/h implies reduction of instrumentation uncertainties to at least this level. This in turn automatically implies successful realization of the technology required for the Josephson voltage standard.

We have attained our goal by improving our Josephson device fabrication to obtain higher voltages, by designing and constructing voltage comparators with performance optimized for this specific experiment and by using improved standard cell comparison techniques. The performance of the special voltage comparators was such that the accuracy of the present experiments was controlled by the stability and accuracy of the voltage standard itself, not the instruments. Accordingly, we here describe the instruments only in sufficient detail to give the reader a fairly complete overall picture of the experiments. Complete descriptionsof the instruments will be published elsewhere.[29,30] On the other hand, we discuss our handling of the voltage standard problem in considerable detail, since only by doing so can we provide the reader with sufficient information to permit him to judge independently our assessment of the dominant source of uncertainty in these experiments. In Section II we describe the fabrication and performance of the Josephson junction devices. Section III contains a brief description of the instrumentation, excluding the voltage comparators. Section IV contains a

description of the maintenance and performance of our local voltage standard and the procedures used to relate it to the NBS as-maintained volt. A rather detailed discussion is necessary here since the data in this section almost completely determine our final assignment of uncertainty. In Section V the voltage comparators are described. Section VI describes the experimental procedures used in comparing the Josephson device with the local voltage standard. Section VII presents the final result and a discussion of the factors contributing to its uncertainty. Section VIII describes the results of differential experiments designed to test the magnetic field, temperature, and step-number independence of the frequency-voltage relation at a level of precision appropriate to the present experiments. Section IX contains a discussion of the significance of our result for the fundamental constants and for a voltage standard based on the ac Josephson effect.

II. JOSEPHSON DEVICE FABRICATION AND PERFORMANCE

A variety of methods for weakly coupling two superconductors to form a Josephson junction have been developed.[31] Precision e/h determinations to date have employed tunnel junctions,[6] point contacts,[6,13,15] and solder-blob junctions.[10,11,14] For experiments like those reported here, the tunnel junction has several advantages over the other types and we have used tunnel junctions exclusively.

The most precise Josephson effect e/h determinations have used microwave-induced (Shapiro) steps. These are steps in the current at voltages $V_n = nh\nu/2e$; the steps occur in the dc current-voltage (I-V) characteristic of a Josephson junction exposed to microwave radiation of frequency ν. An example of this effect is shown in Fig. 1d. Under the proper conditions, steps can readily be induced in the I-V characteristics of all types of junctions. The usefulness of an induced step for e/h determination is characterized by (1) its voltage position, (2) its current amplitude, and (3) its slope (dI/dV). These are interrelated. High voltage measurement accuracy requires the highest possible step voltage consistent with usable step amplitude and large step slope. A "vertical" step ($dI/dV \to \infty$) is desired so that the step voltage is independent of the current when the junction is biased on the step. Parker et al.[6] used both tunnel junctions and point contacts. They were generally able to get usable steps up to about 800 μV (n = 40) in the various junctions used. Nonvertical steps were observed in both types of junctions for junction resistances of order 0.1 Ω and larger. For a junction resistance near 0.1 Ω the voltage variation was about 10 nV over the height of the step and

increased with increasing junction resistance. (Unfortunately no data on the current amplitudes of these steps were reported.) Parker et al. concluded that the voltage position of the center of the step gave the "correct" value of e/h and estimated that it could be determined to about 10% of the total voltage change over the step (i.e., to about 1 nV out of 10 nV). They also surmised that the slope of the steps was due to fluctuation processes within the junction, or external noise. Subsequent theoretical and experimental work has shown that the steps are symmetrical about the "correct" voltage and that the non-vertical steps observed by Parker et al. were almost certainly due to external noise.[27, 32-34] In the case of Finnegan et al.,[27] steps vertical to within the experimental voltage resolution (1 nV at 2 mV) were observed in both a tunnel junction and a point contact with resistances of order 1 Ω. Since these measurements differed from those of Parker et al. primarily in the use of a shielded room to exclude external noise, it was concluded that the nonvertical steps observed by Parker et al. were indeed primarily due to external noise sources, and that essentially vertical steps could be obtained reproducibly by taking care to eliminate such sources. This has been done in the present experiments.

Our approach to the voltage measurement problem (see Section V) required a Josephson device output voltage which was greater than 10mV and could be adjusted (by varying the microwave frequency) to a fixed fraction of the standard cell voltage. An obvious way to achieve such a voltage was to connect several junctions in series. Tunnel junctions appeared more suitable for this purpose than point contacts, since the independent adjustment of an array of point contacts presented formidable mechanical problems. Parker et al. had already

used two tunnel junctions evaporated on a single substrate and connected in series to generate a total voltage of 1.6 mV.[6] Parker et al. used mostly Sn-Sn oxide-Sn tunnel junctions in their work and, as noted earlier, normally obtained usable steps up to about 0.8 mV, or about (2/3) (2Δ/e), where Δ was the Sn energy gap parameter. For $T \ll T_c$, 2Δ for Sn corresponds to 1.2 mV. For Pb, 2Δ corresponds to 2.7 mV, and on the basis of the experience of Parker et al. steps up to about 1.8 mV were expected in Pb-Pb oxide-Pb tunnel junctions. We therefore decided to concentrate on the fabrication of Pb-Pb oxide-Pb series tunnel junctions. Some Sn-Sn oxide-Sn junctions were also made but were not used in the final measurements.

In order to obtain 10 mV, a device containing a minimum of five junctions appeared necessary. The final device design incorporated eight tunnel junctions on a single substrate. The additional junctions were included because (1) individual junctions are occasionally defective (e.g., due to a dust particle penetrating the oxide barrier), and several spares were deemed desirable, and (2) variations in junction dimensions cause the junction resonant frequencies to vary, thus complicating the problem of coupling comparable amounts of microwave power into each junction. The latter is a difficulty peculiar to tunnel junctions. A Josephson tunnel junction is effectively an open circuited section of parallel plate transmission line and hence has resonant modes.[35] The characteristic impedance of the line is very small compared with a typical waveguide impedance, and the junction thus presents a very poor match to a microwave source, except at frequencies near the junction resonant frequencies.[36]

In our junctions, relatively efficient coupling to a microwave source at 11 GHz was restricted to frequencies within several per cent of the fundamental junction resonance frequency. Since the resonant frequency depends on the junction dimensions, efficient and fairly equally distributed coupling of power from a single source to an array of junctions requires careful matching of junction dimensions. Extra junctions in the array permitted selection of an optimal subset.

Fig. 2 shows the device geometry used. The cross hatched region indicates the first evaporated film, which was oxidized to form the insulating barrier. The eight junctions are at the top of the figure, and the nine lands to which external lead wires were soldered are at the bottom. The junctions were arranged close together at the center of the substrate so they could be positioned in a waveguide where the electric field is a maximum and relatively uniform. The lands were located as far as practical from the junctions to minimize degradation from heating during soldering of the leads. The strips connecting the junctions and lands were kept narrow mainly to avoid disturbing the microwave fields in the vicinity of the junctions. In the "in-line" or "linear" geometry shown in Fig. 2, the dc bias current passes through each junction in a straight line and produces no net magnetic flux in the junction. In the more commonly used "cross-type" geometry, the dc current makes a right angle turn in passing through the barrier and produces a net flux in the junction.[37] This magnetic flux is undesirable because it attenuates the Josephson current and hence the microwave-induced step amplitudes.

The devices were fabricated with a conventional evaporating system. Both Pb and Sn tunnel devices were made on 2.5 cm square glass substrates. The

films were approximately 1500 Å thick. The junction dimensions were 0.15 mm x 0.8 mm, with the latter dimension determining the resonant frequency of about 11 GHz. The oxide barriers were grown thermally at about 50° C. A significant factor in the success of our devices was the application of a thin layer (a few thousand angstroms thick) of photoresist to the finished device.[38] This coating protected the junctions (particularly those made of Pb) from the adverse effects of the atmosphere. The coating also permitted storage at liquid nitrogen temperatures (to reduce diffusion through the oxide barrier) and reuse of pretested devices with cycling through room temperature. Devices were stored at liquid nitrogen temperatures up to seven months with no apparent change in I-V characteristics.

It was found that useful induced steps in tunnel junctions could be obtained at voltages much greater than anticipated. In fact, with a sufficiently large microwave field and an appropriate junction resistance (~200mΩ), usable steps could be induced in single Pb-Pb oxide-Pb junctions at voltages greater than 10mV, i.e., for $V > 4\,(2\Delta/e)$! Figure 1 shows the I-V characteristics of one of these junctions. The indicated n = 450 step corresponds to a Josephson frequency ν_J of about 5 THz.

In retrospect, the appearance of steps at very high voltages should not be surprising. Simple theory predicts that the amplitude of the nth step is proportional to $j_1 J_n (2eV_{rf}/h\nu)$, where j_1 is the amplitude of the Josephson supercurrent density, J_n is the ordinary Bessel function of order n, and V_{rf} is the rf voltage induced across the junction at frequency ν.[3] j_1 has a complex frequency and voltage dependence which includes a singularity when $eV + mh\nu = 2\Delta$ for m integer, so that the correct theory of step amplitudes is more complicated.[39]

The important point is, however, that j_1 remains sizeable for $V > 2\Delta/e$, varying as V^{-1}. This, coupled with the fact that the first maxima of $J_n(x)$ (which occur for $x \sim n$) decrease as $n^{-1/3}$, means that the steps should persist for voltages well above $2\Delta/e$. If the microwave power is sufficient to make $(2eV_{rf}/h\nu) \sim n$, the maximum step amplitude should decrease roughly as $n^{-4/3}$. This is not inconsistent with our observations, but we have not made a detailed quantitative study of step amplitudes. Steps have been detected in Nb-Nb point contacts to voltages as high as 17 mV by McDonald et al.,[40] and voltages approaching 10mV have been obtained in tunnel junctions under conditions similar to ours by Fowler et al.[41] Some high accuracy e/h measurements were made using the n = 450 step shown in Fig. 1(d). This step had an amplitude of about 20 μA. In general, it was found that steps smaller than about 10 μA could not be reliably used because (1) small drifts in the dc bias current and microwave power made it difficult to remain biased on very small steps, and (2) very small steps tended to be somewhat nonvertical. Scalapino[16] gives an approximate expression for the intrinsic fractional width of a step, $\Delta V/V = \exp(-\hbar I_s/2ekT)$, where I_s is the step amplitude. This expression predicts a fractional width of less that 10^{-8} at T = 1.2 K for $I_s > 1\ \mu$A. In practice, external noise (from nearby electronic equipment) was usually much larger than the intrinsic junction noise and a larger I_s was required.

It was also found practical to obtain 10 mV using several junctions in series as orginally planned. The principal advantage in this was the availability of larger current steps (at least 50 μA) at the smaller voltages required of individual junctions. Both Pb-Pb oxide-Pb and Sn-Sn oxide-Sn multiple junction devices yielded usable 10 mV outputs. There were three practical difficulties

associated with the use of several junctions in series: (1) The resonant frequencies of the various junctions had to be closely matched in order to couple microwave power into all of the junctions simultaneously. This was accomplished by tightly matching the junction dimensions through the use of precision evaporation masks (0.01 mm tolerance). (2) The microwave power incident on the sample had to be adjusted very carefully in order to obtain a combination of large amplitude steps whose voltages summed to 10 mV. (3) The individual junction bias currents had to be maintained at the proper values despite drifts in operating conditions. The latter two problems were tractable but did result in increased complexity. In practice it was found preferable to use several junctions in series rather than just a single junction, and most of the data were taken on such a device.

As noted above, the voltage measuring technique which was adopted required that the total sample voltage be adjusted to a specific value. This was done by choosing the nearest integer step and then tuning the frequency. Since the step number was about 500, the frequency had to be adjusted at most over a range of 1 part in 500. In practice, the voltage could be continuously adjusted over a somewhat wider range than required in both single and multiple junction devices.

III. MICROWAVE AND DC BIAS EQUIPMENT

In this section we describe the equipment and experimental apparatus used to generate the microwave radiation, measure its frequency, and couple it to the Josephson device, and the Josephson device bias circuitry.

A. Josephson Device Holder

A sketch of the sample holder with multiple junction device in place is shown in Fig. 3. The holder consisted of a length of standard X-band waveguide with a slot milled in its broad wall to approximately half the depth of the waveguide. The device was placed in this slot and held by a close fitting metal cover which maintained continuity of the waveguide walls. The lead wires used to measure the junction I-V characteristics and step voltage were soldered directly to the superconducting thin film lands on the device and passed to the terminals outside through grooves in the waveguide wall. These grooves were lined with mylar tape for high insulation resistance. Insulated superconducting wire was used so that only one lead rather than the customary two normal leads had to be passed through the waveguide wall for each current-voltage connection. This reduced the number of solder joints on the substrate, a definite advantage for testing devices having a large number of junctions. The solder joints on the substrate were made with pure In. All e/h measurements were made well below the In T_c (~3.4 K). It was found useful to scratch the lands on the substrate before soldering in order to assure a good superconducting connection. The photoresist coating which protected the junctions also was observed to strengthen the mechanical bond of the solder to the Pb films. The joints on the teflon-insulated terminals outside the wavequide were made with ordinary Sn-Pb solder. From these terminals, copper magnet wire leads were run to the bias supply and to the voltage

comparator. These leads were run to the top of the cryostat in teflon tubing and passed through small holes in polystyrene plugs which were sealed with polystyrene cement. The portions of the voltage comparator leads inside the dewar were enclosed in a metal tube in order to minimize changes in the thermal emfs in these leads by maintaining a fixed temperature distribution along their length.[42] The lower part of the tube was copper as indicated in Fig. 3; the upper part was stainless steel. This tube was designed so that in use the liquid helium level always intersected the copper section. The portions of the bias and voltage comparator leads outside the cryostat were enclosed in teflon tubing which was wrapped in aluminum foil for electrostatic shielding. An outer covering of cloth tape insulated the foil from the grounded cryostat thereby preventing an undesirable ground loop.

A large microwave field was required to induce steps at high voltages. In order to couple the available microwave power (~0.5 W) into the Josephson device more efficiently, a low-Q cavity was formed around the device using an iris (shunt inductive diaphragm) located a quarter wavelength above the junctions and a sliding short below the device to tune the cavity. The short was operated by a stainless steel tube which extended through an O-ring seal at the top of the cryostat.

B. Microwave Equipment

A block diagram of the microwave generation and frequency measurement equipment appears in Fig. 4. The microwave source was a klystron phase-locked to a continuously tunable quartz crystal oscillator in the stabilizer (Curry, McLaughlin, and Len model MOS-1). The frequency was measured by means of an electronic counting system referenced to the U. S. Frequency Standard. Although the stabilizer kept the

frequency steady, the klyston was mounted in an air cooled oil bath to minimize drifts in klystron tuning which might cause output power variations. Such variations were undesirable since for a high order induced step ($n \sim 300\text{-}500$) to be stable, the power incident on the junction had to remain constant to at least 1% over a few minute measuring interval. Since it was also necessary to adjust the power to better than 1%, a high resolution main attenuator was used. The coupler was a standard 20 dB cross-guide type which was connected to the stabilizer in the standard manner. Since in practice the stabilizer was operated near the upper limit of its frequency-range (12.4 GHz) and had a high input VSWR, the attenuator to it was usually set near 0 dB (i.e. no attenuation). The wave reflected from the stabilizer input passed directly through the cross-arm of the coupler and was sufficient to operate the converter. (Negligible signal coupled to the converter directly because the isolator and main attenuator were well matched.) Isolators are normally used on the inputs of the stabilizer and converter because both generate a series of harmonics at their inputs and can interact with each other. In practice no interaction was observed in the absence of such isolators because of attenuation in the long cables to each of these instruments. A dc block between the isolator and main attenuator prevented ground currents between the electronic equipment in the microwave system and the cryostat, which was directly grounded to the shielded room.

The counter/timebase (Hewlett-Packard model 5245L) was regularly compared with the VLF transmissions of WWVB. Since the counter and VLF receiver (Hewlett-Packard model 117A) were in separate locations, a cable about 100 m long was necessary to connect them. This required a specially designed low-impedance amplifier which was built into the counter and allowed calibration of the timebase during e/h measurements. The aging

rate of the timebase was only a few parts in 10^{11} per day. An independent check of the frequency measuring equipment was made by directly counting the frequency of the quartz crystal oscillator. The frequency obtained in this way agreed with that obtained in the normal way to 1 part in 10^9, the reproducibility of the measurements. (To achieve this precision, a frequency synthesizer was used.) In addition, the frequency spectrum of the phase-locked klystron output was checked with a high resolution spectrum analyzer. The linewidth (full width at half-power) was less than 200 Hz (2 parts in 10^8), the resolution of the spectrum analyzer. No discrete sidebands greater than -60 dB (the noise level of the analyzer) were evident. Late in the series of measurements, the crystal reference oscillator in the stabilizer was replaced by the frequency synthesizer. This significantly improved the short term frequency stability of the system from about 1 part in 10^8 to about 2 parts in 10^9.

C. Josephson Device Bias Equipment

A diagram of the wiring and dc bias circuitry of the Josephson device is shown in Fig. 5. There were two leads on each terminal, one to supply the bias current and the other to measure the voltage. The two voltage comparator leads were connected across the junction(s) to be measured as indicated in Fig. 3. Since the I-V characteristics of the junctions normally differed somewhat, it was necessary to bias each one independently. The nth junction, its leads, and associated bias unit are shown explicitly. Each bias unit supplied an adjustable current to its junction and produced a voltage proportional to the junction current (by means of a shunt) for oscilloscope display. A switch was used to select the current and voltage signals of an individual junction. The polarity switch reversed these signals when the junction current was reversed in order to keep the display polarity fixed. Both signals were then offset in

order to display a small region of the I-V curve on an expanded scale (e.g., (the 4.2 V battery circuit of Fig. 5) Fig. 1(d). The voltage offset control had a calibrated dial (~ 12 mV maximum) so that the total device voltage (the sum of the individual junction voltages) could be independently set to within 1% (100 μV or, equivalently, 5 steps), the maximum range of the voltage comparison null detection system. A current divider circuit was used for this offset to minimize the effects of thermal emfs, which are usually large in 10-turn potentiometers. In order to resolve clearly the induced steps, which were about 20 μV apart, the voltage signal from the junction was passed through a low noise dc amplifier.

Since only 18 leads were used to bias 8 junctions, the individual bias units were joined outside the cryostat. This resulted in some interaction between the adjustments of adjacent bias units. For the system used, the lead resistance was such that the interaction in the worst case was about 10% and was tolerable. Since the voltage comparator leads were independent of the bias leads and the connections from the junctions to the terminals were entirely superconducting, this biasing interaction did not affect the high accuracy voltage measurements.

The circuit diagram of an individual bias unit is shown in Fig. 6. The dc power source was a mercury battery chosen for its small size, low noise and quite constant voltage. Since the I-V characteristics of the junctions used were generally slightly different for the two polarities, separate forward and reverse fine controls were provided in order to reverse rapidly without readjustment of the bias current. The current ranges available were 1 to 50 mA (full scale). A small ac voltage could be added to the dc bias as indicated for oscilloscope display of the I-V curve [see Fig. 1(d)]. The ac sweep (about 1 mA at 60 Hz) was

supplied by the power line through a specially shielded transformer whose input and output were carefully filtered to prevent noise from reaching the junction. A large fraction of the source voltage appeared across the shunt resistor so that no extra amplification was needed for the current display.

The circuit diagram of the dc amplifier necessary for the voltage display is shown in Fig. 7. This amplifier has a voltage gain of approximately 100 and was designed for low noise and minimal drift when used with a low resistance source such as a Josephson junction. The two transistors were a matched pair assembled in a single case; this construction reduces the drift due to ambient temperature changes. Two separate zero controls were provided and could be set so that the zero was independent of the source resistance. The starred resistors were trimmed to center the respective zeroing controls which were a composition type for sufficient resolution. (The two resistors and diodes on the input were included to protect the amplifier from continuous overloads up to 10 V or 100 mA.) The input and output resistances of the amplifier were 5 kΩ and 6 kΩ respectively. Bandwidths of either 5 kHz or 50 kHz could be selected with the switch BW. With the input shorted, the equivalent input noise was about 0.2 μV rms (5 kHz) or 0.6 μV rms (50 kHz). (Fig. 1(d) was made with the 5 kHz bandwidth.) The maximum input signal for a linear output was about 10 mV and the input drift was about 1 μV/hr under steady ambient conditions. The oscilloscope used in these measurements had a maximum sensitivity of 100 μV/cm on both horizontal and vertical axes.

IV. VOLTAGE STANDARD

In this section we discuss the procedures used to establish and maintain our local voltage standard and to determine the relationship between our local volt and the NBS as-maintained volt. Since the voltage standard is the dominant source of uncertainty in the present experiments, a rather detailed discussion is necessary.

The local voltage standard consisted of three groups of standard cells. Group A was composed of six saturated cells housed in a modified commercial standard cell enclosure (Eppley model 106, serial no. 2910). Group B was composed of three saturated cells and Group C was composed of three unsaturated cells. Groups B and C were housed together in an unmodified commercial enclosure (Eppley model 106, serial no. 4130). The function of the enclosures was to provide a constant and uniform temperature environment for the cells. Saturated standard cells have overall temperature coefficients of about -60 $\mu V/^{\circ}C$ near 30° C and internal resistances of about 1 kΩ. Unsaturated cells have overall temperature coefficients of about 2 $\mu V/^{\circ}C$ near 25° C (with sign and magnitude depending on the age of the cell) and internal resistances of about 500 Ω. The temperature coefficients of the individual electrodes of both types of cells are of order 300 $\mu V/^{\circ}C$ and have opposite signs.[43] (The smaller overall temperature coefficients result from partial cancellation of the individual electrode temperature coefficients.) Elimination of temperature fluctuations and of temperature gradients across the cells is therefore essential.

Since the electrolyte solution in an unsaturated cell is unsaturated, its composition changes with time. As a result, the emf of this type of cell decreases

at a rate of about 20 μV/year. Despite their larger temperature coefficients, saturated cells are normally used in precision measurements because they have greater long term stability. They are nevertheless rather sensitive to current flow, charging or discharging, and to mechanical shock and vibrations. Most saturated cells "age" or drift, particularly when new, and exhibit long time constant (months) response to temperature changes. The amount of drift varies from cell to cell and arises primarily from differences in construction and in the histories of individual cells. In our experiments, Group A was transported to and from NBS for calibration in terms of the U.S. legal or as-maintained volt. The enclosure containing Groups B and C was not disturbed during the entire course of the measurements, thus providing a means of assessing the effect of transportation on Group A. The primary function of Group C was to provide information on the effects of temperature fluctuations in the enclosure which it shared with Group B.

The thermal design of the enclosures was similar to that of Mueller and Stimson.[44] Each enclosure had a mercury-in-glass temperature regulator and was designed to minimize both temperature gradients and the effects of cycling of the regulator on the cells. The temperature of the standard cells in each enclosure was monitored by means of the mercury-in-glass thermometer built in by the manufacturer. Three limitations of the original enclosures were (1) relatively low leakage resistance, (2) a residual response to ambient temperature variations, and (3) insufficient accuracy of the thermometer in monitoring enclosure temperature. The insulation resistance between two cells in the same enclosure was as low as 10^9 Ω. The leakage resistance between an individual cell and the external (grounded) portions of the enclosure was as low as 10^{10} Ω. Each enclosure and its 12 V storage battery were therefore insulated (by placing them on plastic foam) and electrostatically shielded with a cage of wire mesh. The enclosures were each powered

by a 12 V battery (see Fig. 8) during all measurements to eliminate ac voltages from this source in the standard cell circuit and to facilitate this necessary insulation.

The reading uncertainty of the mercury-in-glass thermometers read by different observers using a low power microscope was about $\pm$ 0.002° C (1σ). This corresponds to an emf uncertainty of about 0.1 μV, or 0.1 ppm. (The random uncertainty for a single observer was about half of this.) Other possible sources of error involved in using the thermometer as the temperature monitor included ambient stem temperature corrections, variation in mechanical pressure on the bulb of the thermometer, and correlated barometric pressure effects on the bulbs of both the temperature regulator and the thermometer. Most of these sources of error are particularly serious if the enclosure is transported from one laboratory to another for comparison. Therefore, the enclosure containing Group A was modified internally before e/h measurements were begun. The modifications were as follows: (1) The thermostat was replaced/ with a similar thermostat supplied by the enclosure manufacturer. (This raised the operating temperature of the enclosure by about 0.2° C). (2) A thermistor was installed to monitor the temperature of the cells. Using a high accuracy resistance bridge, the relative temperature could readily be resolved to better than 5×10^{-4} °C. (3) The leads from the standard cell rack to the binding posts were replaced with much lighter ones (32 gauge, or about 0.2 mm) to reduce heat conduction along this path.[45] All of these leads were taken from a single spool of wire to minimize thermoelectric voltages.

The local voltage standard was monitored and maintained by almost daily intercomparisons of the cells in the three groups. A block diagram of the standard cell comparison system is shown in Fig. 8. In standard cell comparisons, it is common to connect potentiometer leads directly to the cell enclosure

binding posts. This procedure has at least two drawbacks: (1) The cells may be disturbed mechanically. (2) Transient thermals are generated which take an appreciable time to become negligible (i.e. less than 10 nV). The use of silver contact selector switches on both enclosures permitted permanent connections to the binding posts and avoided both of the above problems. The two standard cell emfs were connected in opposition at the junction box and the voltage difference was measured with a potentiometer which had nanovolt resolution. An unsaturated standard cell and a null detector were used to set the potentiometer working current in the usual manner. The null detector was the same one used in the e/h measurements and consisted of a photocell amplifier (Guildline type 9460) and a galvanometer (Leeds and Northrup no. 2430-D). Since standard cells are known to rectify,[46] measurement errors will occur if sufficient ac is present. Therefore, all components in this system were battery operated (including the lamps on the photocell amplifier and galvanometer) and the standard cell enclosures to avoid ac pickup. A modified low-thermal reversing switch (Guildline type 9145A) was used to eliminate the effects of zero drift in the photocell amplifier. All wiring in the comparison system was twisted pair to reduce magnetic pickup and was enclosed in an overall electrostatic shield.

Standard cell comparisons were carried out almost daily throughout the period during which e/h determinations were made. Each comparison consisted of observations of the emf difference between twelve separate pairs of cells, one of each pair in each enclosure. Twelve observations were made in the sequence $X_1 - Y_1$, $X_1 - Y_2$, $X_2 - Y_2$, $X_2 - Y_3 \ldots$, $X_6 - Y_6$, $X_6 - Y_1$ where X_i and Y_i indicate the i^{th} cell emf in enclosures X and Y respectively. From these data the difference in emf between any two cells and other useful quantities

could be computed. The random uncertainty for a particular day's comparison was estimated by summing the twelve observations in the sequence with alternating signs so that the sum (termed a "residual") would be zero in the absence of any (random) measurement error. (The initial or fiducial point in the sequence of observations was systematically advanced by one in successive comparisons.) Fig. 9 is a histogram of a series of 78 such daily residuals and gives some idea of the level of precision of the standard cell comparisons. The standard deviation of the residuals was 25 nV, implying a random error for a single observation of 25 nV/ $\sqrt{12}$ or about 7 nV.

Two types of computed voltage differences were routinely evaluated from the comparison data. The first type consisted of the differences between each cell and its respective group mean (e.g., $X_1 - \overline{X}$). These differences permitted monitoring of the relative stability of the cells within a group and were insensitive to small variations in the operating temperature of the enclosure. (The temperature coefficients of the cells in a group were very nearly equal.) The second type consisted of the voltage differences between the group means (e.g., $\overline{X} - \overline{Y}$). These differences were mainly dependent on the relative stability of the groups and on variations in the operating temperatures of the enclosures. In addition, the emf differences between individual pairs of cells were also computed for those days on which e/h runs were made. The linear combination (the over determined set) of observations used to compute each voltage difference was chosen (uniquely) to give the minimum random error in the computed result. For individual cell differences, the random error for the worst case (e.g., cell pairs with cyclic sequence positions differing by three) was only slightly greater ($\sqrt{3/2}$ times 7 nV) than the random

error for a single observation. (The systematic error associated with the effects of thermoelectric emfs in the standard cell comparison circuitry was about 10 nV as determined from direct measurements and from the results of the NBS Volt Transfer Program.)

Examples of the first type of data are shown in Fig. 10 for two cells used as working standards during e/h runs. (In the standard cell comparison data shown in Figs. 10 and 11, no error bars are indicated because the random uncertainty of each point is not larger than the circle marking the point. The time scale corresponds to a period extending from December, 1969 to July, 1970. The time scales on succeeding figures are numbered correspondingly.) The mean of a group X is denoted $\overline{X}$. Most of the time the day-to-day scatter was several parts in 10^8. Group B was not disturbed mechanically during this period. Group A, however, was transported to NBS twice for "calibration". The first of these calibrations was made over a three week period just prior to Day 1.

The second calibration was made over the three week period indicated in the figure. The occasional "jumps" in the B3-$\bar{B}$ data are typical of the behavior of standard cells, even when maintained under carefully controlled conditions, and illustrate the importance of frequent cell comparisons in any voltage standard maintenance program. The jumps are not necessarily attributable to B3, since $\bar{B}$ includes the effects of the other cells in the group. For example, the large voltage jump on Day 88 was apparently caused by an abrupt shift of about -0.5 μV in B2 alone. The cell B2 was identified as the one which changed by examining the B1-$\bar{B}$ and B2-$\bar{B}$ data together with the B3-$\bar{B}$ data shown. The voltage jump in B3-$\bar{B}$ on Day 190, however, does represent an abrupt change of approximately +0.1 μV in cell B3.

The A5-$\bar{A}$ data prior to the transport to NBS indicated in the figure show no large voltage jumps. The shift and subsequent drift in A5-$\bar{A}$ as the result of transfer to and from and calibration by NBS is apparent. The corresponding data for the other cells in Group A indicate that some of the cells changed more, others less. A more detailed examination of the stability of the individual cells in the local voltage standard including the unsaturated cells forming Group C is presented in Sec. VIIB.

The comparison data for the difference of the group means $\bar{A}$ and $\bar{B}$ during the same 200 day period are shown in Fig. 11. Since the apparent temperature variation of Group B as measured using the thermometer did not exceed the reading error, no temperature corrections were applied to this mean. The mean $\bar{A}$, however, was corrected for temperature variation using the thermistor data. Most of the day-to-day scatter in $\bar{A}$-$\bar{B}$ was less than 0.1 ppm and is

attributed to the uncorrected temperature variations in $\bar{B}$. (Recall that an uncertainty of 10^{-3} °C in temperature is equivalent to 0.06 ppm.) Some of the scatter, however, was due to shifts in individual cells. For example, the effect of the -0.5 μV jump in B2 cited earlier (on Day 88) is readily apparent. Note that there is an apparent discontinuity between the data before and after the transfer to NBS.

In the first of the two separate transfers of Group A to NBS during these experiments, the group was calibrated by NBS using their normal calibration procedure (described in NBS Fee Schedule 211.021e) and the temperature of the enclosure was monitored only with the mercury-in-glass thermometer. The stated uncertainty in this calibration procedure is 1 ppm [NBS Form 532a(11-68)] and is meant to be interpreted as 3 σ.[47] This uncertainty includes an allowance "for the random errors in the measurement procedure and variability in the emf of the cell during test" and an allowance "for the possible effects from known sources of systematic errors", such as temperature monitor errors and leakage resistance paths. It does not include an allowance for the effects of transport, for which an additional contribution of 0.5 ppm (3 σ) has been recommended to us.[48] Assuming a normal distribution of error, the root-sum-square combined 1 σ uncertainty is thus 0.37 ppm. For reasons discussed in Section VIIC, we have chosen to expand this uncertainty to 0.45 ppm.

Two factors which contributed to a substantial reduction in the uncertainty of the subsequent transfer of Group A to NBS about four months later were improved temperature monitoring through use of the thermistor in the enclosure, and the use by NBS of an improved measuring procedure developed for the NBS

Volt Transfer Program (see below). The NBS calibration data for the group mean $\bar{A}$ are shown in the upper part of Fig. 12. The dotted line indicates the NBS assigned value of the mean. No day-to-day temperature corrections were applied to these data. The apparent mean enclosure temperature as measured by three different observers during the calibration period using the mercury-in-glass thermometer was 30.193 °C. The resistance of the thermistor was also measured by NBS over part of this period (between Days 109 and 118) using the same type of resistance bridge used in our laboratory. Using thermistor data from these and from our own prior and subsequent measurements, all $\bar{A}$ data obtained in our laboratory before and after this transfer have been corrected to an apparent temperature of 30.193 °C unless otherwise noted.[49] Corrections derived from the less precise thermometer data are in reasonably good agreement with the thermistor data. (It may be of interest to note that a significant factor in this temperature correction was a reproducible and reversible shift of about 0.01 °C in the temperature of the A enclosure associated with the transport to and from NBS. This was observed in both transfers on the thermometer and in the second transfer on the thermistor also. The cause is unknown, but it may conceivably be an effect of changes in ambient pressure on the mercury-in-glass temperature regulator.) We have assigned an uncertainty of 0.2 ppm to this volt tranfer. The justification for this assignment requires a discussion of the apparent shift in $\bar{A}$ during the transfer (see Fig. 11) using the e/h data. We defer discussion of this point to Section VIIC.

A third volt transfer was carried out using a new NBS service known as

the Volt Transfer Program (VTP).[50] The transfer consisted of three steps: (1) NBS calibrated a transportable group of cells, hereafter called Group D, in terms of the U. S. Secondary Reference Group. Group D consisted of three saturated standard cells housed in a thermistor-regulated enclosure (Guildline Model 9152T/4, Serial No. 24834) operating near 35°C. The apparent temperature of the enclosure, measured with the built-in thermistor bridge and dial, could be resolved to about 10^{-3} °C. The leakage resistance between the cells and grounded portions of the enclosure were all greater than 10^{12} Ω. The group was then transported to the University of Pennsylvania under continuous power, as in the transfers of Group A. (2) Group D was compared with our cell groups in our laboratory using the same measurement sequence (design) used by NBS. (3) Group D was returned to NBS and recalibrated in terms of the Secondary Reference Group by NBS. The value of the group mean $\overline{D}$ during the period in which Group $\overline{D}$ was in our laboratory was derived from the data obtained in steps (1) and (3). The NBS calibration data for $\overline{D}$ in terms of the U. S. Secondary Reference Group are shown in the lower part of Fig. 12. (All data for Group D were corrected to a temperature of 35.000° C.) The NBS assigned value of $\overline{D}$ while at our laboratory (from approximately Day 130 to Day 150) is indicated by the dashed line. It is the value indicated by a linear least-squares fit to the data shown for the midpoint of the period during which Group D was in our laboratory.

The comparison data for $\overline{A} - \overline{D}$ at the University of Pennsylvania are shown in Fig. 13. The voltage differences are large because the operating temperature of Group D was about 5° C higher than the operating temperature of Group A. In

order to achieve an accuracy of one part in 10^8 in the voltages being compared, their difference had to be measured with an accuracy of 35 ppm. The calibration of the potentiometer and its reference standard cell used in the comparison was determined to about 10 ppm. In Fig. 13(a) $\bar{A}$-$\bar{D}$ is plotted versus time, in Fig. 13(b), versus ambient temperature. The dashed lines are linear least-squares fits to the data. The slopes together with

their random uncertainties are indicated. Over this time period the difference $\bar{A} - \bar{D}$ did not drift significantly and the standard deviation (the day-to-day scatter) was about 0.04 ppm. The plot of the data versus ambient temperature [Fig. 13(b)], however, reveals that some of this scatter was due to the non-negligible sensitivity of the temperature sensors in both groups to the ambient temperature. Taking the dependence on ambient temperature into account reduces the standard deviation of $\bar{A} - \bar{D}$ to 0.03 ppm and reveals a possible source of systematic error. Because the mean ambient temperatures of our laboratory and the NBS laboratory differed by less than 1° C, this possible source does not contribute significantly to the overall transfer uncertainty in our case. It could be important, however, in transfers between laboratories with larger ambient temperature differences.

On the basis of experience with many similar VTP transfers, NBS has assigned an uncertainty of 0.14 ppm (1 σ) to the mean $\bar{A}$ during the transfer period.[51]

V. VOLTAGE COMPARISON INSTRUMENTATION

As noted in the Introduction, the improved accuracy of the present measurements resulted partly from major improvements in voltage comparison instrumentation. These included the design and construction of two new voltage comparators (specialized potentiometers) and substantial modification of the photocell-galvanometer null detector system. In this section we present a brief description of the two comparators and the modified null detector system, and a detailed analysis of the sources of error in the voltage comparison system. A complete description of the design, construction, and performance of the comparators will be published elsewhere.[29,30]

Since the voltage supplied by a Josephson device depends on the frequency of the incident microwave radiation and is therefore precisely "tunable", the comparison of the device voltage with a standard cell voltage can be rather simply accomplished by the use of a fixed voltage ratio as illustrated in Fig. 14. Two voltages with an appropriate ratio (here 100:1) are generated by passing a stable working current through two series resistances. The working current is adjusted so that the voltage across the larger resistance is equal to the standard cell emf (~ 1 V). The microwave frequency is then adjusted until the Josephson device voltage is equal to the voltage across the smaller resistance (~10 mV). The ratio of the two compared voltages is then equal to the ratio of the two resistances. The voltage comparison problem reduces to one of establishing a sufficiently stable and accurately determinable resistance ratio. An important advantage of this fixed-ratio comparison technique, made feasible by the tunability of the Josephson device voltage, is the elimination of the adjustable resistance

element of the conventional potentiometer together with its attendant complexity and sources of uncertainty.

The two voltage comparators we used were based on two different methods of establishing the critical resistance ratio. Although one would have sufficed for e/h determination, two were designed and built because each had different advantages, disadvantages, and dominant sources of systematic error. A comparison of their performances was expected to reveal any unexpected sources of systematic error, test our estimates of the uncertainties associated with expected sources of systematic error, and perhaps indicate which method was more suitable for use in practical Josephson voltage standards.

A. Series-Parallel Comparator

The design of the first voltage comparator was based on a method called double series-parallel exchange.[12] The method depends on the fact that if n nominally equal resistors are connected first in series and then in parallel, the ratio of the resistances of the two combinations is n^2 with an error second order in the degree of resistance matching.[52] A simplified circuit diagram of the Series-Parallel Comparator (SPC) is shown in Fig. 15. A resistance ratio of 100:1 was obtained by using two sets of ten matched resistors, one set in series and one in parallel. The use of tetrahedral junctions between these main resistors and of compensating resistors (fans) for paralleling the series-parallel network permitted achievement of high accuracy in the series-to-parallel transfer despite relatively high lead and connection resistances.[53-55] The resistance network was fed by a high stability (0.5 ppm/hr current drift) power supply regulated by a mercury battery under essentially no load. If the two sets of

resistors are "exchanged", i.e., the set originally in series reconnected in parallel, and the other set reconnected in series, and a second pair of balances made, the effect of inequality of resistance between the two sets of resistors is reduced to second order if the results from the two pairs of balances are averaged. The effects of thermoelectric voltages in the circuit were eliminated by reversing the SPC current, the standard cell, and the junction bias current. The main advantage of this method is that the overall ratio can have considerably greater accuracy than that with which the individual main resistors can be compared. The main disadvantage is that the power dissipated in each of the series-parallel networks changes by a factor of 100 when they are switched from series to parallel connection. The resultant heating effects can introduce error.

Table I summarizes the sources of uncertainty in e/h associated with the
All uncertainties are intended to be one standard deviation.
SPC./ The following comments apply to the indicated items:

(a) The random uncertainty of the mean in an average e/h run was about 2 parts in 10^8 (see Section VII). If the results of several such runs are combined, the overall random uncertainty is reduced to 1 part in 10^8.

(b) Seven checks of the matching of the resistors in the main resistor strings were carried out during the seven month period in which e/h runs were made. The matching remained within tolerance throughout the period. An uncertainty of 4 parts in 10^9 due to resistor mismatch was estimated by computing the second order corrections to the resistance ratio using the data from each of the tolerance checks. The total resistances (1kΩ) of the two series-parallel networks remained matched within 10 ppm, and contributed negligible uncertainty to the measurements.

(c) The fan resistor mismatch uncertainty was estimated in a similar manner

from fan check data. The direct paralleling of the end main resistors through a single fan introduced an additional error[29] and required application of a correction of 2 parts in 10^8 to the data. The estimated uncertainty from both of these sources was 1 part in 10^8.

(d) The two independent transfer resistances of all 18 tetrahedral junctions (these are not required at either end of a series-parallel network since only three connections are required at these points) were measured at the beginning and end of the seven month period. The junction asymmetries introduced an uncertainty of 4 parts in 10^9.

(e) The physical arrangement of the main resistors was chosen to minimize heating effects through thermal coupling of the two strings. (If the two strings were perfectly thermally coupled, the heating error would be zero since the total power dissipated in both strings would be the same before and after exchange. Thus, this error is smaller than the individual resistor string self-heating errors by a factor which depends on the degree of thermal coupling between the strings.) The heating effects in the SPC were measured <u>in situ</u> using the usual "bridge within a bridge".[56] The two series-parallel resistor strings formed two arms of the bridge, and additional ac power was applied to one of the strings. The quantity of interest was thus directly measured, i.e., one of the strings was heated while the ratio of the resistances of the two was monitored. The heating effect was measured at several different added powers (between 5 and 20 times normal operating power) and the results extrapolated to the normal operating power. On the basis of these tests, a correction of about 3 parts in 10^8 was applied to the e/h data with an uncertainty of 2 parts in 10^8.

(f) Another source of uncertainty in any single series-parallel network is the fact that the resistance ratio is not established simultaneously, i. e., one measurement is made with the network in series and at a different time a second one is made with the network in parallel. Any change in the average resistance between the two measurements (e. g., from temperature variations) will cause a first order ratio error even though the individual resistor matching remains within tolerance. In the present instrument, the largest contribution to this type of error is internal temperature drift resulting from a systematic ambient temperature drift during e/h runs. Since the SPC was enclosed in a temperature-regulated oven which reduced the effects of ambient temperature variations by a factor of about 100 and a double series-parallel exchange was used, the uncertainty due to temperature drift was only 3 parts in 10^9. (The double exchange method further reduces the effects of temperature drifts to the extent that the temperature coefficients of the two series-parallel strings are matched, i. e., the resistance ratio can remain fixed even though the resistance of both networks changes.)

(g) Since in practice the junction and standard cell balances were made consecutively rather than simultaneously (see Section VI) a correction was required for drift of the comparator power supply. This correction averaged about 2 parts in 10^8 with an uncertainty of 1 part in 10^8.

(h) The balancing procedure used required interpolation of the null detector deflections and employed a calibrating signal to normalize these deflections (see Section VI and Fig. 15). Although the resistors used to produce the calibrating signal had a 1% tolerance, the actual values were measured in order to

compute the magnitude of the calibrating signal. The interpolated corrections averaged about 1 ppm and the uncertainty in generating the calibrating signal was about 1% (primarily due to resistor aging),[57] resulting in a measurement uncertainty of 1 part in 10^8.

(i) The effects of leakage resistance in the SPC were estimated in two ways. First, the individual leakage paths were measured directly. This was possible because the construction included extensive guarding. These leakage measurements were each made over a time interval comparable to the usual balancing times (about one minute) and thus yielded realistic values. Such tests were made several times to verify that the insulation had not deteriorated during actual use. Second, the leakage effects were evaluated during actual e/h measurements by individually grounding (one at a time) each portion of the circuit (Josephson device, standard cell, SPC, null detector, etc.) and observing the effect on the null detector balance. On the basis of these two types of leakage measurements, the estimated uncertainty from this source was 1 part in 10^8.

(j) A related source of uncertainty was dielectric polarization. If the direct leakage measurements described above were made over a long time interval (greater than one hour), a much larger value of leakage resistance could often be obtained than in a measurement made over several minutes. This was due to a component of the insulator dielectric polarization which required several hours to reach its equilibrium value. Another source of polarization currents is piezoelectricity induced by stresses resulting from machining or mounting insulators. In practice this could produce small unwanted currents in various parts of the circuit. In order to minimize these currents, the various parts of

the
/measuring circuit were grounded when not in use. The polarization currents
using an electrometer
were measured in the SPC/and were found to contribute an uncertainty of about 2 parts in 10^9.

(k) The last source of uncertainty considered here (associated with the SPC) is variations in the thermal emfs. These arise from both the SPC and the leads to the Josephson device (which traverse a large temperature gradient). The variations of the thermal emfs in the instrument were reduced by specially selecting the low-thermal solder used for each particular type of joint and in the junction leads by the thermal shielding. From the results of the step-number/bias-voltage differential experiment discussed in Section VIII, we estimate 5 parts in 10^9 for this uncertainty.

The root-sum-square total uncertainty is 3.1 parts in 10^8 and represents an estimate of the total uncertainty associated with the SPC voltage comparison system.

B. Cascaded Interchange Comparator

The design of the second voltage comparator was based on the use of a series of high-accuracy resistance comparisons to establish the critical 100:1 resistance ratio.[58] A simplified circuit diagram of this Cascaded Interchange Comparator (CIC) in the measurement mode is shown in Fig. 16. The calibration of the voltbox was carried out using a second independently powered voltbox incorporated in the instrument. Figure 17 shows the circuit arrangement for the first step in the calibration procedure. With the switches set as shown, a 10 Ω equal-arm Wheatstone bridge was formed. These resistors were trimmed until the null detector indicated a balance for both positions of the "interchange"

switch. The pair of 10 Ω resistors in each voltbox were then equal. The next position of the "select ratio" switch was then used to form a 20 Ω bridge with which the two 20 Ω resistors were matched to the two series pairs of 10 Ω resistors. Each of the remaining resistors were matched to a previously measured combination in this way until, on the last (seventh) calibration step, the 360 Ω resistor was matched to the sum of the 320 Ω and 40 Ω resistors. Lead compensation required by the low resistor values employed was provided by use of an independent power supply for each voltbox. Only one voltbox was required for e/h voltage comparisons, but the second could be used to check the results obtained with the first since both were calibrated equally well. The main advantage of this method is that the resistors are always subjected to the same power and hence heating effects should be negligible. The main disadvantage is the chain of precision resistance comparisons required for calibration, in which first order errors can arise.

Table II summarizes the sources of uncertainty in e/h associated with the CIC. Some of the sources of uncertainty for the CIC are the same as those for the SPC since the overall construction for the two was similar. The leading sources of uncertainty, however, are quite different in the two instruments. The following comments apply to the indicated CIC uncertainty items:

(a) The random uncertainty of the mean for a typical e/h run using the CIC was about the same as that for the SPC, i.e. 2 parts in 10^8. In addition, there was a random uncertainty associated with the CIC calibration procedure. This amounted to about 3 parts in 10^8 for a single calibration. During a typical e/h run two calibrations (one at the beginning and the other at the end) were performed

which resulted in a net calibration uncertainty of about 2 parts in 10^8. The total random error for a run using the CIC was obtained by combining the contributions from the measurements and from the calibrations. The final random uncertainty for several such runs was estimated to be 2 part in 10^8.

(b) Since the lead compensation in the CIC depended on matching both the connection resistances in the calibration (Wheatstone) bridges and the voltages across the two voltboxes moderately well, an uncertainty which was essentially the product of these two mismatches resulted. Nearly all variations in the connection resistances arose from switch contacts because the wiring resistances were carefully matched during construction. These contact resistance variations were directly estimated by performing a series of calibrations using only a single power supply, thus making the voltage mismatch 100%. The first step in the standard calibration procedure consisted of equalizing the voltages across the two voltboxes. During the calibration these voltages drifted apart, and an estimate of this drift was made by measuring the lack of equality as the last step of the standard calibration procedure. The estimates were 5 parts in 10^4 for the connection variations and 4 parts in 10^5 for the relative power supply drift. Thus, the systematic calibration uncertainty from the combination of these two factors was 2 parts in 10^8.

(c) Because the trimmer resistors on adjacent main resistors of the CIC resistance strings shared a common lead, there was a small difference between the ratio as measured during calibration and the ratio which existed during actual use of the comparator.[30] We have estimated an uncertainty of 7 parts in 10^9 from this source.

(d) Since the temperature of the CIC oven drifted between calibrations during a run and the temperature coefficient of the 100:1 resistance ratio was not negligible, a small systematic uncertainty resulted. The main contributor to this uncertainty was the nonlinearity in the temperature drift which was not eliminated by simple averaging of the calibration data. The uncertainty from this source was about 3 parts in 10^9.

(e) The power supply in the CIC was of the same design and construction as that in the SPC. Since during measurements both instruments were used in the same manner and the CIC power supply was observed to be as stable as the one in the SPC, an uncertainty of 1 part in 10^8 was also assigned to this source for the CIC.

(f) The uncertainty in generating the calibrating signal in the SPC was mainly due to aging of the calibrating resistors. The corresponding uncertainty for the CIC was significantly smaller because this instrument was used over a much shorter time interval. An additional calibrator signal uncertainty arose from the CIC calibration procedure. The combined uncertainty from both sources was about 5 parts in 10^9.

(g) The effects of leakage resistance in the CIC were evaluated in a manner similar to those in the SPC. The associated uncertainty in the CIC was about 4 parts in 10^9. This uncertainty was smaller than that in the SPC, probably as a result of the somewhat simpler circuitry in the CIC.

(h) The dielectric polarization current was also measured in the CIC and an uncertainty of 2 parts in 10^9 was assigned to this source.

(i) The effects of thermoelectric voltages on CIC measurements were estimated

in the same way as for the SPC and again contributed an uncertainty of 5 parts in 10^9.

The root-sum-square total uncertainty is 3.2 parts in 10^8 and represents an estimate of the total uncertainty associated with the CIC voltage comparison system. The estimated total uncertainties for the SPC and CIC, although made up of quite different components, are almost identical. This indicates that in use, the two instruments should give results of comparable accuracy which agree to within the joint instrument uncertainties provided no significant source of systematic error has been overlooked in either instrument. The results of comparisons of the performance of the two instruments in actual use are presented in Section VII.

C. Null Detector System

A single null detector system was used for both the Josephson device and standard cell balances. (In Fig. 14 two separate null detectors are indicated for conceptual simplicity.) The null detector system consisted of a photocell-galvanometer amplifier (Guildline type 9460) with negative feedback, modified to drive a strip chart recorder. Other improvements in the amplifier included (1) reduction of variations in the thermal emfs, (2) increasing the input resistance for standard cell balances, and (3) complete electrostatic shielding of the unit. The photocell amplifier employed two types of feedback. Series (voltage) feedback, which produces a high input resistance, was used in the standard cell balance to minimize the off-null currents. Parallel (current) feedback, which does not add any resistance in series with the input circuit, was used in the Josephson device balance for minimum Johnson noise (the dominant source of uncertainty in

this balance). When used with the SPC and CIC comparators, the null detector resolution for the standard cell balance was about 1 part in 10^8 (10 nV in 1 V) and for the Josephson device balance was about 2 parts in 10^8 (0.2 nV in 10 mV).

For the routine standard cell comparisons discussed in Section IV, the same photocell amplifier was used with series feedback (to minimize off-null currents). In this case, a display galvanometer was used rather than the strip chart recorder which was neither essential nor desirable. The resolution for the standard cell comparisons was about 5 parts in 10^9 (5 nV in 1 V).

VI. EXPERIMENTAL PROCEDURE AND RESULTS

In this section the experimental procedure for a typical e/h run is described and the results are presented.

A block diagram of the dc measuring system and the Josephson device biasing system as arranged for an e/h run is shown in Fig. 18. Since the Josephson devices used in these e/h measurements could be stored at liquid nitrogen temperature for long periods of time, they were maintained at this temperature in the cryostat and repeatedly reused. Before each run a complete standard cell comparison was carried out. Several hours or more after the cryostat was filled and all electronic equipment was turned on, data taking began. The Josephson device was biased and the microwave power adjusted to produce a total step voltage of about 10 mV. The comparator was connected to the Josephson device, standard cell, and null detector system. While the Josephson device voltage was monitored with the comparator, the step number and then the microwave frequency were adjusted to within about 1 ppm of the proper values. By this time the temperatures in both the cryostat (1.2 K) and the shielded room (about 25° C) had essentially stabilized. The e/h data were obtained by alternately balancing the comparator against the Josephson device and the standard cell and measuring the microwave frequency. The polarity of all voltages was reversed between certain pairs of balances in a sequence (usually + - - +) which would average out not only thermoelectric emfs but also uniform drifts in these emfs. A total of 16 pairs of balances were made in about $2\frac{1}{2}$ hours during a typical run. Since the operating conditions varied somewhat during the run, the dc bias current, the microwave power, the microwave frequency, and the thermoelectric

voltage offset in the comparator were adjusted as required. During most runs the counter time base was compared with the WWVB standard frequency broadcast. After most runs, a second complete standard cell comparison was made.

The raw e/h data consisted of a strip chart recording of a series of comparator balances. During a run the strip chart recorder was operated continuously to permit accurate interpolation of the null detector balance data (versus time) and elimination of the effects of the various drifts. Operating parameters such as temperatures and relative microwave power incident on the Josephson device were monitored and noted on the chart recording. A typical section of analyzed data is shown in Fig. 19. Straight lines were fit by eye to each portion of the balance and the numerical values of the deflections were determined by measuring the distances between appropriate pairs of the fitted lines. These distances were measured at the mean time (as indicated, for example, by the arrows in Fig. 19) of each comparator balance. Each balance yielded three quantities: the comparator imbalance (GJ or GS), the calibration signal (MS), and the mean time of the balance. The normalized comparator imbalance was calculated as the ratio of GJ or GS to MS and was independent of the gain of the null detector system. Three or four normalized pairs of imbalances were then combined as required by the particular sequence of polarity reversals used and combined with the respective microwave frequencies and standard cell voltage to obtain an independent 2e/h value. In a typical run, four such values were measured.

Experimental values of 2e/h were calculated from the equation $2e/h = \beta n\nu/V_S$, where β is the compared voltage ratio V_S/V_J (very nearly 100), n is the step

number (about 500), ν is the microwave frequency (about 11 GHz), V_S is the standard cell voltage (about 1 V), and V_J is the total Josephson voltage (about 10 mV). Since the uncertainty associated with the voltage standard used in these measurements was larger than that from all other sources combined (particularly in the later runs), it was found useful to treat the standard cell voltage as a possible variable. It was therefore convenient to rewrite this equation in the form $(2e/h)V_S = \beta n\nu \equiv F_S$, the equivalent standard cell Josephson frequency. Expressing the results in terms of F_S is particularly desirable since the standard cell comparison data (Section IV) clearly indicate that at least some of the cell emfs were changing in time, while e/h is presumably constant.

Results for three of the later runs which coincided with the NBS VTP transfer of Group D to the University of Pennsylvania are shown in Fig. 20. These data were obtained using as a working standard cell A5 (shortly after group A had been returned from NBS). The standard deviation of the individual points within a run and the standard deviation of the mean for each of these runs are indicated.

Altogether there were 23 e/h runs. For Runs 1 through 11, the working standard cell was B1, for Runs 12 through 18, cell B3, and for Runs 19 through 23, cell A5. Equivalent standard cell Josephson frequencies were obtained for the other cells using the standard cell comparison data taken on the same days as the runs. The standard cell frequency F_S for the group mean $\bar{\bar{A}}$ is plotted in Fig. 21 as a function of time. Only 21 experimental points are indicated because two runs were made while Group A was at NBS being calibrated. The error bars on the individual points represent the random uncertainty of the mean

for the run plus an estimate of the uncertainty in the standard cell emfs caused by the disturbing effects of the run itself on the ambient conditions, particularly the temperature of the standard cells. These two uncertainties were generally comparable in magnitude. Figures 22, 23, and 24 show the corresponding data for the individual cells comprising Group A. Since the random uncertainty in the standard cell comparison data was only about 1 part in 10^8, the net uncertainties for the F_S of the individual cells are essentially the same as those shown for $\overline{A}$ in Fig. 21.

The standard cell frequency data for the group mean $\overline{B}$ are shown in Fig. 25. The error bars for these points were obtained in a manner similar to those for Group A. The dashed line in a least-squares fit to the data from Runs 11 through 23, assuming equal weighting for each point and excluding Run 12 on Day 64. (The significance of this line is discussed in Section VII.) Figure 26 shows the corresponding data for the individual cells in Group B. Note that the points for both B1 and B3 are offset vertically.

The F_S data for the three cells in Group C are shown in Fig. 27. On the scales shown, the experimental uncertainty in each point is smaller in magnitude than the symbol indicating the point. The solid straight lines represent least-squares fits to the corresponding solid points, and the slope for each fitted segment is indicated in the figure. The broken lines indicate times at which apparently irreversible shifts in cell emfs occurred. (The final aging rate (about 0.04 ppm/day) for cells C5 and C6 is typical for unsaturated standard cells.) The data points with open symbols had significantly greater uncertainties than the others and were not used in fitting the straight lines. In Fig. 28, the deviations

of these data from the least-squares fitted lines are plotted on an expanded scale. The standard deviations for the solid points about the fitted lines are indicated.

VII. DISCUSSION AND ASSIGNMENT OF UNCERTAINTIES

The various contributions to the final total uncertainty of our result can be separated fairly unambiguously into three categories: (1) Uncertainties associated with the measurement system exclusive of the local voltage standard. These we call "measurement uncertainties". (2) Uncertainties associated with fluctuations and drifts in the local voltage standard. (3) Uncertainties associated with volt transfers between our local volt and the NBS volt. In this section we discuss each of these in turn, and then combine them to obtain our final result and its uncertainty.

A. Measurement Uncertainties

The sources of random uncertainty in an individual e/h run were of two types: (1) Random uncertainties associated with the measurement system exclusive of the voltage standard, such as fluctuations in the frequency stabilization system, thermal noise in resistors, variations in the thermal emfs in the cryostat leads, and any randomly varying components of the sources of systematic uncertainty in the voltage comparator system; (2) Random uncertainties associated with very short term fluctuations in the working standard cell emf. The latter are to be distinguished from drifts in standard cell emf during the course of a run due to changes of ambient temperature. These were corrected for; the additional uncertainty associated with these corrections is discussed in Section VIIB. Random uncertainties due to short term fluctuations of standard cell emf were not distinguishable from those due to other sources in the measuring system and are therefore included in the total random measurement uncertainty.

In the early runs the random uncertainty of the mean was about 0.1 ppm.

This was reduced to about 0.02 ppm in the later runs (see, for example, Fig. 20) by refinements and improvements in the measurement procedure. These included: (1) Comparison of the standard cells and measurement of the cell enclosure temperature both before and after the run, beginning with Run 8; (2) Improved statistics resulting from an increase in the number of experimental points measured in a run from about two to five; (3) Use of a multiple junction device. Three junctions connected in series were used beginning with Run 4. The current amplitudes of the individual steps were then all greater that 50 μA, thus reducing the effects of external noise on the steps; (4) Use of the regulated power supply in the SPC beginning with Run 6. Prior to this, the instrument had been operated in the unregulated mode; (5) Avoidance of rapid variations in the microwave power incident on the junction. This was important because variations in the microwave power were observed to cause changes in the drift of the thermal emfs in the junction leads from the cryostat. Particular attention was given to this problem beginning with Run 13.

We have assigned a total uncertainty of 1 part in 10^8 to the frequency measurement. This is primarily due to drift in the frequency stabilization system during the period of a single Josephson-device balance (about 3 min.) and the consequent lack of exact simultaneity of balance and frequency measurement. It also includes an estimate of the uncertainty associated with the calibration and maintenance of the frequency-counting system, which was a few parts in 10^9.

The possible dependence of the step voltage on bias current (nonvertical steps) was checked experimentally by varying the bias current and simultaneously monitoring the step voltage under operating conditions with the SPC. Within the voltage

resolution of about 0.2 nV, the step voltage did not change while the current was varied over the full height of the step. During measurements all junctions were biased near the center of the step. This bias point could be maintained to within about 20% of the total step height for single junction steps near 10 mV. For larger steps near 3 mV in a three-junction device, the mid-step position could be maintained roughly three times better. An uncertainty of 4 parts in 10^9 has been assigned to take into account possible systematic error due to non-vertical steps.

The estimated uncertainties associated with each of the two voltage comparators have been discussed in Section VA and VB and are summarized in Tables I and II. The total uncertainties for both instruments were about 3 parts in 10^8. These uncertainties were obtained by evaluating all known possible sources of systematic error in each system and may be termed a priori uncertainties. A crucial question is whether these a priori uncertainties are a true representation of the accuracies of the instruments and of the voltage measurements made with them, or whether some important sources of systematic error may have been overlooked. Our purpose in building two instruments based on different principles was to check just this point by comparison of the two instruments.

The SPC was used in all 23 runs. The CIC was used together with the SPC in Runs 22 and 23. The individual F_S data for these two runs are plotted in Fig. 29. From these data the difference in the apparent voltage ratio provided by the two instruments was deduced. The principal source of uncertainty in determining this difference was the drift which is apparent in Fig. 29. That this is not primarily due to a real difference between the two instruments is evident from

the fact that the order in which they were used was reversed in the second run and the fact that this drift appeared in all runs which extended over such relatively long times. The drift is attributable to drift in the emf of the working standard cell due to increase of the ambient temperature during the course of a run (see Section VIIB). Two different procedures were used to take into account this drift in Runs 22 and 23. In the first, the F_S data for each instrument were treated independently and a correction for the drift of the cell was computed from the observed temperature change of the cell measured before and after the run. The difference in the voltage ratio of the two instruments evaluated in this manner was 2.8 ± 2.6 parts in 10^8. In the second procedure, a straight line was least-squares fitted to all the F_S data within each run. (These are the dashed lines shown in Fig. 29.) An average ratio difference of 1.5 ± 1.5 parts in 10^8 was computed from the two slopes and the appropriate time intervals.

In a separate experiment performed two days after Run 22 and two days before Run 23, the 100:1 voltage ratios established by the two instruments were compared directly by connecting their 10 mV (Josephson device) inputs together and employing a separate working standard cell for each. Sixteen sets of balances were made with the two instruments. Each set consisted of two standard cell balances and a common "Josephson device" balance. The CIC was calibrated at the beginning, midway through, and at the end of this instrument comparison run. The voltage difference between the two cells determined from the instrument data was 3.092 ± 0.018 ppm. The average cell difference measured via the direct standard cell comparisons made before and after the run was 3.108 ± 0.020 ppm. (These uncertainties include only the random component.) The voltage ratio

difference computed from these data was -1.6 ± 2.8 parts in 10^8. The weighted mean of this result and the more precise result from Runs 22 and 23 is 0.8 ± 1.3 parts in 10^8. The weighted mean with the less precise result from Runs 22 and 23 is 0.8 ± 1.9 parts in 10^8. Comparing these with the voltage ratio difference expected from the a priori estimated uncertainties, 0 ± 4.5 parts in 10^8, we conclude that the two instruments agree to within about 1 part in 10^8, that there are probably no significant unsuspected systematic errors in either instrument, and that the estimated a priori uncertainties assigned to the two instruments are realistic.

Combining root-sum-square either instrument uncertainty with the frequency measurement and nonvertical step uncertainties, we estimate a total "measurement uncertainty" of 3.3 parts in 10^8.

B. Local Volt Uncertainties

The uncertainties associated with our local voltage standard may be discussed in three categories: (1) contributions to the random uncertainty; (2) uncertainties due to standard cell temperature drifts during e/h runs; (3) uncertainties due to long term drifts and sporadic shifts in cell emfs over long times (months). As noted in Section VIIA, the first category is indistinguishable from random uncertainties due to other components of the measuring system and has been included in the overall random measurement error.

Drifts of the emfs of all the standard cells during e/h runs occurred because the cell enclosure temperature regulators failed to compensate completely for (1) the increase in ambient temperature in the shielded room (typically several degrees) due to power dissipation in electronics and a less-than-ideal room

temperature control system, and (2) a change in power dissipation in the enclosure temperature regulator circuitry caused by switching from the ac power source normally used to the dc battery source used during runs. This was not a problem during our routine standard cell comparisons because there was much less power dissipation in the shielded room and because these measurements required less than an hour. Typical e/h runs extended over several hours, and the drifts of cell emfs were not negligible. Measurements of the temperature within each cell enclosure before and after e/h runs and evaluation of the F_S data taken during the runs indicated that the changes in emf of the standard cells were smooth and monotonic. This was confirmed in a separate experiment in which a series of standard cell comparisons was made at 1.5 hr. intervals under typical e/h run operating conditions. It was found that individual cell differences relative to the appropriate group mean varied randomly by amounts between 0.2 and 1.2 parts in 10^8, while the group mean differences varied smoothly and monotonically by much larger amounts. This strongcorrelation among the cell emfs in a particular group indicates that each enclosure maintained a fairly uniform temperature in the face of ambient temperature changes, but the variation of the group mean differences shows that each enclosure responded to ambient temperature drifts by different amounts. The cell emf drifts varied from run to run and were generally about a factor two greater for the enclosure containing Group B than for the modified A enclosure. Corrections for these drifts were made for cells in Group A using thermistor temperature data and for cells in Group B by assuming that the emfs of the unsaturated cells in Group C (in the same enclosure with Group B) were constant between the standard cell comparisons before and after

the run. (Recall that the temperature coefficients of the unsaturated cells were about a factor of thirty smaller than for the saturated cells.) The F_S data for the individual cell being used as a working standard generally showed a monotonic increase with time in very good agreement with that implied by the observed temperature change in the cell enclosure. The drift was more severe for runs in which the data were taken over a long time interval, e.g., contrast the data for Runs 22 and 23 (Fig. 29) with those for Runs 19,20, and 21 (Fig. 20) Runs 1 through 18 were made using cells from Group B as working standards and the drift was usually between 0.1 and 0.2 ppm. The drift rate in Runs 19 through 23 (in which a cell from Group A was used) was smaller.

The uncertainties associated with the temperature corrections applied to the mean of the F_S data for each run depended on a number of factors including the size of the correction and the timing of the temperature measurements and standard cell comparisons. The uncertainties varied between 0.07 ppm in some of the earlier runs (excluding the first two) and 0.02 ppm in the later runs. This uncertainty has <u>not</u> been included in the uncertainty budgets for the two voltage comparators (Tables I and II) because these are meant to characterize the performance of the voltage measuring systems using a hypothetical perfectly stable voltage standard. The temperature correction uncertainties <u>have</u> however been incorporated in the error bars on the final F_S data shown in Figs. 21 and 25, since these error bars are intended to reflect the total random uncertainty from all sources, <u>before</u> allowance for uncertainties associated with possible systematic effects. (It should be noted that the error bars on the points in Fig. 21 also apply to the corresponding points in Figs. 22-24, and the error bars on

the points in Fig. 25 apply to the corresponding points in Fig. 26. They have been omitted from the individual cell F_S plots for clarity. The standard cell comparisons required for the necessary F_S transfers had a negligible uncertainty of 0.007 ppm [see Sec. IV].)

We have assigned an uncertainty of 5 parts in 10^8 to the short term local volt stability. This includes an estimate of the uncertainty in our standard cell temperature drift correction procedure and a small contribution from effects of changing thermoelectric emfs in the standard cell comparison circuitry.

Consideration of the third category of local voltage standard uncertainty, that associated with long term stability, requires some discussion of the F_S data displayed in Figs. 21-28. First, we must reemphasize that our presentation of the data in this manner rests on the assumptions that neither the Josephson devices nor the voltage comparison system used in these experiments exhibit any significant long term drift, and that the nonsystematic uncertainties assigned to the comparison of Josephson device and standard cell voltages (the error bars in Figs. 21 and 25) are realistic. Our previous discussion of the stability and performance of the two voltage comparators and careful study of all of the e/h and standard cell comparison data strongly support this assumption! It follows that the significant variations evident in the F_S data are to be attributed to the standard cells. This allows us to draw some important conclusions about the properties of our standard cells and, by inference, any standard cells maintained under similar circumstances.

Consider the F_S data for $\bar{A}$ shown in Fig. 21. The largest difference between any two values of $F_S(\bar{A})$ was about 0.3 ppm. Prior to the indicated

transfer of Group A to NBS, a small but significant downward drift is apparent. The data immediately after the transfer imply that $F_S(\bar{A})$ had increased by about 0.2 ppm. This shift is also reflected in the $\bar{A}$-$\bar{B}$ direct cell comparison data (Fig. 11). When the final two runs were made about two months later, $F_S(\bar{A})$ had decreased to a value smaller than that which it had just prior to the transfer. The transfer shift can be traced in more detail in Figs. 22-24. Cells A2 and A3 do not appear to have been significantly disturbed by the transfer. Cells A4 and A6 had increased by about 0.2 ppm when measured (Runs 19, 20 and 21) immediately after their return from NBS. Cells A1 and A5 exhibited the most drastic changes. A5 had increased by about 0.5 ppm but then decreased over a period of several months (see also Fig. 10) to a value consistent with that expected on the basis of the pre-transfer data. A1 exhibited the greatest instability of any of the cells in Group A. Before the transfer, the emf of this cell steadily decreased at the rate of about 0.01 ppm/day. This accounts for most of the negative slope apparent in the data for $F_S(\bar{A})$ prior to the transfer. The emf of A1 after the transfer differed by about 0.5 ppm from that obtained by extrapolating the pre-transfer data. Note also the abrupt change in A1 between the last two runs. (This exceptional instability of A1 was not entirely unexpected. It is by far the most shopworn of the Group A cells, having been used as the working standard throughout the experiments of Parker et al. and in other work, and having suffered at least one momentary short circuit. It does however indicate the importance of a cell's life history in determining its behavior.) A1 might have been deleted from Group A for purposes of computing $\bar{A}$, but this would not have altered any of our conclusions, so it was retained.

The F_S data for $\bar{B}$ shown in Fig. 25 show a relatively large upward drift for the first several months which is reflected in the individual cell data (Fig. 26) and the $\bar{A} - \bar{B}$ cell comparison data (Fig. 11). This again is most likely a history effect. The Group B cells had been aged about three years at a relatively constant temperature before they were mounted in their enclosure by the manufacturer about three months before Run 1. The operating temperature of the enclosure was about 2^{o} C higher than the aging temperature. The large initial drift lasting for about five months is probably a recovery from this temperature shock.

A linear least-squares fit to the $F_S(\bar{B})$ data for Runs 11 (Day 59) through 23, excluding Run 12 (Day 64), is indicated by the dashed line in Fig. 25. This fit was made to see whether the data were really consistent with a linear drift of Group B (after the large temperature shock transient had died away) plus scatter of the magnitude expected from the a priori estimated uncertainties indicated by the error bars together with possible day-to-day temperature fluctuations in the Group B enclosure. The result for Run 12 was omitted from the fit because it was based on only one e/h datum (due to technical difficulties during the run) whereas the others were based on about five e/h data points. All the data were weighted equally because it was expected that the enclosure temperature fluctuations might account for most of the scatter. The slope of the fitted line corresponds to an apparent drift in $\bar{B}$ of about 3×10^{-9}/day (about 1 ppm/year). The standard deviation of the points about the fitted line is 0.06 ppm. This corresponds rather well with the a priori uncertainties indicated by the error bars. On the other hand, this standard deviation could be entirely accounted for by a day-to-day enclosure temperature fluctuation of just 10^{-3} ^{o}C, an amount which is entirely

consistent with our experience with the performance of both enclosures. Note also that the large deviation of the point for Run 16 (Day 102) from the fitted line can be traced to a large fluctuation in cell B2 which is also evident in the F_S(B2) data (Fig. 26) and the $\bar{A} - \bar{B}$ data (Fig. 11).

Consider now the F_S data for the cells in Group C shown in Fig. 27. The significance of these data is twofold. First, the average standard deviation of 0.04 ppm for cells C4 and C6 is in excellent agreement with the a priori uncertainties. (The a priori uncertainty for each of these cells is essentially identical to that for the corresponding $F_S(\bar{B})$.) Second, the smooth aging of cell C4 between Runs 11 and 21 and to a lesser extent that of cell C5 between Runs 11 and 23 are additional evidence that both the dc measurement system and the Josephson device voltage used to compare and evaluate $\bar{A}$ before and after the final transfer to NBS did not change during this transfer period. This implies that the apparent shift in $\bar{A}$ during this transfer really is associated with Group A, not the remainder of the system.

Taken as a whole, our standard cell comparison and F_S data show that the long term behavior of standard cells is characterized by drifts at various rates and by occasional sudden shifts. By careful study of frequently obtained direct comparison data on a relatively large number of cells and of data obtained by comparing cells with a stable Josephson voltage standard (the F_S data), the drifts and shifts can be identified with specific cells or groups of cells and can often be connected with causal events in the history of the cells. The scatter of the F_S data for cells which show no abnormal drifts or shifts is consistent with the a priori uncertainties estimated from knowledge of the measurement system and procedures.

We therefore conclude that it is unnecessary to include in the total uncertainty of our e/h result any contribution associated with the long term behavior of our local voltage standard, except insofar as this behavior influences the assignment of uncertainties to volt transfers between our laboratory and NBS. This is discussed in the next section.

Another very important conclusion which can be drawn from the data discussed in this section is that the ac Josephson effect can be used to maintain standards of electromotive force with short and long term precisions of several parts in 10^8 using the instrumentation and techniques we have used in these experiments. This demonstrated capability surpasses by an order of magnitude the demonstrated performance of emf standards based on electrochemical standard cells.

C. Volt Transfer Uncertainties

The three volt transfers by which our local volt was related to the NBS volt have been described in Section IV. The procedure we have adopted for analyzing our data and obtaining a final value of e/h involves treating the three transfers independently and deriving a value of e/h for each. Accordingly, we now consider the final uncertainty to be assigned each transfer.

As noted in Section IV, the uncertainty in the first transfer of Group A derived from standard NBS uncertainty estimates is 0.37 ppm. In a preliminary report of our experiments we assigned an uncertainty of 0.45 ppm to this transfer.[12] The components of the transfer uncertainty given in Section IV differ from those given in this preliminary report because of subsequent clarification of the meaning of the uncertainty estimates contained in NBS Form 532a (11-68).[51] Rather than

adopt the new (smaller) uncertainty, we have chosen to retain the 0.45 ppm uncertainty for the following reasons: (1) The enclosure housing Group A had been modified by replacing the temperature regulator and changing the leads to the cells only about one month before NBS began measuring the cells. This may have been insufficient time for the cells to recover from the accompanying trauma. (2) We have been informed that NBS had a power failure during the calibration period which caused a brief shutdown of the temperature regulator of the oil bath

containing their reference cells.[48] The value of 2e/h associated with this transfer and based on the first ten runs is thus the one given in Ref. 12,

$$(2e/h)_I = 483.593\ 65 \pm 0.000\ 22\ \text{MHz}/\mu\text{V}_{\text{NBS 69}}\ (0.46\ \text{ppm})$$

The second NBS calibration of Group A was made in April, 1970. (It is important to note this date to facilitate future comparisons of our result with those of workers in other countries. This calibration coincides with the final measurements made by NBS as part of the 1970 international voltage comparisons at BIPM.)[47] The F_S data for Group A, temperature corrected using the thermistor data (Fig. 21), indicate that the group mean $\bar{A}$ increased by about 0.2 ppm as a result of the transfer, then decreased to a value near that which it had just prior to the transfer. The same F_S data temperature corrected using the thermometer data showed an apparent shift in $\bar{A}$ of about 0.5 ppm. (The temperature changes indicated by the thermometer and the thermistor differed by about 5×10^{-3} °C.) With no temperature correction at all, the apparent shift was 0.55 ppm. Our data and the NBS $\bar{A}$ data (Fig. 12) suggest that physical transport of Group A both to and from NBS caused an upward shift in $\bar{A}$ which was followed after both transports by relaxation downward. Because the thermistor was less sensitive to mechanical shock and vibration and could be resolved much more accurately than the thermometer, we believe it provides better temperature correction data and therefore, the real overall (transient) shift associated with the transfer was about 0.2 ppm.

In order to obtain a value of 2e/h associated with this transfer it is necessary

to determine the value of $F_S(\bar{A})$ which corresponds to the mean voltage $\bar{A}$ assigned by NBS ($\bar{A}$ dashed line, Fig. 12). This was done as follows: (1) A value of $F_S(\bar{B})$ on Day 116 (the central day of the transfer) was calculated from the least-squares fit to the $F_S(\bar{B})$ data from Runs 11 through 23, excluding Run 12 (dashed line, Fig. 25). (2) A value of $\bar{A} - \bar{B}$ on Day 116 was obtained by least-squares fitting a straight line to the $\bar{A} - \bar{B}$ data taken on the same days as Runs 11, 13 through 16, and 19 through 21. (The fitting of a single straight line may be objected to because it does not take into account the transfer shift in $\bar{A}$. The corresponding shift in $\bar{A} - \bar{B}$ is barely significant, however, because $\bar{B}$ was drifting upward during the transfer period. As a result, the Day 116 $\bar{A} - \bar{B}$ obtained from the mean of separate fits to the pre- and post-transfer $\bar{A} - \bar{B}$ data is almost identical to that obtained from a single fitted line.) (3) These numbers were then combined with the value assigned $\bar{A}$ by NBS to yield

$$(2e/h)_{II} = 483.593\,730 \pm 0.000\,101\ \text{MHz}/\mu\text{V}_{\text{NBS69}} (0.21\ \text{ppm})$$

Because the NBS measurements of Group A during this transfer were made following the procedure of the NBS VTP rather than the usual calibration procedure, the uncertainty associated with the transfer might be taken as that recommended by NBS for a typical VTP transfer, 0.14 ppm.[51] However, because of the apparent shift of $\bar{A}$ as a result of the transfer and the uncertainty associated with corrections for this shift, we have chosen to expand the uncertainty assigned this transfer to 0.2 ppm. The uncertainty quoted for $(2e/h)_{II}$ is a root sum square of this uncertainty with the measurement and local volt uncertainties discussed above.

The VTP transfer of Group D between the University of Pennsylvania and NBS was made nearly simultaneously with the second transfer of Group A. The procedure used to determine a value of $2e/h$ for this transfer was to combine the $F_S(\bar{A})$ data for Runs 19, 20, and 21 with the $\bar{A} - \bar{D}$ data obtained on the same three days using VTP procedures. The resulting mean value of $F_S(\bar{D})$ was then combined with the mean $\bar{D}$ assigned by NBS for the transfer, yielding

$$(2e/h)_{III} = 483.593\,720 \pm 0.000\,074 \text{ MHz}/\mu V_{NBS69} (0.15 \text{ ppm})$$

The uncertainty is the root sum square of the measurement and local volt uncertainties with the 0.14 ppm transfer uncertainty recommended by NBS on the basis of NBS experience with a large number of similar transfers.[51] This estimate of the transfer uncertainty is supported by the following observations: (1) The mean of the $\bar{A} - \bar{D}$ data for the three days on which the runs were made and the mean $\bar{A} - \bar{D}$ for all standard cell comparisons made in our laboratory during the VTP transfer (Fig. 13) agreed to 1 part in 10^8. (2) The $F_S(\bar{D})$ data indicate that $\bar{D}$ drifted during the three week period during which Group D was at the University of Pennsylvania with about the same slope as that indicated by the NBS calibration data before and after the transport of Group D to our laboratory. Our data yield a slope of $(-8.2 \pm 3.7) \times 10^{-9}$/day; the NBS data yield $(-6.2 \pm 2.3) \times 10^{-9}$/day. (3) The relative stability of the three cells comprising Group D was significantly better than that for some of the cells in Group A. (4) The mean ambient temperature of the two laboratories was about the same ($23^{\circ}C$).

The final value of 2e/h and its uncertainty were determined on the basis of the following considerations: NBS interprets the 0.14 ppm uncertainty for a VTP-type transfer as almost entirely random, i.e., the effects of systematic errors are believed to be negligible at this level of accuracy. The enclosures of the two different standard cell groups transferred were of different construction and the dominant uncertainties in each case were the effect of the physical transport itself either directly on the cells or indirectly by way of the temperature sensing elements. We have therefore assumed that for the last two transfers the uncertainties are uncorrelated. The net transfer uncertainty for these two transfers together, calculated in the usual manner, is thus about 0.11 ppm. The value of 2e/h to be associated with Runs 11 through 23 was then calculated as the mean of $(2e/h)_{II}$ and $(2e/h)_{III}$, each weighted as the inverse square of the corresponding transfer uncertainty alone. (Note that $(2e/h)_{II}$ and $(2e/h)_{III}$ agree to within 2 parts in 10^8. Since the two transfers were made at essentially the same time, possible uncertainties associated with long term aging or drift of the NBS as-maintained volt do not affect this comparison.) The result was $483.593\,723 \pm 0.000\,063$ MHz/μV_{NBS69}, where the uncertainty is the root-sum-square of the net transfer uncertainty and the measurement and local volt uncertainties estimated above. Our final value of 2e/h is the weighted mean of this value with the value previously obtained for the first ten runs, $(2e/h)_I$, and is

$$2e/h = 483.593\,718 \pm 0.000\,060 \text{ MHz}/\mu V_{NBS69} \quad (0.12 \text{ ppm})$$

The components of this final uncertainty are summarized in Table III. It must be emphasized that the uncertainty assigned this result is a measure of its accuracy in terms of the NBS as-maintained volt, V_{NBS69}, as it existed and was disseminated at a particular epoch, i.e., during the first half of 1970. Any drift of V_{NBS69} will introduce an additional source of uncertainty into comparisons of our value with future values determined in terms of V_{NBS69}. On the basis of an extended series of measurements of the proton gyromagnetic ratio designed to monitor the stability of the NBS ampere, and a number of international volt comparisons via BIPM, it is believed that the drift in V_{NBS69} does not exceed 0.1 ppm/yr.[7, 47] This upper limit is sufficiently large to require consideration in future applications of our result.

VIII. CHECKS ON THE VALIDITY OF THE JOSEPHSON FREQUENCY-VOLTAGE RELATION

In the course of these experiments we looked for possible effects of several experimental parameters on the frequency-voltage ratio.

The effect of an externally applied magnetic field of about 1 G on the measured value of 2e/h was investigated during Run 14. The first half of the F_S data for this run was taken with the magnetic field in the plane of the junction and perpendicular to the waveguide axis. The remainder of the data were taken in the usual way in essentially zero magnetic field. The external magnetic field was produced by a modified pair of Helmholtz coils located within the multiple-layer magnetic shield used to reduce the effect of the earth's field to less than 1 mG. A magnetic field of 1 G is a relatively large field for a Josephson junction resonant at X-band; the first minimum in the Fraunhofer pattern of the zero-voltage current would occur at about 0.3 G. Theoretically, an external magnetic field small compared with the film critical field should change the amplitude of the steps but not their voltage position. Experimentally, the difference in the two subsets of data for this run was

$$(2e/h)_{H = 1\ G} - (2e/h)_{H = 0} = -3.2 \pm 4.1 \text{ parts in } 10^8 .$$

The effect of temperature was investigated during Run 15. The first half of the data was taken at 1.2 K, our usual operating temperature, and the remainder of the data were taken at 2.0 K. The difference in the two values was

$$(2e/h)_{T = 2.0\ K} - (2e/h)_{T = 1.2\ K} = -7.6 \pm 4.1 \text{ parts in } 10^8 .$$

The step-number or dc-bias-voltage dependence of 2e/h was tested in several different ways. The first three runs were made using a single junction biased at 10 mV ($V_n > 7\Delta/e$) with $n = 450$. In the next five runs, a series connection of three junctions was used to obtain the 10 mV, with the individual junction voltages (or step numbers) in the ratio $(n_1:n_2:n_3) \cong (1:1:2)$. On the basis of these first 8 runs,

$$(2e/h)_{\Sigma V_n} - (2e/h)_{V_n} = 4.2 \pm 6.8 \text{ parts in } 10^8 .$$

A more accurate differential experiment was done in which two junctions were connected in series opposition to a third (all on the same substrate), irradiated with microwaves in the usual way, and biased so that $n_1 + n_2 = n_3$ and $n_1 \cong n_2$. The two junctions in series were each biased near 2.4 mV so that both V_{n1} and V_{n2} were less than the lead energy gap $2\Delta/e$ (2.7 mV); the third junction was biased near 4.8 mV so that $3\Delta/e < V_{n3} < 4\Delta/e$. The power incident on the junctions was approximately equal to that used in the later runs. The effects of constant and linearly drifting thermal emfs (about 25 nV/hr) were eliminated by appropriately averaging the data. The difference between the junction voltages was $(V_{n1} + V_{n2}) - V_{n3} = 53 \pm 66$ pV. The standard deviation of a single datum computed from the random scatter of the data was 0.20 nV, the resolution of the null detector system. The difference in 2e/h between the two bias points was

$$(2e/h)_{V_n < 2\Delta/e} - (2e/h)_{V_n > 3\Delta/e} = 1.1 \pm 1.4 \text{ parts in } 10^8$$

Combining this result with the result for the single and series connection of junctions, we find the Josephson frequency voltage ratio is independent of the dc bias point between $V_n < 2\Delta/e$ and $V_n > 7\Delta/e$, or equivalently between n = 110 and n = 450 (for ν = 11 GHz), to within about 7 parts in 10^8. The voltage independence at high bias voltages ($V_n > 2\Delta/e$) is particularly significant because it demonstrates that the induced step voltages are not sensitive to the amplitude of the quasi-particle background current. In many of the later runs (11 through 23), the individual step numbers varied significantly from run to run. The most common ratios were either 1:1:2 or 1:1:3. However, voltages as low as 1 mV (n = 45) in one junction and as high as 8 mV (n = 360) in another were used. Thus, the step-number or voltage-bias dependence was indirectly checked at many voltages between about 1 mV and 10 mV (or step numbers from about 45 to 450) to within the overall precision of the measurements.

Taken together with the experiment of Clarke,[27] these results indicate that the Josephson frequency voltage ratio is independent of all of the important experimental parameters to a precision of a few parts in 10^8. A possible exception is our result for the temperature dependence. This will be reinvestigated in an experiment specifically designed for this purpose.

IX. CONCLUSIONS

The final result of the present work is compared with all previously published Josephson effect values of 2e/h in Fig. 30. The recent more accurate results are shown on an expanded scale in Fig. 31. Not all of these are independent: UP2, UP3, UP4, and UP5 are from successive reports on a single set of experiments, the final result being UP5. Similarly, NPL1 and NPL2 are preliminary and final results respectively of a single set of experiments. The NPL, NSL, and PTB values were expressed in terms of V_{NBS69} using conversion factors derived from linear interpolation or extrapolation of the appropriate time-dependent national volt differences obtained from the 1967[7] and 1970[59] BIPM volt comparisons, using central dates provided by BIPM.[7,59] The dates of the 2e/h values were taken to be the dates of receipt by the publisher of the first report of each experiment, i.e., Refs. 10, 13, 14 and 15. The volt differences obtained in this way were $V_{NPL69} - V_{NBS69} = 0.54$ ppm for NPL1 and NPL2, $V_{NPL69} - V_{NBS69} = 0.505$ ppm for NPL3, $V_{NSL69} - V_{NBS69} = -0.19$ ppm for NSL1, and $V_{PTB69} - V_{NBS69} = -0.54$ ppm for PTB 1.[60] The uncertainties shown in Figs. 30 and 31 are those reported by the authors, with no additional allowance for the uncertainty of the volt comparisons through BIPM. (We note in passing that the comparison of NPL2, UP7 and NSL1 shown in Fig. 1 of Ref. 13 is somewhat misleading because the three values were not converted to a common voltage scale.)

We see in Figs. 30 and 31 that the rather tiresome unanimity of the early results has yielded to some diversity of position. Using the uncertainties quoted by the authors, we find NPL3-UP8 = -0.95 ± 0.82 ppm, NSL1-UP8 = 0.44 ± 0.24 ppm and PTB1-UP8 = 0.50 ± 0.43 ppm. If we take the 0.1 ppm uncertainty suggested by BIPM for each BIPM-national-volt

transfer[59] to imply a 0.14 ppm uncertainty in the relation between any two national volts (the root sum square of two 0.1 ppm uncertainties), these become NPL3-UP8 = -0.95 ± 0.83 ppm, NSL1-UP8 = 0.44 ± 0.28 ppm,[61] and PTB1-UP8 = 0.50 ± 0.45 ppm. These differences are not necessarily cause for alarm but they are not insignificant either. We believe that they are partly and perhaps almost entirely due to discrepancies in the relations between the national volts. It has become apparent in recent years that differences between two national volts obtained indirectly via the BIPM comparisons and by direct transfer between the two national laboratories can be discrepant by an appreciable part of a ppm.[47] Discrepancies of this size could quite easily account for the 2e/h differences noted above. They also emphasize the need for an international volt maintenance system which does not rely on the physical transport of electrochemical standard cells.

It has been clear for some time that a voltage standard with extremely desirable properties could in principle be based on the ac Josephson effect. We have demonstrated in the present work that this can be done in practice with ample precision. The uncertainty we have assigned our voltage measurement system, about 0.03 ppm, represents the precision with which a drift-free and readily reproducible volt can be maintained with this system. If and when an internationally agreed upon value can be assigned 2e/h, this 0.03 ppm uncertainty then represents the presently achievable accuracy with which a common international volt or perhaps even the absolute volt can be made available. Indeed, further advances in voltage comparison technology (perhaps by a factor ten or more in precision) can be expected long before any such international agreement. We must emphasize, however, that further improvements in voltage comparison

methods cannot be expected to yield greatly improved accuracy in the determination of e/h. We have already reached a point in the present work where the accuracy with which the voltage across a Josephson device can be compared with an electrochemical voltage standard considerably exceeds the accuracy with which that standard can be maintained and transferred, especially over long periods of time. Further improvement in our knowledge of e/h from the ac Josephson effect will depend primarily on improvements in our knowledge of the various national as-maintained volts and the relations between them.

Probably the most interesting and important fundamental constant which is affected by an increase in the accuracy of e/h is the fine structure constant. In their 1969 review of the fundamental constants, Taylor, Parker and Langenberg obtained an adjusted value of α^{-1} using only data from experiments which could be analyzed without essential use of quantum electrodynamic theory.[7] This α^{-1}_{WQED} (WQED = "without quantum electrodynamic theory") depended heavily on the Josephson effect e/h determination of Parker et al.[6] and was $\alpha^{-1}_{WQED} = 137.03608 \pm 0.00026$ (1.9 ppm). In order to see the effect on α of our present more accurate value of e/h, Taylor[47] has recomputed α^{-1}_{WQED} using the same procedure and data except for two changes: (1) Our present value of 2e/h was substituted for that of Parker et al. (2) The experimental uncertainties of c (0.33 ppm) and $c^2\Omega_{ABS}/\Omega_{NBS}$ (0.20 ppm) were taken into account. In the earlier adjustment they were negligible compared with the uncertainties of other pertinent quantities, but in the new adjustment they are larger than the uncertainty in e/h and must be taken into account. The result is $\alpha^{-1}_{WQED} = 137.03611 \pm 0.00021$ (1.5 ppm).[62] Two features of the new result are obvious: First, it agrees

very well with the earlier value, a result of the fact that our new e/h agrees very well with that of Parker et al. Second, an increase in the accuracy of e/h by a factor of nearly twenty has resulted in a much smaller decrease in the uncertainty of α^{-1}_{WQED}. This is a consequence of the fact that the Parker et al. value of e/h contributed less than half of the total uncertainty in the Taylor et al. value of α^{-1}_{WQED}, so that the almost complete elimination of this contribution has a relatively small effect on the net uncertainty of α^{-1}_{WQED}. The uncertainty in α^{-1}_{WQED} is now completely dominated by the uncertainty in γ'_p (see Eq. 1). Because of this, the twenty-fold increase in accuracy of our present result does have the important consequence that any forseeable increase in the accuracy of the determination of γ'_p will be directly reflected in a corresponding decrease of the uncertainty of the fine structure constant. For purposes of comparison, we note the final recommended value of Taylor et al., $\alpha^{-1} = 137.03602 \pm 0.00021$ (1.5 ppm). Because there were apparent discrepancies among the results of the various QED experiments (e.g., determinations of electron and muon g-factors and fine and hyperfine splittings in hydrogenic atoms) which give information on α, this recommended value of α rested entirely on α_{WQED} together with a value of α derived from hydrogen hyperfine structure determinations. Recent theoretical and experimental work has largely removed these discrepancies.[63]

In summary, then, we have determined e/h using the ac Josephson effect with an accuracy approximately twenty times greater than that of the early measurements of Parker et al. Our result is in excellent agreement with the earlier result but differs somewhat from more recent accurate determinations by other workers. The intrinsic precision of our measurement is nearly two orders of

magnitude greater than that of the Parker et al. determination and establishes the basis for a practical Josephson voltage standard with significant advantages over existing electrochemical standard cell standards. The large improvement in accuracy of the present result yields a slightly more accurate indirect value of the fine structure constant, and clears the way for a significant improvement in our knowledge of the fine structure constant through more accurate determination of the proton gyromagnetic ratio.

X. ACKNOWLEDGEMENTS

We are grateful to members of the staff of the Electricity Division of the National Bureau of Standards, particularly B. N. Taylor and W. G. Eicke, for their cooperation in relating the University of Pennsylvania volt to the National Bureau of Standards volt, and for helpful discussions of the problems of voltage standard maintenance. We thank RCA for supplying evaporation masks and J. B. Gross for writing the computer programs used in analysis of the standard cell comparison data. One of us (A. D.) thanks the National Research Council for a NRC-NAS-NAE NBS Postdoctoral Research Associateship which he held during an early stage of the present experiments.

REFERENCES

* Supported by the National Science Foundation and the Advanced Research Projects Agency. This paper is based on a thesis submitted by T. F. Finnegan in partial fulfillment of the requirements for the Ph. D. degree at the University of Pennsylvania.

† Present address: National Bureau of Standards, Washington, D. C. 20234.

1. A tutorial review has recently been published by J. Clarke, Am. J. Phys. 38, 1071 (1970).

2. See, for example, B. D. Josephson, Advan. Phys. 14, 419 (1965).

3. S. Shapiro, Phys. Rev. Letters 11, 80 (1963); S. Shapiro, A. R. Janus, and S. Holly, Rev. Mod. Phys. 36, 223 (1964).

4. W. H. Parker, B. N. Taylor, and D. N. Langenberg, Phys. Rev. Letters 18, 287 (1967).

5. D. N. Langenberg, W. H. Parker, and B. N. Taylor, Proc. Third Int. Conf. on Atomic Masses, edited by R. C. Barber (University of Manitoba Press, Winnipeg, Canada, 1968), p. 439.

6. W. H. Parker, D. N. Langenberg, A. Denenstein, and B. N. Taylor, Phys. Rev. 177, 639 (1969).

7. B. N. Taylor, W. H. Parker, and D. N. Langenberg, Rev. Mod. Phys. 41, 375 (1969); reprinted as a monograph under the title, The Fundamental Constants and Quantum Electrodynamics (Academic Press, New York, 1969).

8. B. N. Taylor, W. H. Parker, D. N. Langenberg, and A. Denenstein, Metrologia 3, 89 (1967).

9. A. Denenstein, T. F. Finnegan D. N. Langenberg, W. H. Parker, and B. N. Taylor, Phys. Rev. B1, 4500 (1970).

10. B. W. Petley and K. Morris, Phys. Letters 29A, 289 (1969).

11. B. W. Petley and K. Morris, Metrologia 6, 46 (1970).

12. T. F. Finnegan, A. Denenstein, and D. N. Langenberg, Phys. Rev. Letters 24, 738 (1970).

13. I. K. Harvey, J. C. Macfarlane, and R. B. Frenkel, Phys. Rev. Letters 25, 853 (1970).

14. B. W. Petley and J. C. Gallop, Proceedings of the International Conference on Precision Measurement and Fundamental Constants, edited by D. N. Langenberg and B. N. Taylor (National Bureau of Standards Special Publication 343, U. S. Government Printing Office, Washington, D. C., 1971).

15. V. Kose, F. Melchert, H. Fack, and H.-J. Schrader, PTB-Mitt. 81, 8 (1971).

16. For a recent review of the theoretical status of the Josephson frequency-voltage relation question, see D. J. Scalapino, Proceedings of the International Conference on Precision Measurement and Fundamental Constants, edited by D. N. Langenberg and B. N. Taylor (National Bureau of Standards Special Publication 343, U.S. Government Printing Office, Washington, D. C., 1971).

17. C. N. Yang, Rev. Mod. Phys. 34, 694 (1962).

18. N. Byers and C. N. Yang, Phys. Rev. Letters 7, 46 (1961); F. Bloch, Phys. Rev. 137, 787 (1965).

19. F. Bloch, Phys. Rev. Letters 21, 1241 (1968); Phys. Rev. B2, 109 (1970).

20. K. Nordtvedt, Jr., Phys. Rev. B1, 81 (1970).

21. D. N. Langenberg and J. R. Schrieffer, Phys. Rev. B3, 1776 (1971).

22. J. B. Hartle, D. J. Scalapino, and R. L. Sugar, Phys. Rev. B3, 1778 (1971).

23. A pertinent analysis of the nature of the electrochemical potential in superconductors has been given by B. D. Josephson, Phys. Letters 16, 242 (1965).

24. M. J. Stephen, Phys. Rev. Letters 21, 1629 (1968); M. O. Scully and P. A. Lee, Phys. Rev. Letters 23, 1228 (1969).

25. D. E. McCumber, Phys. Rev. Letters 23, 1228 (1969).

26. J. Clarke, Phys. Rev. Letters 21, 1566 (1968).

27. T. F. Finnegan, A. Denenstein, D. N. Langenberg, J. C. McMenamin, D. E. Novoseller, and L. Cheng, Phys. Rev. Letters 23, 229 (1969).

28. Having emphasized above that it is actually an electrochemical potential measurement, we here and hereafter revert to the convenient if misleading term "voltage measurement". Any attempt to discuss such a measurement in detail without this term becomes clumsy in the extreme, such is the depth of its entrenchment in our technical vocabulary.

29. T. F. Finnegan and A. Denenstein, to be published; T. F. Finnegan, Ph. D. Thesis, University of Pennsylvania, 1971.

30. A. Denenstein and T. F. Finnegan, to be published; T. F. Finnegan, Ph. D. Thesis, University of Pennsylvania, 1971.

31. For a discussion of the characteristics of various types of Josephson junction devices, see the review by D. N. Langenberg in Proceedings of the International Conference on Precision Measurement and Fundamental Constants, edited by D. N. Langenberg and B. N. Taylor, (National Bureau of Standards Special

Publication 343, U. S. Government Printing Office, Washington, D. C., 1971).

32. M. J. Stephen, Phys. Rev. 182, 531 (1969).

33. V. E. Kose and D. B. Sullivan, J. Appl. Phys. 41, 169 (1970).

34. J. R. Waldram, A. B. Pippard, and J. Clarke, Phil. Trans. Roy. Soc. (London) 268, 265 (1970).

35. J. C. Swihart, J. Appl. Phys. 32, 461 (1961).

36. D. N. Langenberg, D. J. Scalapino, B. N. Taylor and R. E. Eck, Phys. Rev. Letters 15, 294 (1965); D. N. Langenberg, D. J. Scalapino, and B. N. Taylor, Proc. IEEE 54, 259 (1966).

37. T. Yamashita, M. Kunita, and Y. Onodera, J. Appl. Phys. 39, 5396 (1968).

38. W. Schroen, J. Appl. Phys. 39, 2671 (1968).

39. E. Riedel, Z. Naturforsch. 19A, 1634 (1964); N. R. Werthamer, Phys. Rev. 147, 255 (1966); D. J. Scalapino and T. M. Wu, Phys. Rev. Letters 17, 315 (1966); C. A. Hamilton and S. Shapiro, Phys. Rev. Letters 26, 426 (1971).

40. D. G. McDonald, V. E. Kose, K. M. Evenson, J. S. Wells, and J. D. Cupp, Appl. Phys. Letters 15, 121 (1969).

41. H. A. Fowler, T. J. Witt, J. Toots, P. T. Olsen, and W. Eicke, Proceedings of the International Conference on Precision Measurement and Fundamental Constants, edited by D. N. Langenberg and B. N. Taylor (National Bureau of Standards Special Publication 343, U. S. Government Printing Office, Washington, D. C., 1971).

42. This method was suggest to us by R. L. Powell, private communications.

43. W. J. Hamer, National Bureau of Standards Monograph 84, 1965.

44. E. F. Mueller and H. F. Stimson, J. Res. Nat. Bur. Std. 13, 699 (1934).

45. G. B. Jennings, private communication.

46. J. C. E. Jennings and R. J. O'Connor, J. Phys. E-J. Sci. Instr. 2, 353 (1969).

47. B. N. Taylor, private communication.

48. W. G. Eicke, private communication.

49. The thermistor resistance showed an appreciable long term drift (aging). A linear least-squares fit was made to our thermistor data, and the temperature corrections were made on the basis of the deviations of individual data points from the fitted line. The standard deviation of the points about the fitted line corresponded to 1.0×10^{-3} °C.

50. Volt Transfer Program Instructions (Electricity Division, National Bureau of Standards, 1970).

51. W. G. Eicke and B. N. Taylor, private communication.

52. F. Wenner, J. Res. Nat. Bur. Std. 25, 253 (1940).

53. B. V. Hamon, J. Sci. Instr. 31, 450 (1954).

54. J. C. Riley, IEEE Intern. Conv. Record 13, Pt. 11, 136 (1965).

55. C. H. Page, J. Res. Nat. Bur. Std. 69C, 181 (1965).

56. F. Wenner, op. cit., p. 287.

57. In addition, a small correction (less than 1%) was applied to the amplitude of the calibration signal for the particular setting of the variable dropping resistor in Fig. 15.

58. T. F. Finnegan, A. Denenstein, and D. N. Langenberg, Proceedings of

the International Conference on Precision Measurement and Fundamental Constants, edited by D. N. Langenberg and B. N. Taylor (National Bureau of Standards Special Publication 343, U. S. Government Printing Office, Washington, D. C. 1971).

59. J. Terrien, private communication.

60. An alternative procedure would have been simply to take the volt differences from the 1970 BIPM volt comparisons, $V_{NPL69} - V_{NBS69} = 0.52$ ppm, $V_{NSL69} - V_{NBS69} = -0.17$ ppm, and $V_{PTB69} - V_{NBS69} = -0.43$ ppm. We consider this procedure somewhat less desirable than the one we have used because it does not take into account the relative drifts of the various national volts. If we had used it, however, the differences between the 2e/h values would not have been significantly different from those shown in Figs. 30 and 31.

61. In a private communication, I. K. Harvey has informed us that the NSL result has been reassessed in the light of subsequent data and is now approximately 0.1 ppm less than the value quoted in Ref. 13.

62. We have quoted a value of α^{-1} simply to give an indication of how our new value of e/h would affect the conclusions of Taylor et al. (Ref. 7) if no other changes in their input data were made. However, improved values of several other quantities affecting the values of the fundamental constants have recently become available. Although the value of α^{-1} quoted here and the Taylor et al. recommended value do not differ significantly, the recommended value should be used in computations pending a new adjustment of the constants which takes into account all of the new data.

63. See, for example, S. J. Brodsky and S. D. Drell, Ann. Review of Nuc. Sci. 20, 147 (1970).

Table I - Sources of uncertainty in e/h associated with the Series-Parallel Comparator.

		Uncertainty (1σ) Parts in 10^8
(a)	Random uncertainty of the mean	1
(b)	Main resistor mismatch	0.4
(c)	Fan resistor mismatch	1
(d)	Transfer resistances of tetrahedral junctions	0.4
(e)	Main resistor heating effects	2
(f)	Comparator temperature stability	0.3
(g)	Working current stability	1
(h)	Calibrating signal accuracy	1
(i)	Leakage resistances	1
(j)	Dielectric polarization	0.2
(k)	Effects of thermal emfs	0.5
	RSS Total	3.1

Table II - Sources of uncertainty in e/h associated with the Cascaded-Interchange Comparator.

		Uncertainty (1σ) Parts in 10^8
(a)	Random uncertainty of the mean (measurement and calibration)	2
(b)	Switch and power supply variations during calibration	2
(c)	Trimmer lead resistance	0.7
(d)	Comparator temperature stability	0.3
(e)	Working current stability	1
(f)	Calibrating signal accuracy	0.5
(g)	Leakage resistances	0.4
(h)	Dielectric polarization	0.2
(i)	Effects of thermal emfs	0.5
	RSS Total	3.2

Table III - Sources of final uncertainty (1σ)

		Uncertainty Parts in 10^8
1. Measurement uncertainty		
(a) Frequency measurement and stability	1	
(b) Voltage comparison	3.1	
(c) Effects of possible nonvertical steps	0.4	
RSS Subtotal		3.3
2. Short term local volt stability		5
3. Transfer to NBS Volt		11
RSS Total		12

FIGURE CAPTIONS

Fig. 1 I-V characteristics of a Pb-Pb oxide-Pb tunnel junction. (a) Vertical scale 2.5 mA/cm, horizontal scale 1 mV/cm; (b) Same characteristic with vertical scale 10 mA/cm, horizontal scale 5 mV/cm; (c) 11 GHz microwave power applied, same scales as (b); (d) Expanded portion of (c), vertical scale 50 μA/cm, horizontal scale 25 μV/cm. The arrow indicates an induced step at about 10.2 mV corresponding to n = 450. This voltage is also indicated by arrows in (b) and (c). The magnetic field was $\lesssim$ 1 mG.

Fig. 2 Josephson device geometry. The cross-hatched region indicates the first evaporated film with an oxide insulating barrier. Eight Josephson junctions are formed by the overlap of the second film on the first film and oxide barrier at the top of the figure.

Fig. 3 Waveguide holder with Josephson device in place. Some of the bias leads have been omitted for clarity.

Fig. 4 Block diagram of microwave generation and frequency measurement system.

Fig. 5 I-V characteristic display circuitry, dc bias circuitry, and wiring of Josephson device.

Fig. 6 Individual junction dc bias unit.

Fig. 7 dc amplifier for junction voltage display.

Fig. 8 Block diagram of the standard cell comparison system.

Fig. 9 Standard cell comparison residuals.

Fig. 10 Comparison data for two standard cells used as working standards during e/h runs.

Fig. 11 Standard cell comparison data for the group mean difference $\overline{A} - \overline{B}$. The solid points are from comparisons made on days of e/h runs.

Fig. 12 NBS calibration data for Groups A and D. The measurements were made with respect to the U.S. Secondary Reference Group using the procedures of the NBS Volt Transfer Program. The error bars indicate random error only. The dashed lines indicate the final NBS-assigned means.

Fig. 13 Standard cell comparison data for the group mean difference $\overline{A} - \overline{D}$ obtained at the University of Pennsylvania.

Fig. 14 Basic circuit of 1 V:10 mV voltage comparison system. The voltage comparator instrument includes all elements inside the dashed line. ND stands for "null detector."

Fig. 15 Simplified circuit diagram of the series-parallel voltage comparator.

Fig. 16 Simplified circuit diagram of the cascaded-interchange voltage comparator in the measurement mode.

Fig. 17 Simplified circuit diagram of the cascaded-interchange voltage comparator in the calibration mode.

Fig. 18 Block diagram of the dc measurement system.

Fig. 19 Section of typical recorded data showing Josephson device and standard cell balance analysis. The Josephson device balance is shown in the lower portion of the figure. The "+GJ" and "-GJ" indicate the relative polarity of the null detector (galvanometer switch). The calibrating signal labelled "+MS" was introduced midway through the balance. The standard cell balance is shown in the upper part of the figure. The "+GS" and "-GS" indicate the relative polarity of the null detector and "+MS" again indicates the calibrating signal.

Fig. 20 Typical equivalent standard cell Josephson frequency F_S data for three later runs.

Fig. 21 Equivalent standard cell Josephson frequency F_S for the group mean $\overline{A}$, versus time.

Fig. 22 Equivalent standard cell Josephson frequencies F_S for standard cells A1 and A2, versus time.

Fig. 23 Equivalent standard cell Josephson frequencies F_S for standard cells A3 and A4, versus time.

Fig. 24 Equivalent standard cell Josephson frequencies F_S for standard cells A5 and A6, versus time.

Fig. 25 Equivalent standard cell Josephson frequency F_S for the group mean $\overline{B}$, versus time.

Fig. 26 Equivalent standard cell Josephson frequencies F_S for standard cells B1, B2, and B3, versus time. The ordinate scale indicated is that for B2; the B1 points have been displaced upward by 0.00035 THz, and the B3 points have been displaced upward by 0.00050 THz.

Fig. 27 Equivalent standard cell Josephson frequencies F_S for standard cells C4, C5, and C6, versus time.

Fig. 28 Deviations of the data of Fig. 27 from the least-squares fitted lines.

Fig. 29 Comparison of equivalent standard cell Josephson frequency F_S using both the series-parallel comparator (SPC) and the cascaded-interchange comparator (CIC). The time scales indicate elapsed time during each run.

Fig. 30 Comparison of present result with published Josephson effect values of 2e/h. All values have been expressed in terms of V_{NBS69} using the results of the 1967 and 1970 international volt comparisons(see text for details). The sources are: UP1, D. N. Langenberg, W. H. Parker, and B. N. Taylor, Phys. Rev. 150, 186 (1966); UP2, Ref. 4; UP3, Ref. 8; UP4, Ref. 5; UP5, Ref. 6; NPL1, Ref. 10; NPL2, Ref. 11; UP6, Ref. 9; UP7, Ref. 12; NPL3, Ref. 14; NSL1, Ref. 13; PTB1, Ref. 15; UP8, present work.

Fig. 31 Comparison of the recent more accurate values of 2e/h of Fig. 30 on an expanded scale.

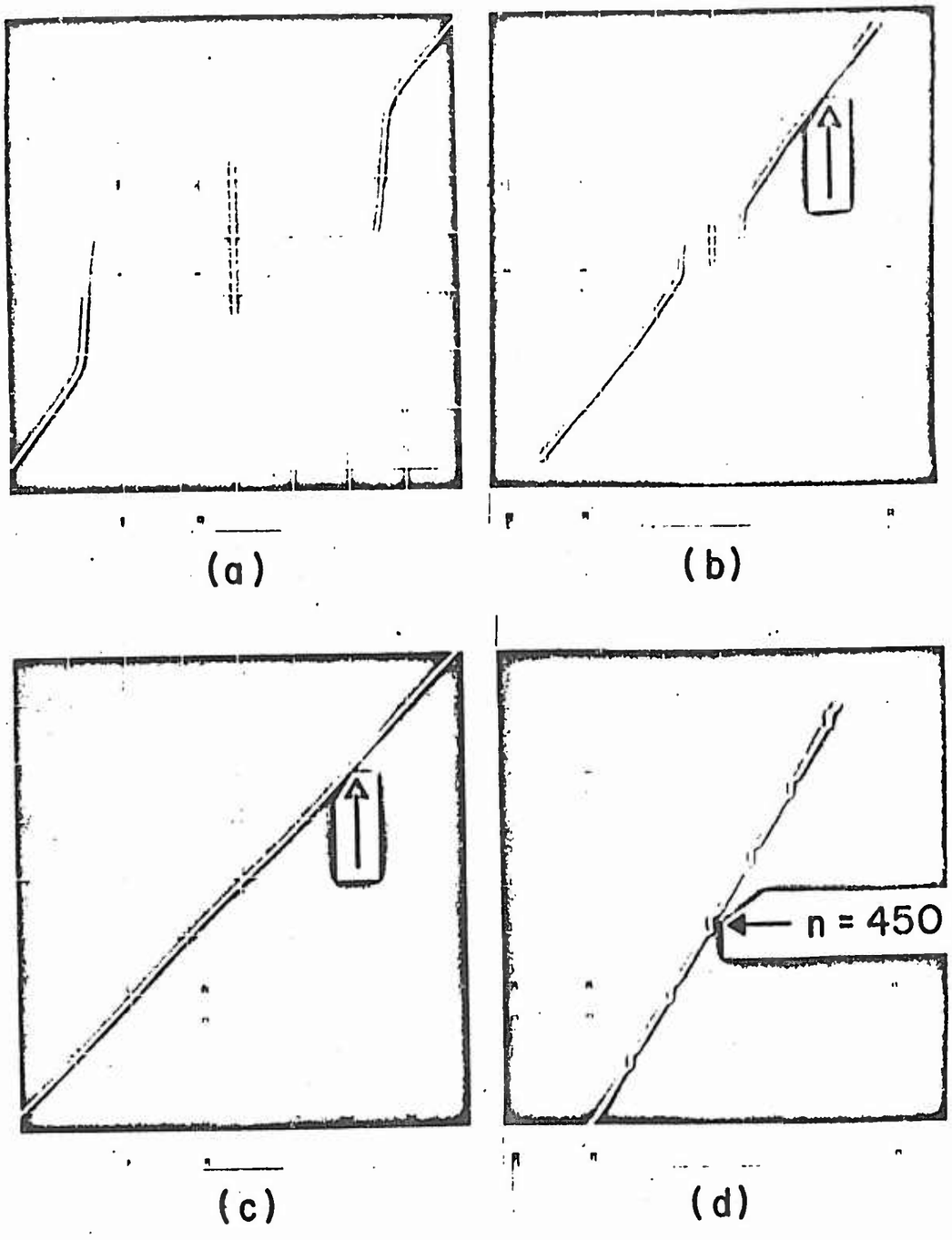

Fig. 1

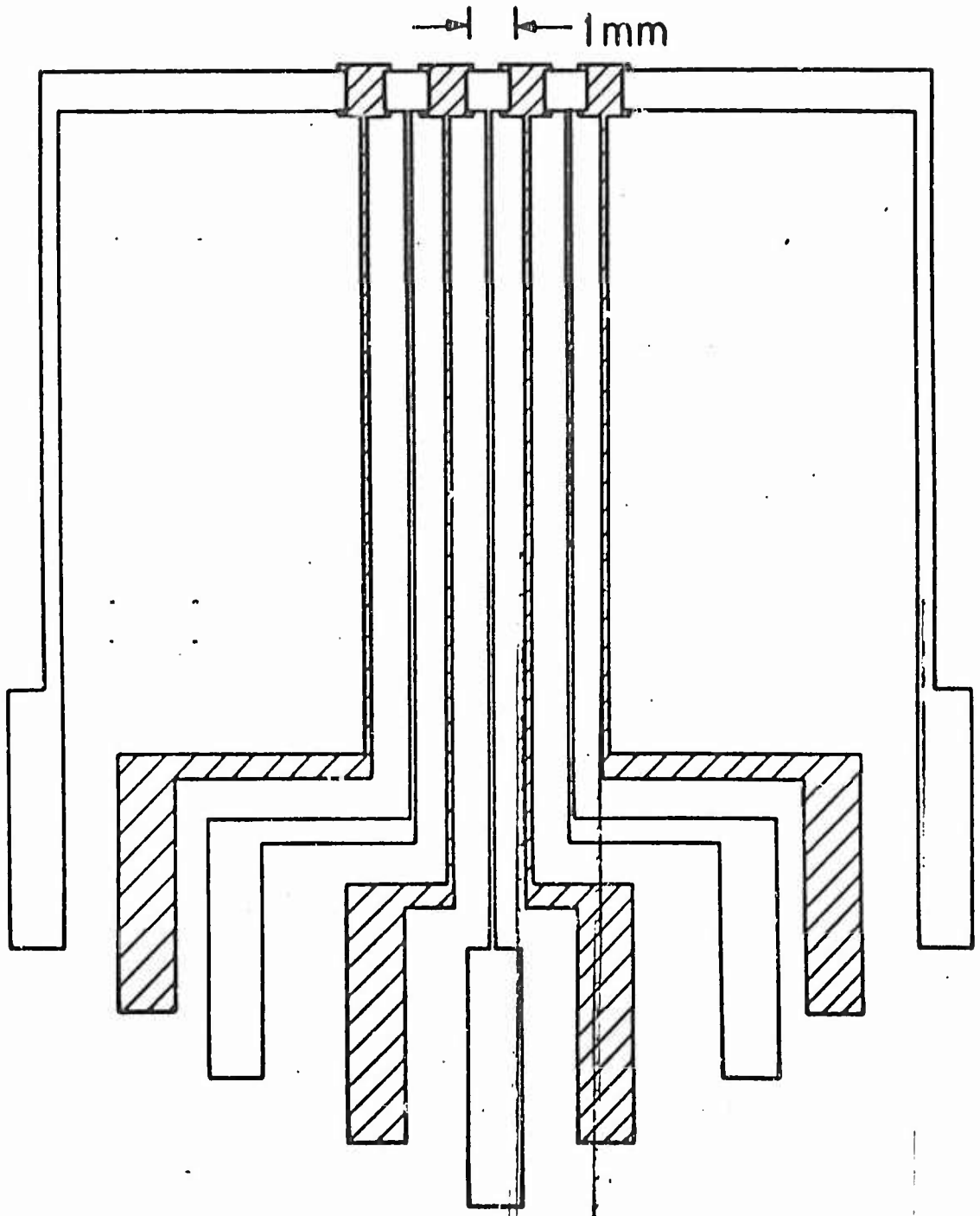

Fig. 2

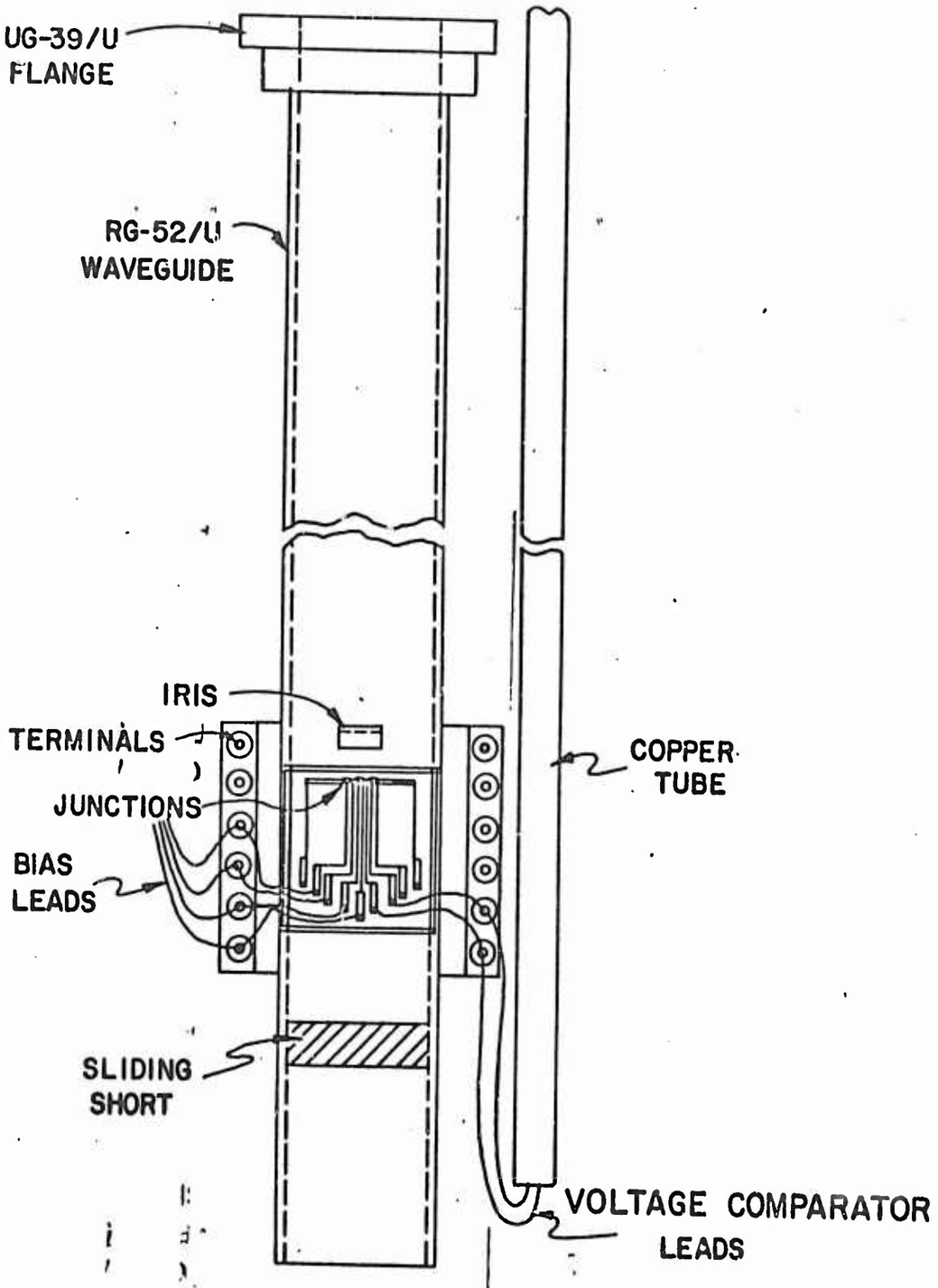
UG-39/U
FLANGE
RG-52/U
WAVEGUIDE
IRIS
TERMINALS
JUNCTIONS
BIAS
LEADS
COPPER
TUBE
SLIDING
SHORT
VOLTAGE COMPARATOR
LEADS

Fig. 3

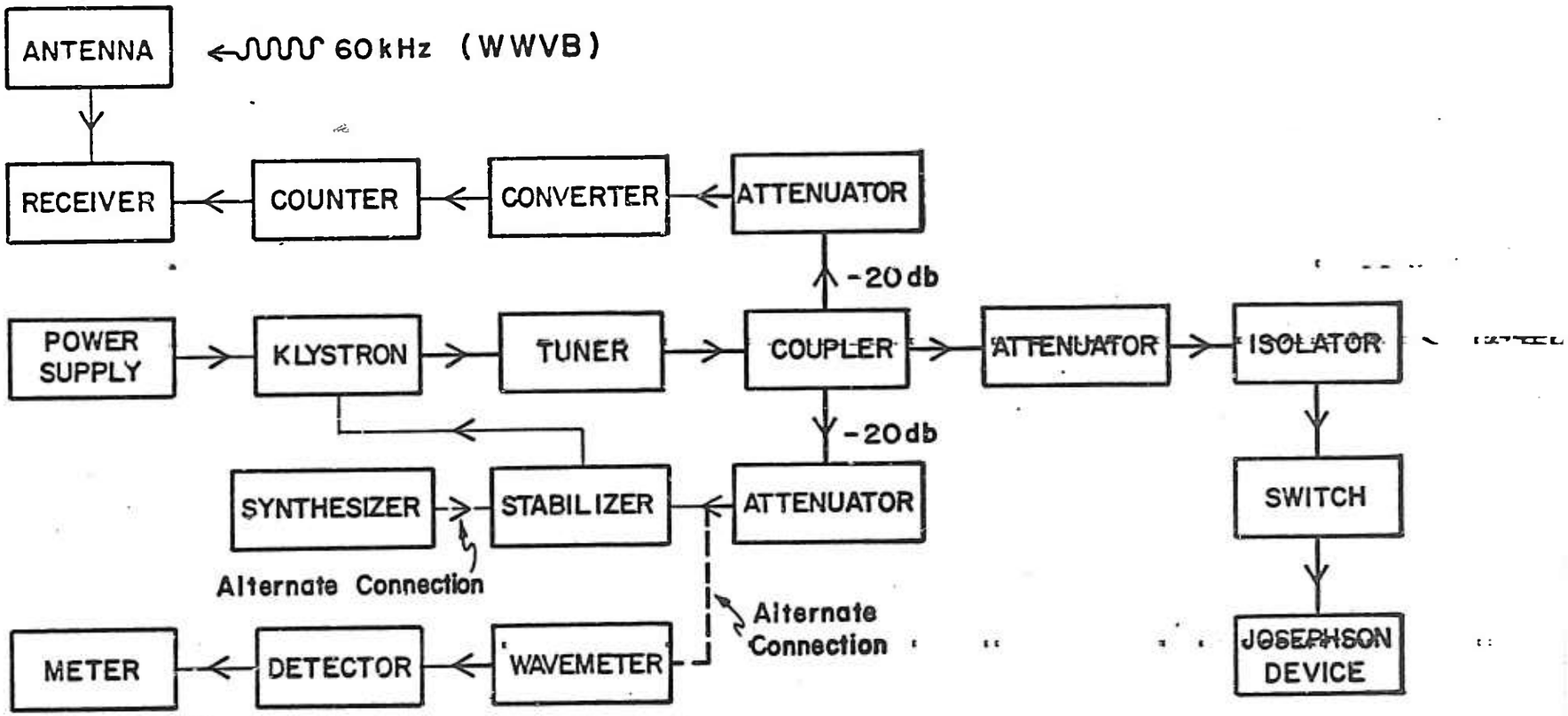
ANTENNA
60 kHz (WWVB)
RECEIVER
COUNTER
CONVERTER
ATTENUATOR
-20 db
POWER SUPPLY
KLYSTRON
TUNER
COUPLER
ATTENUATOR
ISOLATOR
-20 db
SYNTHESIZER
STABILIZER
ATTENUATOR
SWITCH
Alternate Connection
Alternate Connection
METER
DETECTOR
WAVEMETER
JOSEPHSON DEVICE

Fig. 4

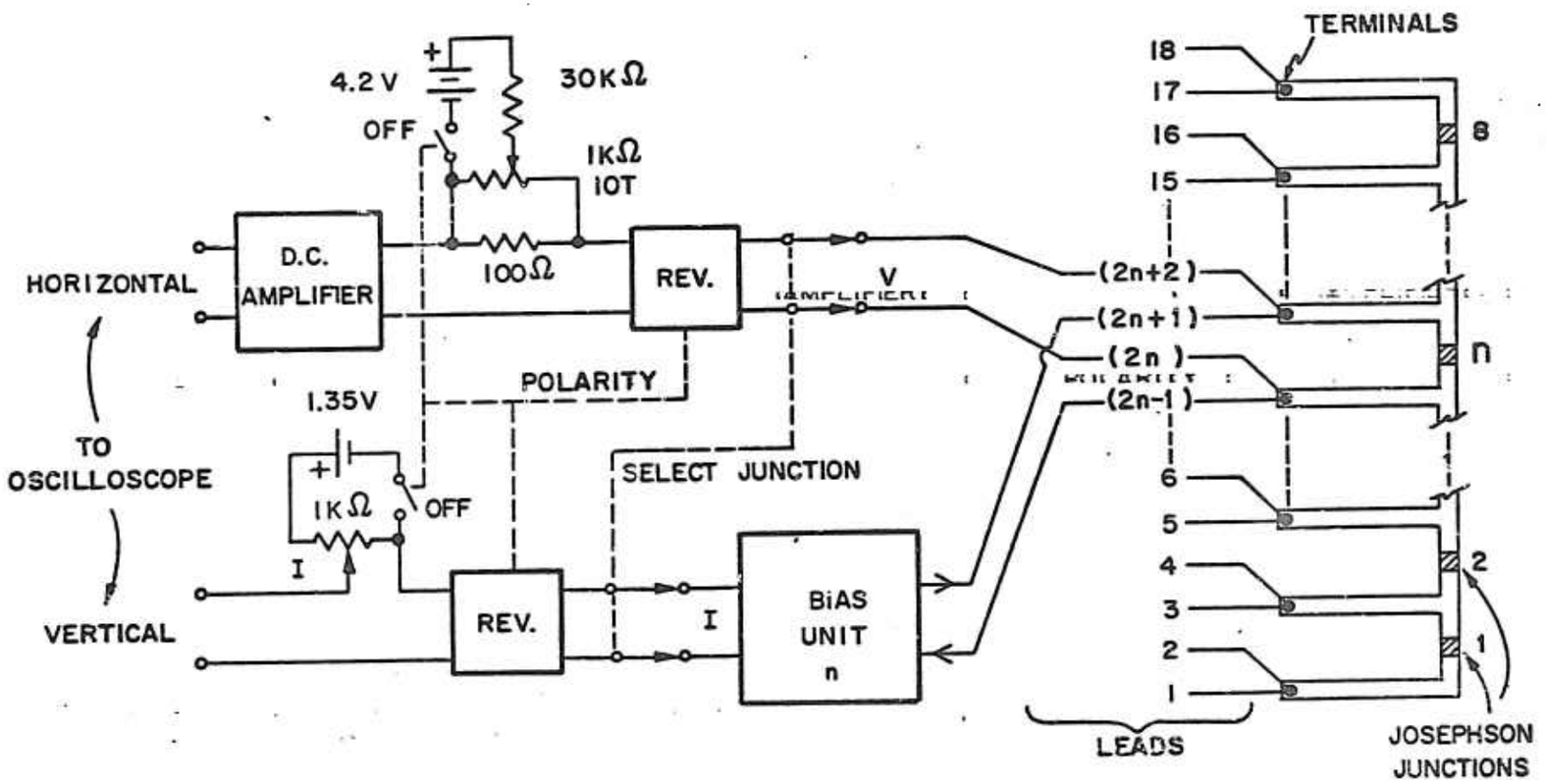
4.2 V
30KΩ
OFF
1KΩ
10T
100Ω
HORIZONTAL
D.C.
AMPLIFIER
REV.
V
POLARITY
1.35V
TO
OSCILLOSCOPE
1KΩ
OFF
I
SELECT JUNCTION
VERTICAL
REV.
I
BIAS
UNIT
n
TERMINALS
18
17
16
15
8
(2n+2)
(2n+1)
(2n)
(2n-1)
n
6
5
4
3
2
1
2
1
LEADS
JOSEPHSON
JUNCTIONS

Fig. 5

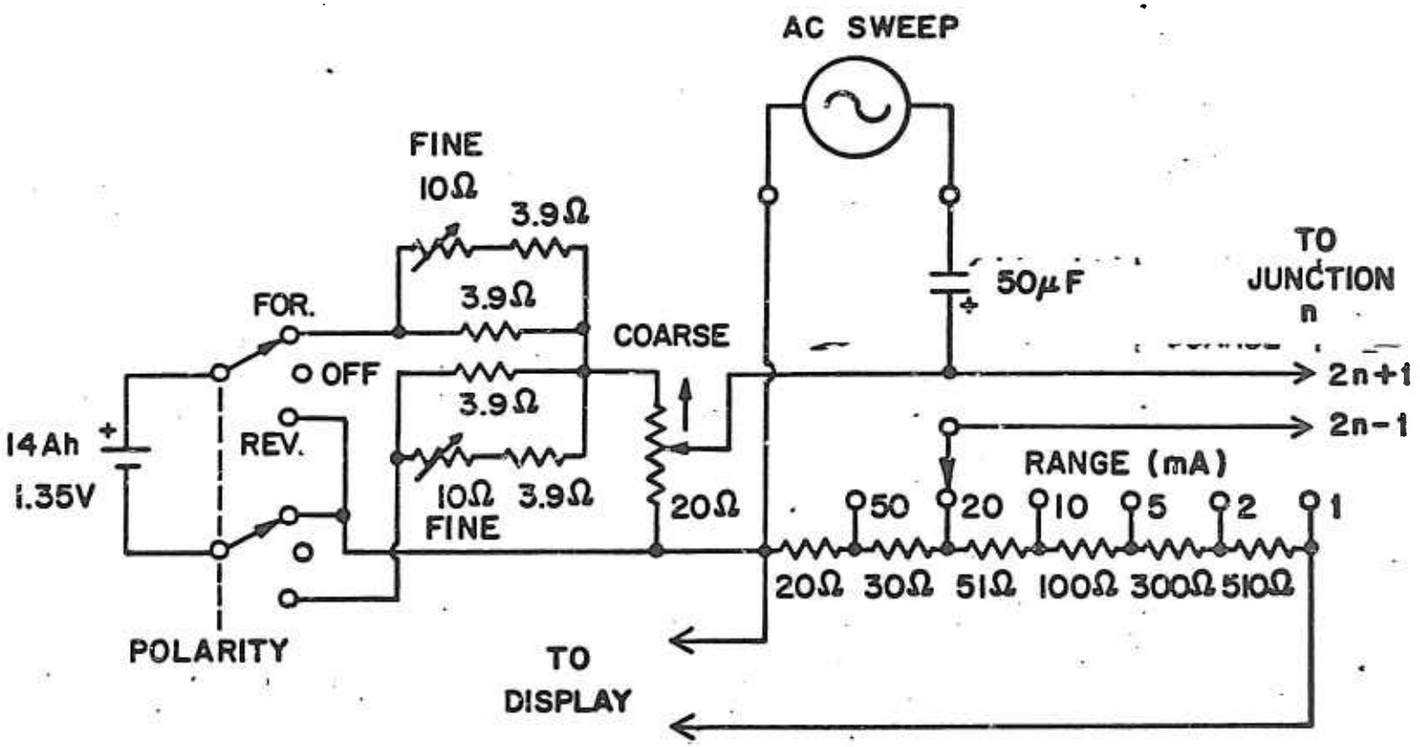
AC SWEEP
FINE
10Ω
3.9Ω
3.9Ω
FOR.
OFF
REV.
3.9Ω
10Ω 3.9Ω
FINE
COARSE
20Ω
50μF
TO
JUNCTION
n
2n+1
2n-1
14Ah
1.35V
RANGE (mA)
50 20 10 5 2 1
20Ω 30Ω 51Ω 100Ω 300Ω 510Ω
POLARITY
TO
DISPLAY

Fig. 6

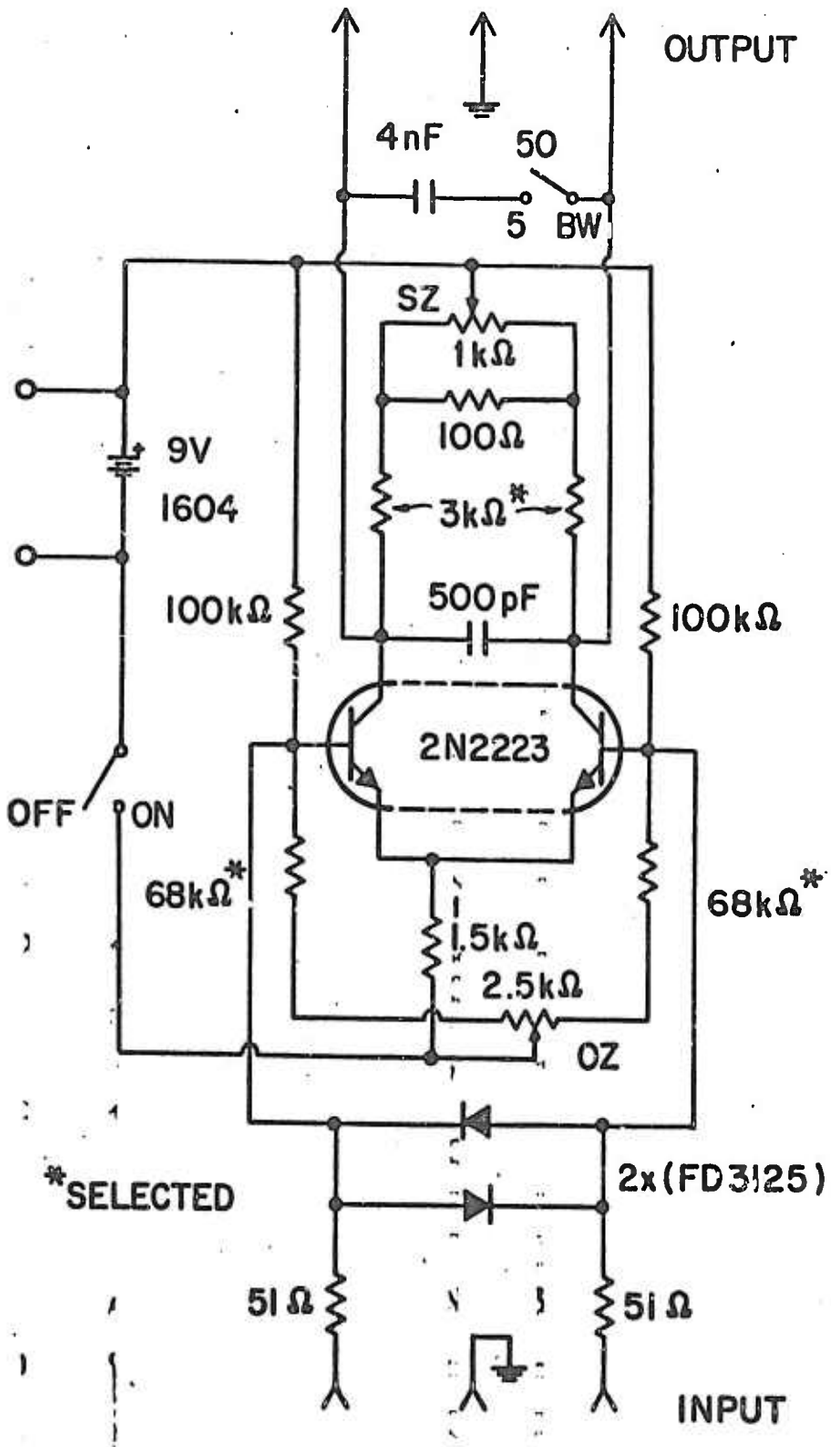
OUTPUT
4nF
50
5
BW
SZ
1kΩ
100Ω
3kΩ*
9V
1604
100kΩ
500pF
100kΩ
2N2223
OFF
ON
68kΩ*
68kΩ*
1.5kΩ
2.5kΩ
OZ
*SELECTED
2x(FD3125)
51Ω
51Ω
INPUT

Fig. 7

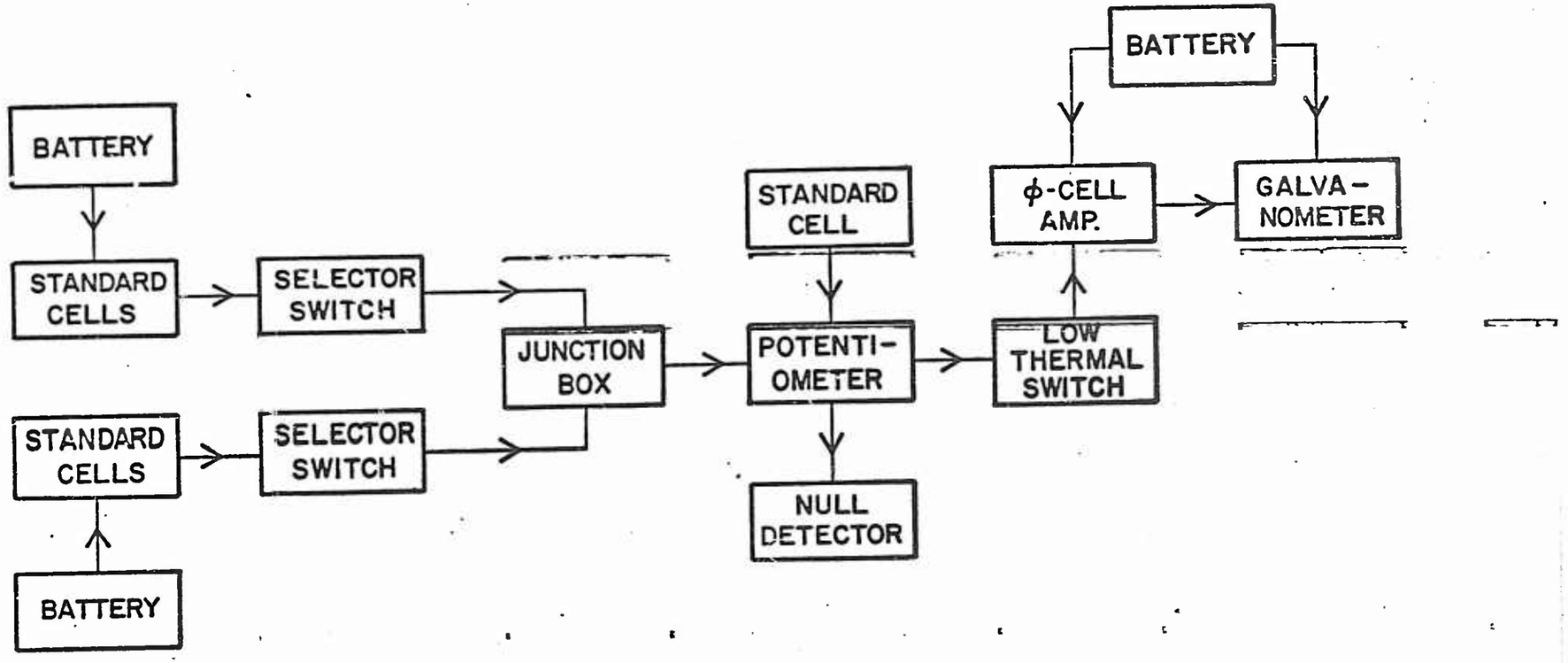
BATTERY
STANDARD CELLS
SELECTOR SWITCH
STANDARD CELLS
SELECTOR SWITCH
BATTERY
JUNCTION BOX
STANDARD CELL
POTENTI-OMETER
NULL DETECTOR
BATTERY
ϕ-CELL AMP.
LOW THERMAL SWITCH
GALVA-NOMETER

Fig. 8

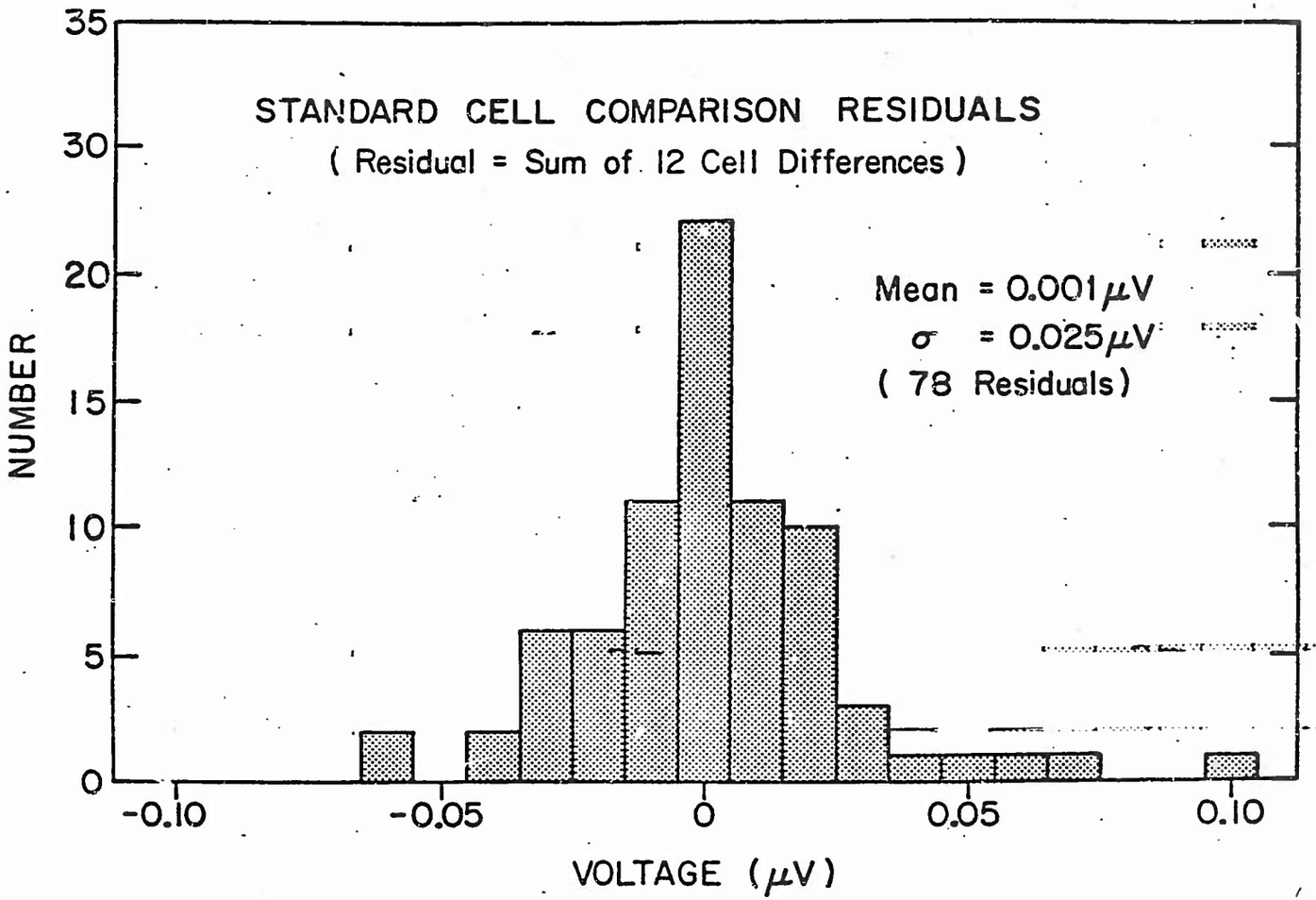
STANDARD CELL COMPARISON RESIDUALS
(Residual = Sum of 12 Cell Differences)
Mean = 0.001μV
σ = 0.025μV
(78 Residuals)
NUMBER
VOLTAGE (μV)
35
30
20
15
10
5
0
-0.10
-0.05
0
0.05
0.10

Fig. 9

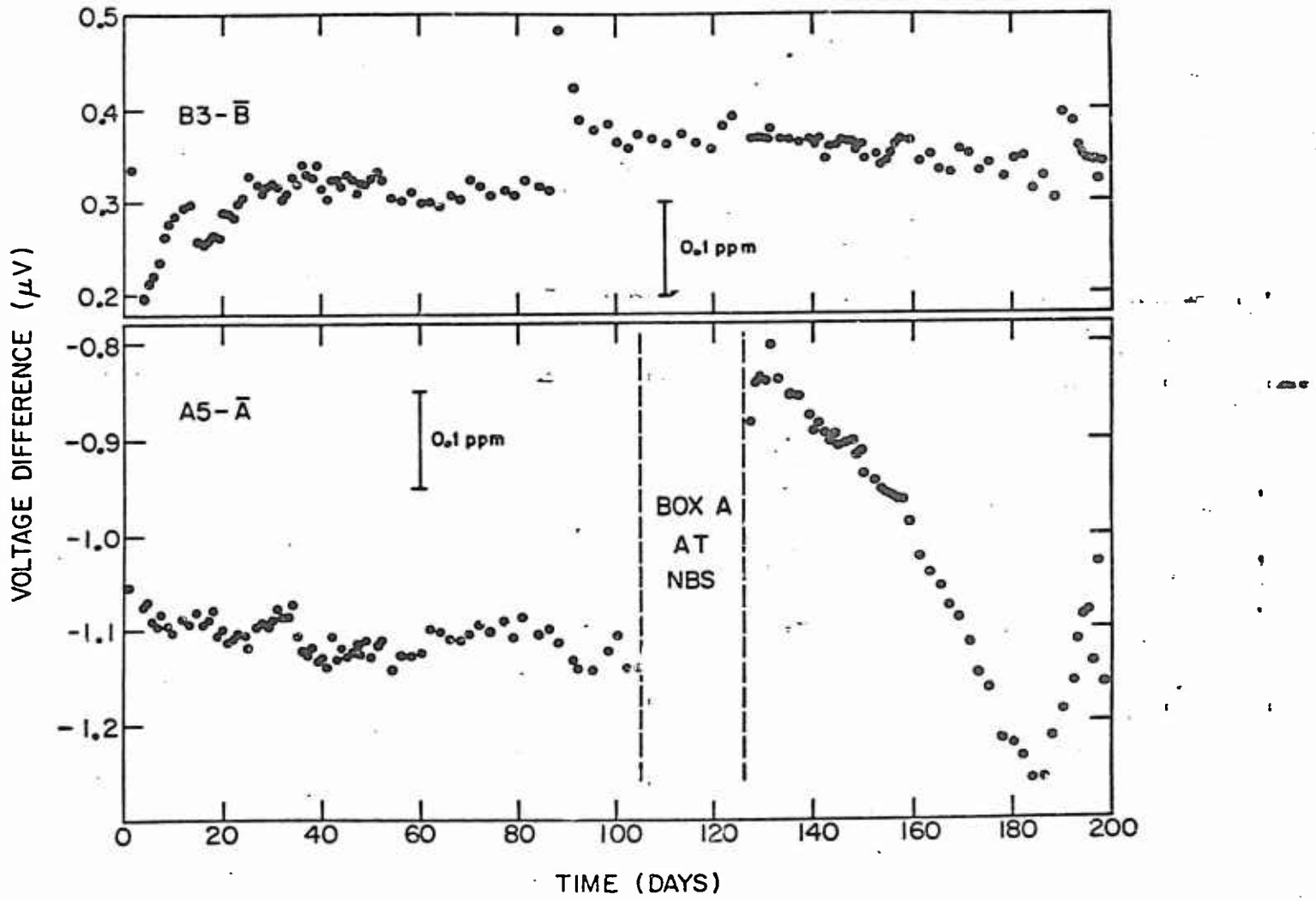
0.5
0.4
0.3
0.2
B3-B̄
0.1 ppm
-0.8
-0.9
-1.0
-1.1
-1.2
A5-Ā
0.1 ppm
BOX A
AT
NBS
VOLTAGE DIFFERENCE (μV)
0
20
40
60
80
100
120
140
160
180
200
TIME (DAYS)

Fig. 10

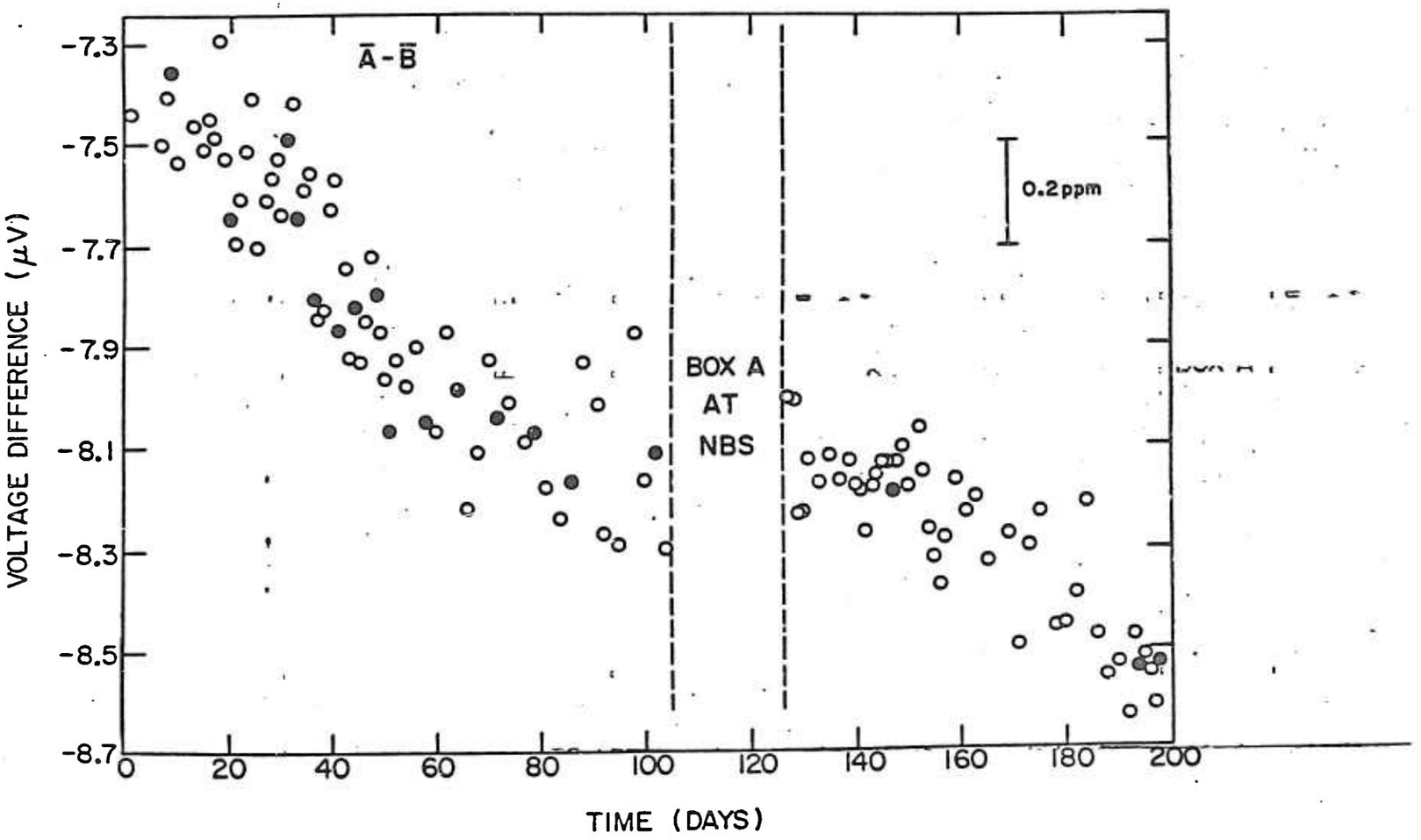
Ā-B̄
0.2ppm
BOX A
AT
NBS
VOLTAGE DIFFERENCE (μV)
-7.3
-7.5
-7.7
-7.9
-8.1
-8.3
-8.5
-8.7
0
20
40
60
80
100
120
140
160
180
200
TIME (DAYS)

Fig. 11

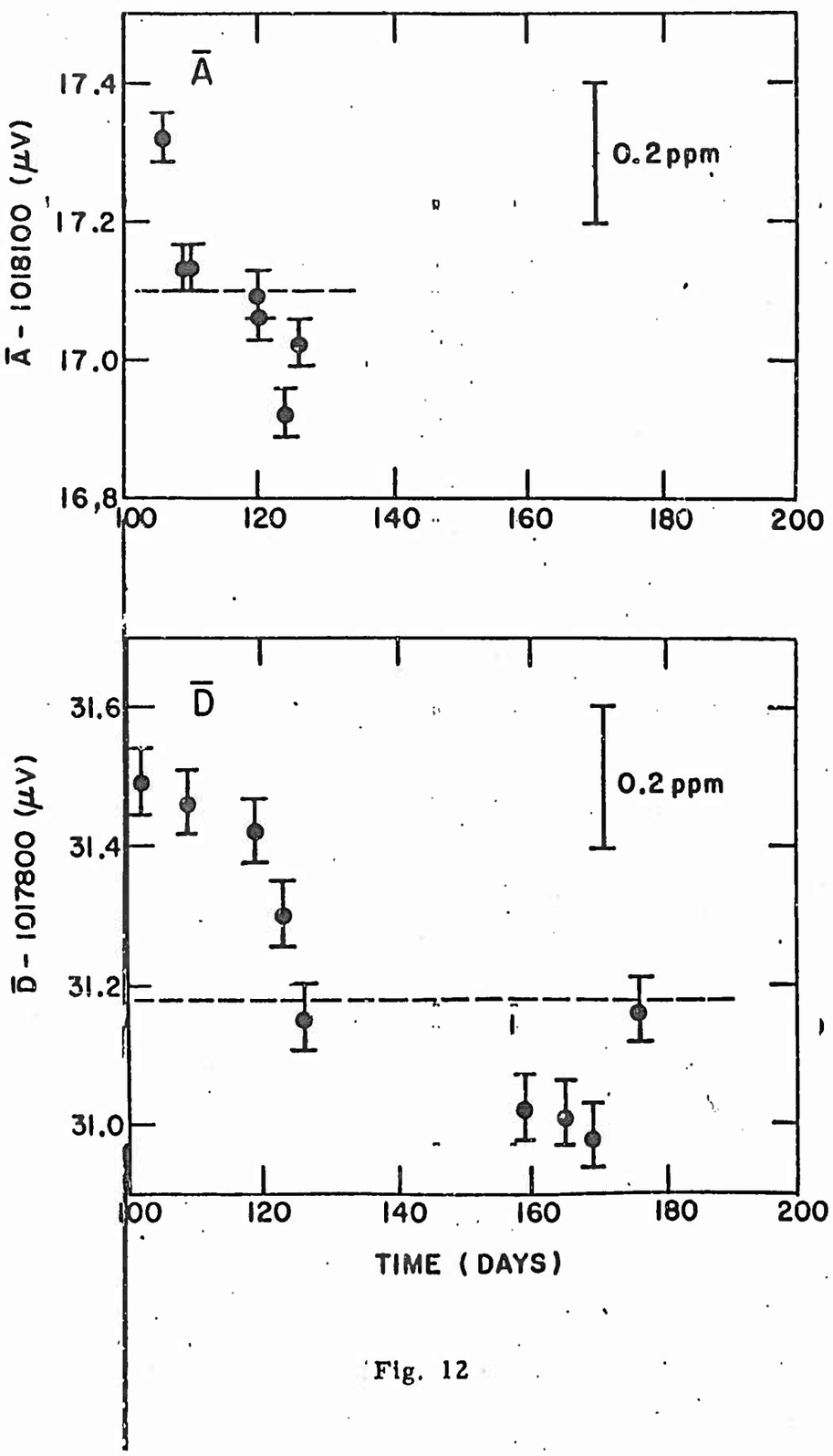
Ā
17.4
17.2
17.0
16.8
Ā - 1018100 (μV)
0.2 ppm
100
120
140
160
180
200
D̄
31.6
31.4
31.2
31.0
D̄ - 1017800 (μV)
0.2 ppm
TIME (DAYS)

Fig. 12

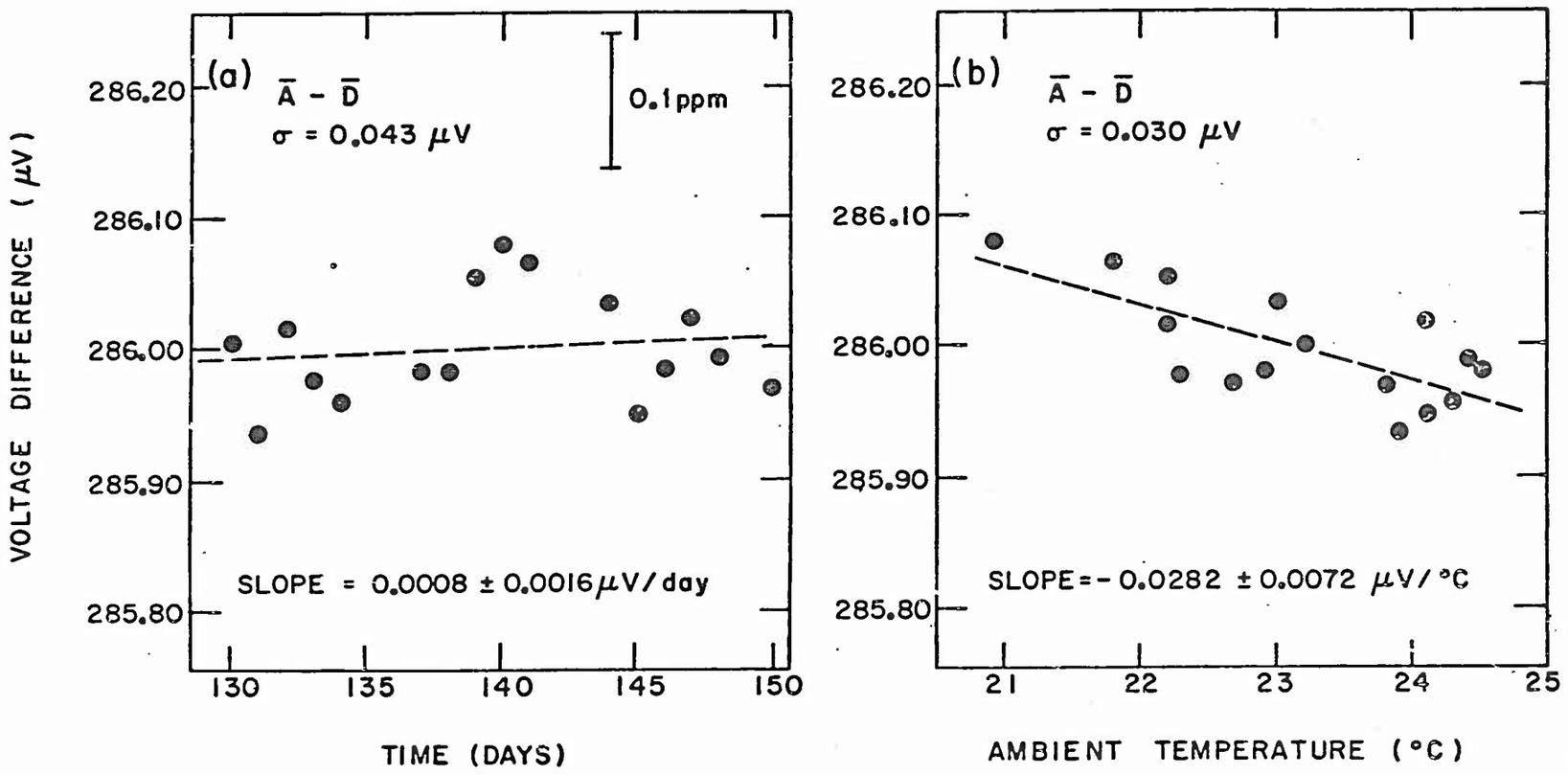
(a)
$\bar{A} - \bar{D}$
σ = 0.043 μV
0.1ppm
SLOPE = 0.0008 ± 0.0016μV/day
VOLTAGE DIFFERENCE (μV)
286.20
286.10
286.00
285.90
285.80
130
135
140
145
150
TIME (DAYS)
(b)
$\bar{A} - \bar{D}$
σ = 0.030 μV
SLOPE = - 0.0282 ± 0.0072 μV/°C
286.20
286.10
286.00
285.90
285.80
21
22
23
24
25
AMBIENT TEMPERATURE (°C)

Fig. 13,

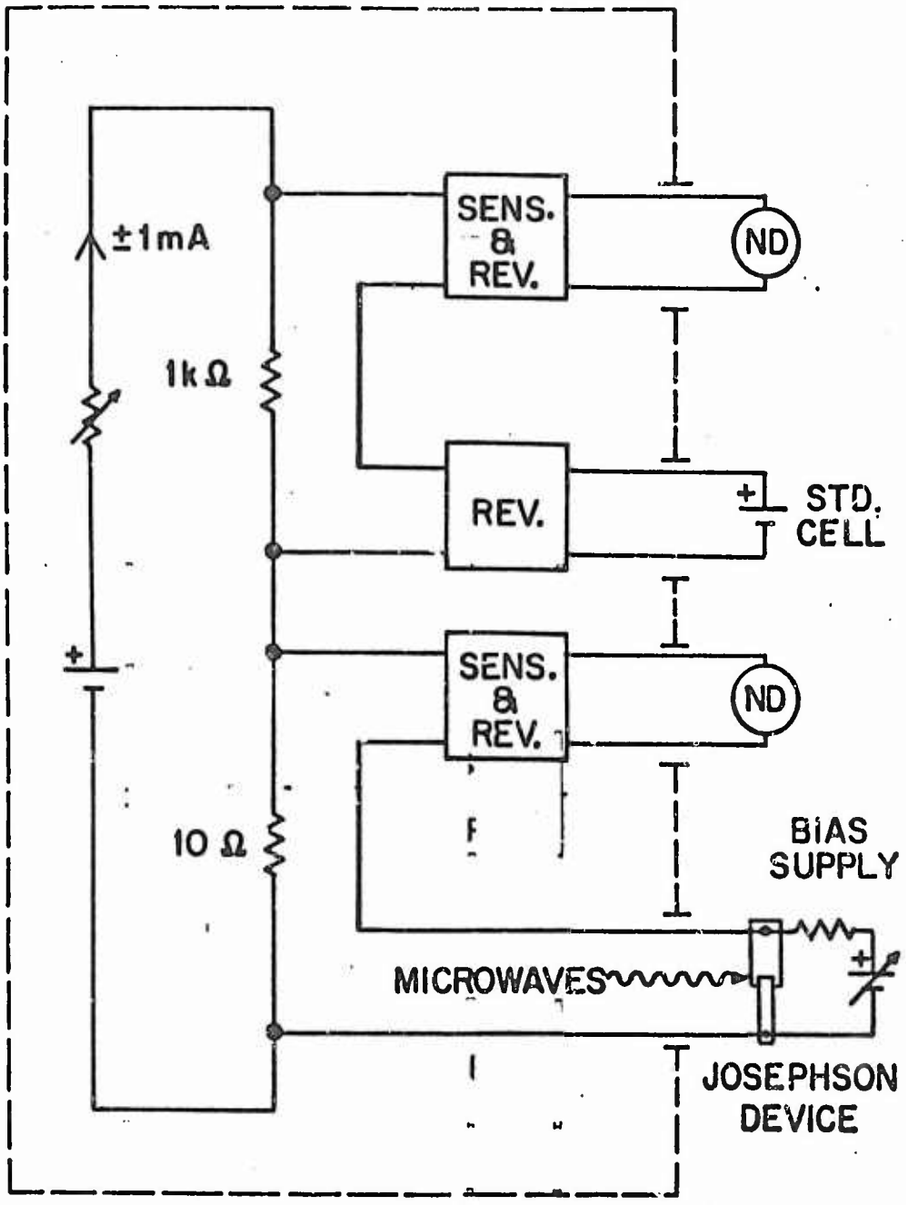
±1mA
1kΩ
10 Ω
SENS. & REV.
ND
REV.
STD. CELL
SENS. & REV.
ND
BIAS SUPPLY
MICROWAVES
JOSEPHSON DEVICE

Fig. 14

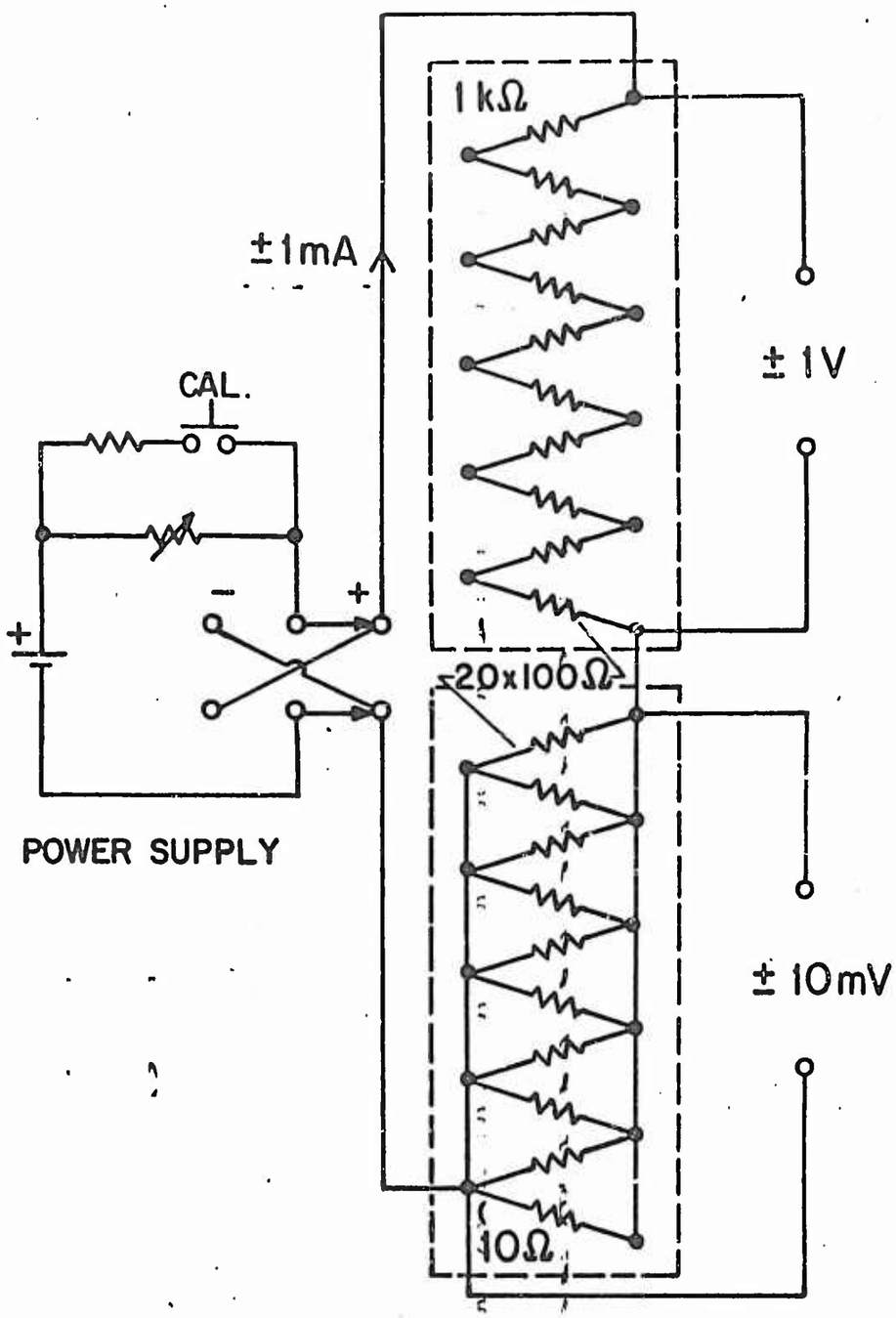

Fig. 15

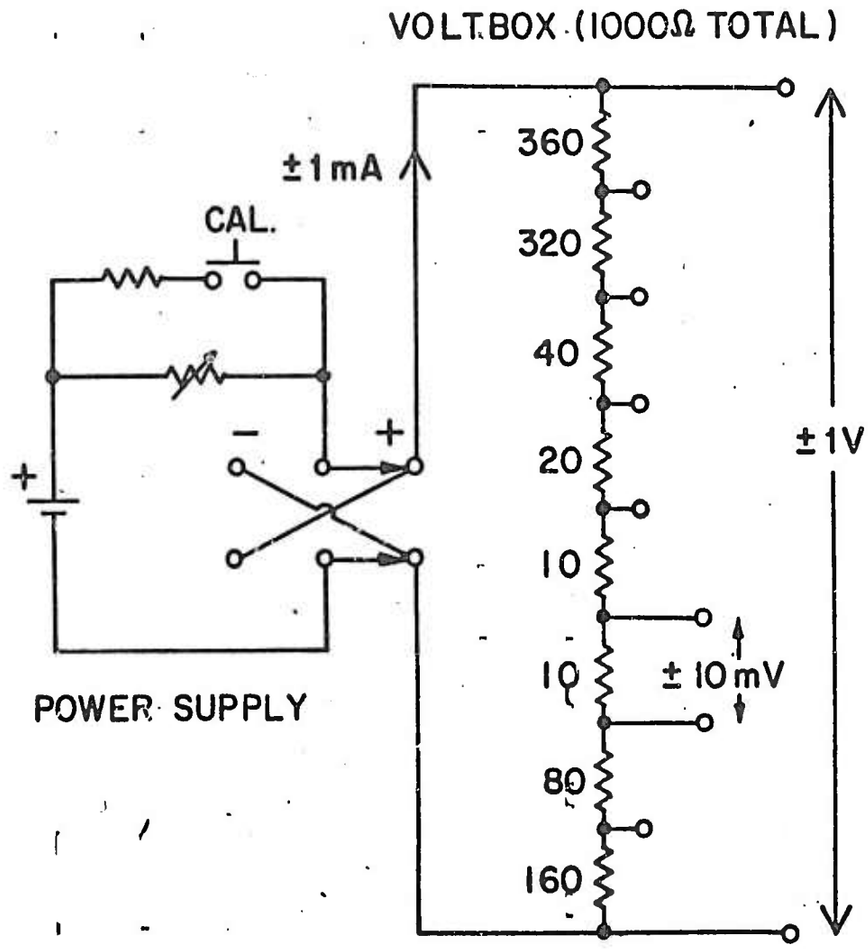
VOLTBOX (1000Ω TOTAL)
±1mA
CAL.
360
320
40
20
10
10
80
160
±1V
±10mV
POWER SUPPLY

Fig. 16

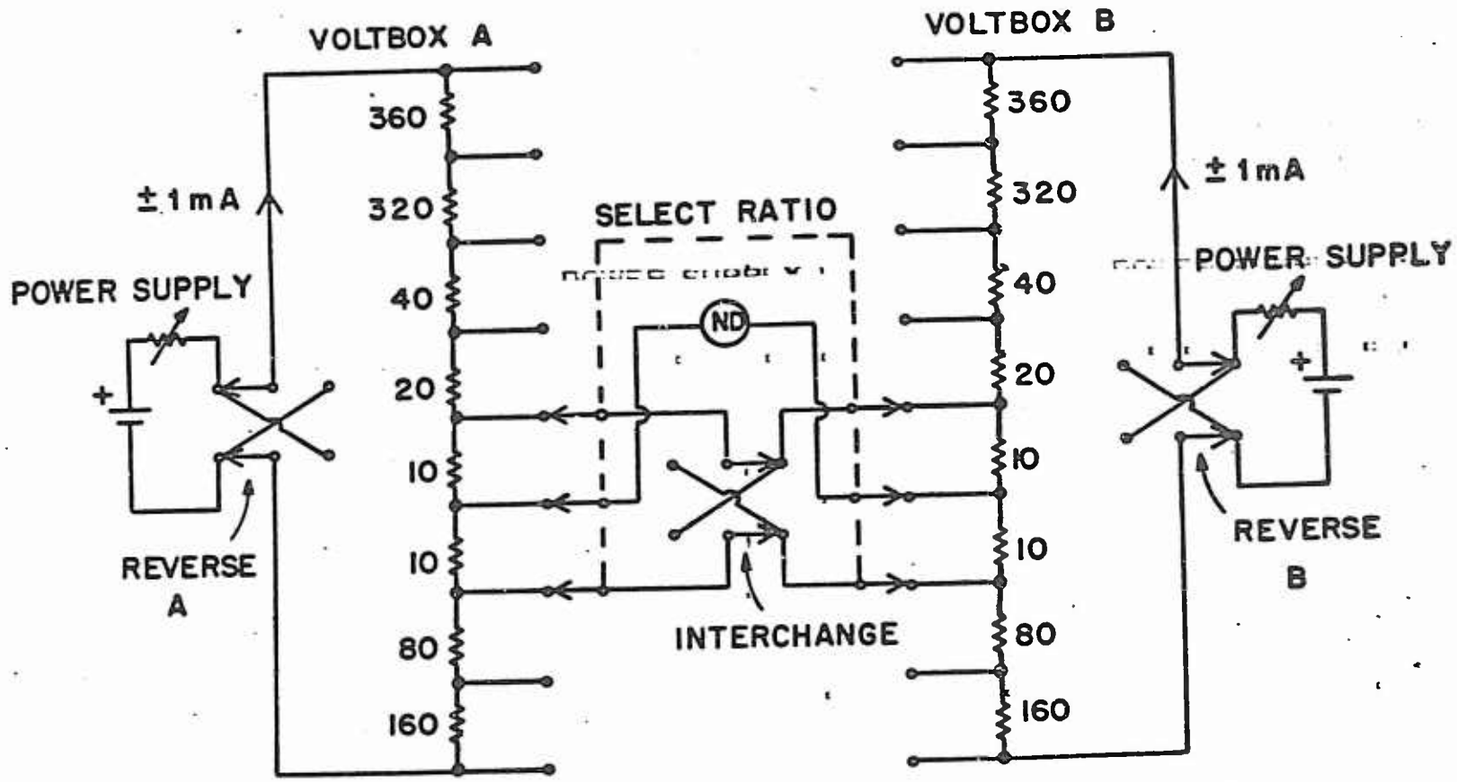
VOLTBOX A
VOLTBOX B
360
320
40
20
10
10
80
160
±1mA
±1mA
SELECT RATIO
POWER SUPPLY
POWER SUPPLY
ND
REVERSE
A
REVERSE
B
INTERCHANGE

Fig. 17

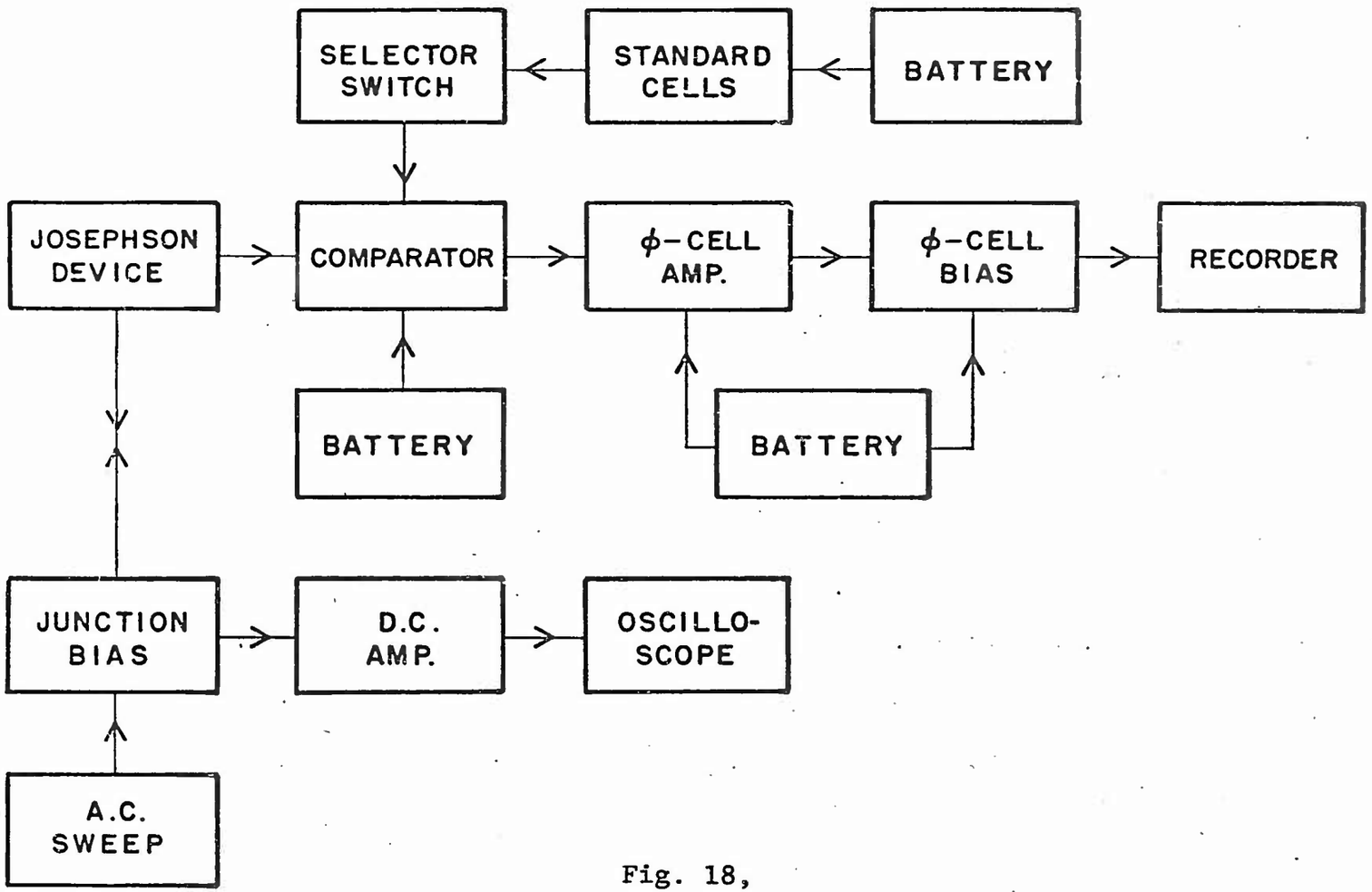
SELECTOR SWITCH
STANDARD CELLS
BATTERY
JOSEPHSON DEVICE
COMPARATOR
ϕ-CELL AMP.
ϕ-CELL BIAS
RECORDER
BATTERY
BATTERY
JUNCTION BIAS
D.C. AMP.
OSCILLO-SCOPE
A.C. SWEEP

Fig. 18,

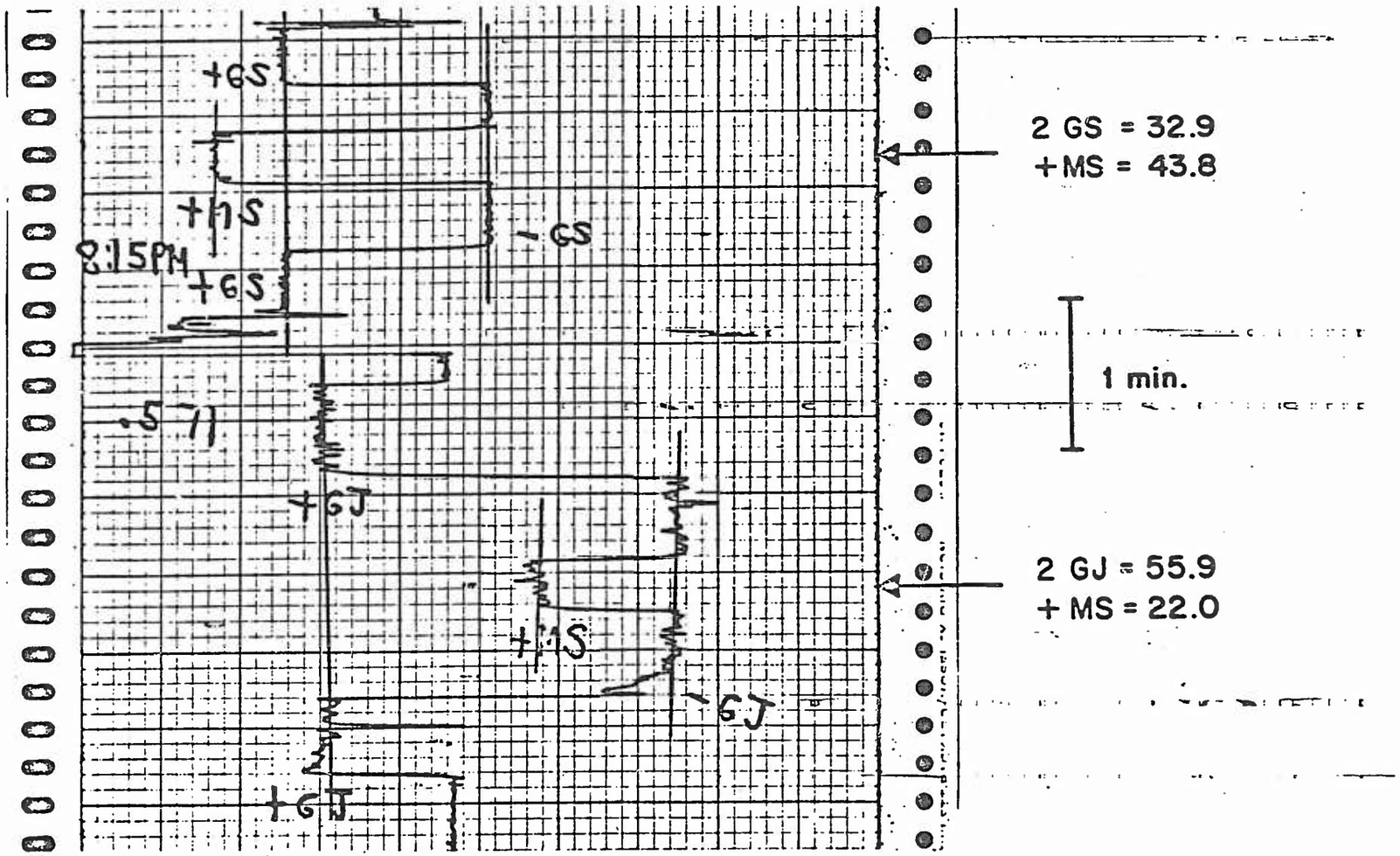

Fig. 19

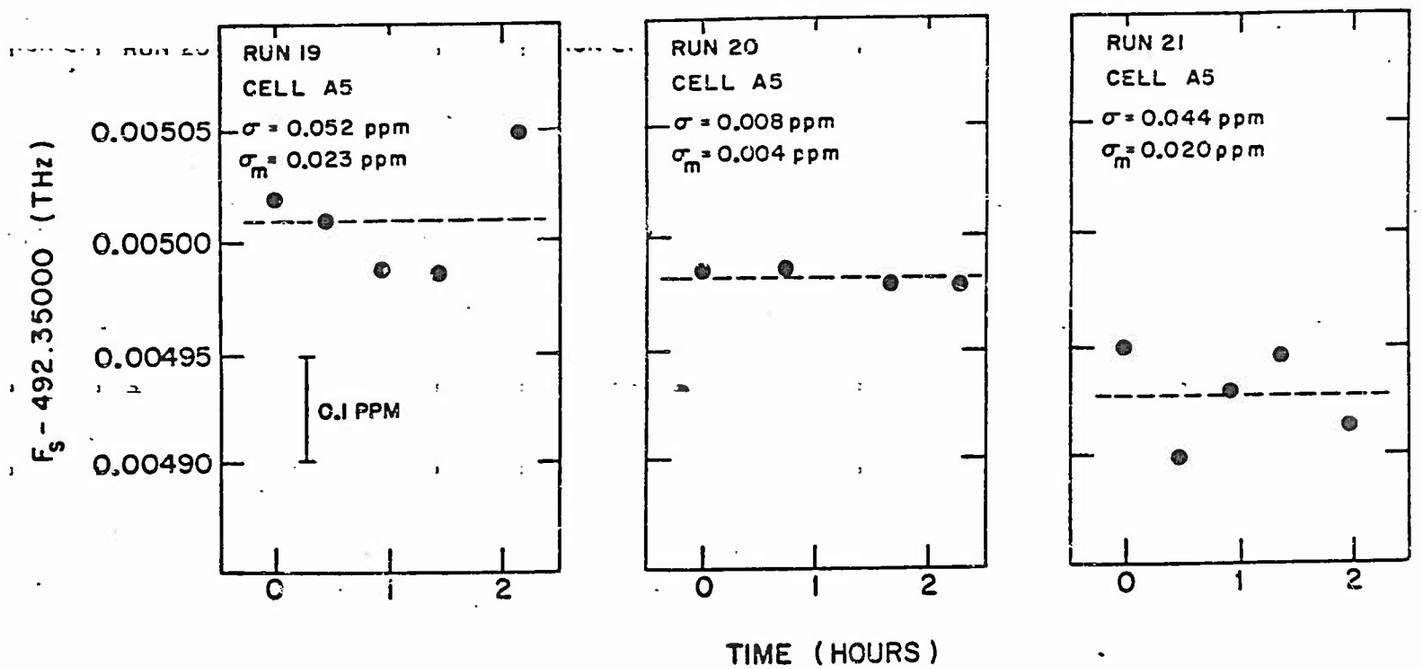
RUN 19
CELL A5
σ = 0.052 ppm
σm = 0.023 ppm
RUN 20
CELL A5
σ = 0.008 ppm
σm = 0.004 ppm
RUN 21
CELL A5
σ = 0.044 ppm
σm = 0.020 ppm
0.00505
0.00500
0.00495
0.00490
0.1 PPM
Fs - 492.35000 (THz)
0
1
2
TIME (HOURS)

Fig. 20

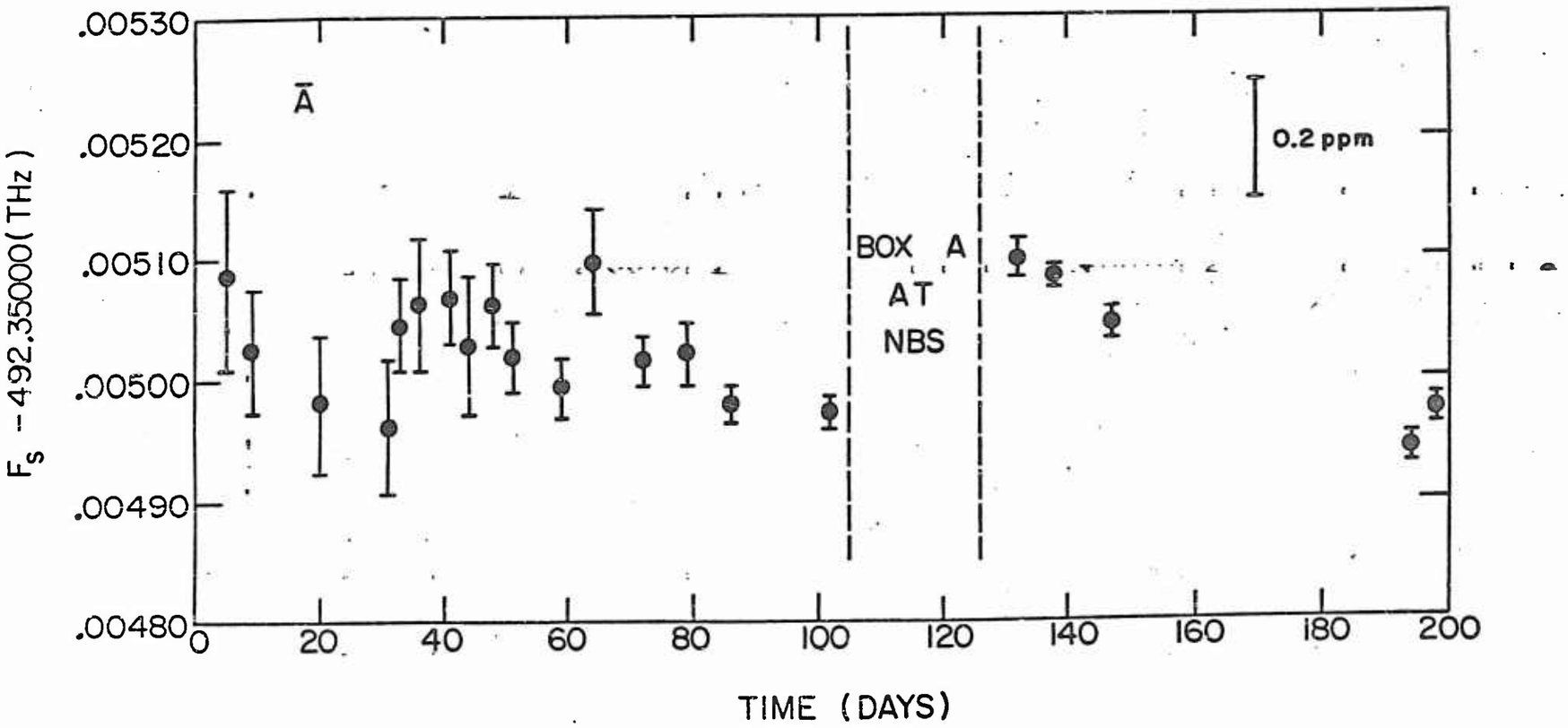
.00530
.00520
.00510
.00500
.00490
.00480
F_s - 492.35000 (THz)
Ā
BOX A
AT
NBS
0.2 ppm
0
20
40
60
80
100
120
140
160
180
200
TIME (DAYS)

Fig. 21

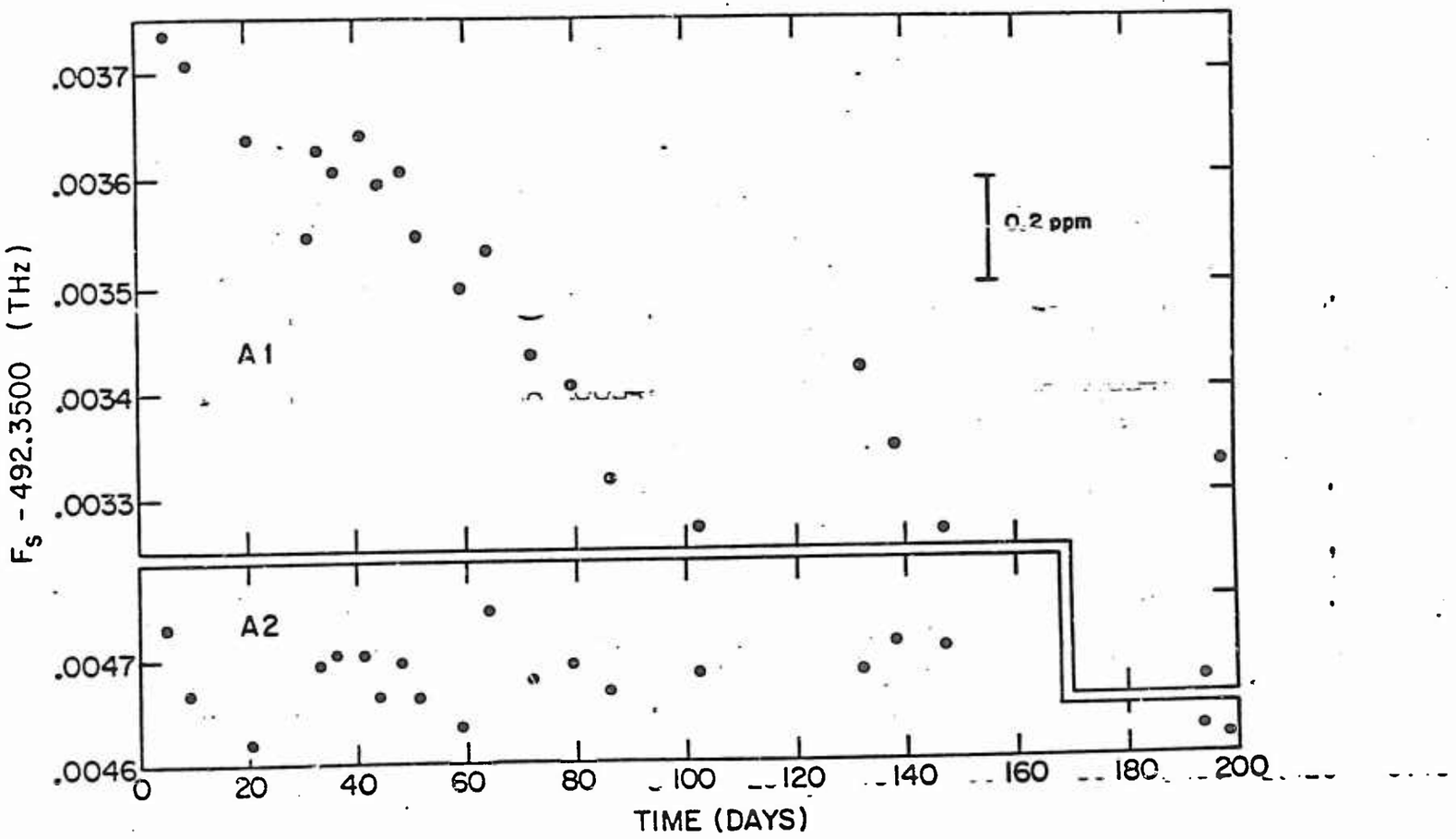
.0037
.0036
.0035
.0034
.0033
.0047
.0046
F_s - 492.3500 (THz)
A1
A2
0.2 ppm
0
20
40
60
80
100
120
140
160
180
200
TIME (DAYS)

Fig. 22

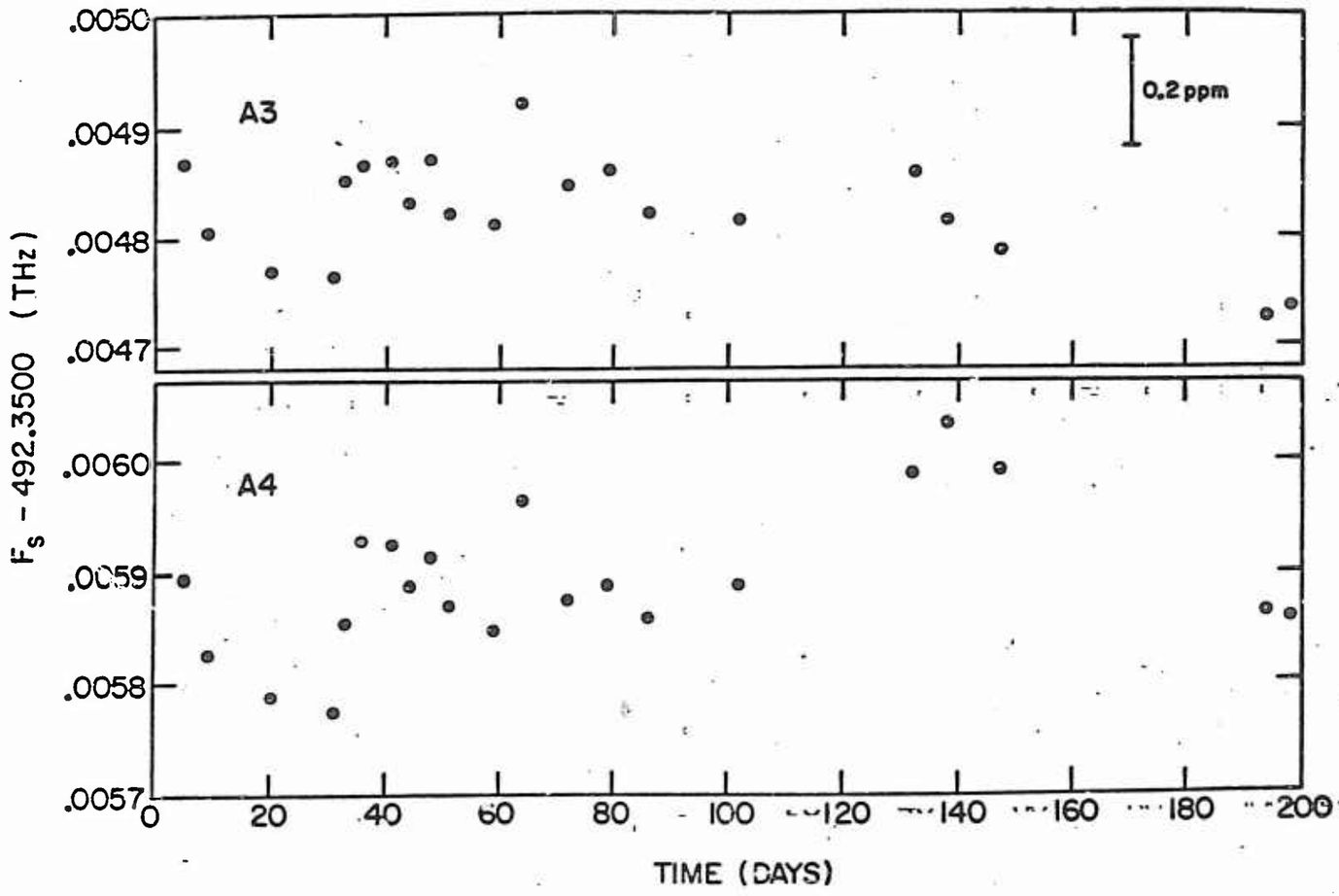
.0050
.0049
.0048
.0047
A3
0.2 ppm
.0060
.0059
.0058
.0057
A4
F_s - 492.3500 (THz)
0
20
40
60
80
100
120
140
160
180
200
TIME (DAYS)

Fig. 23

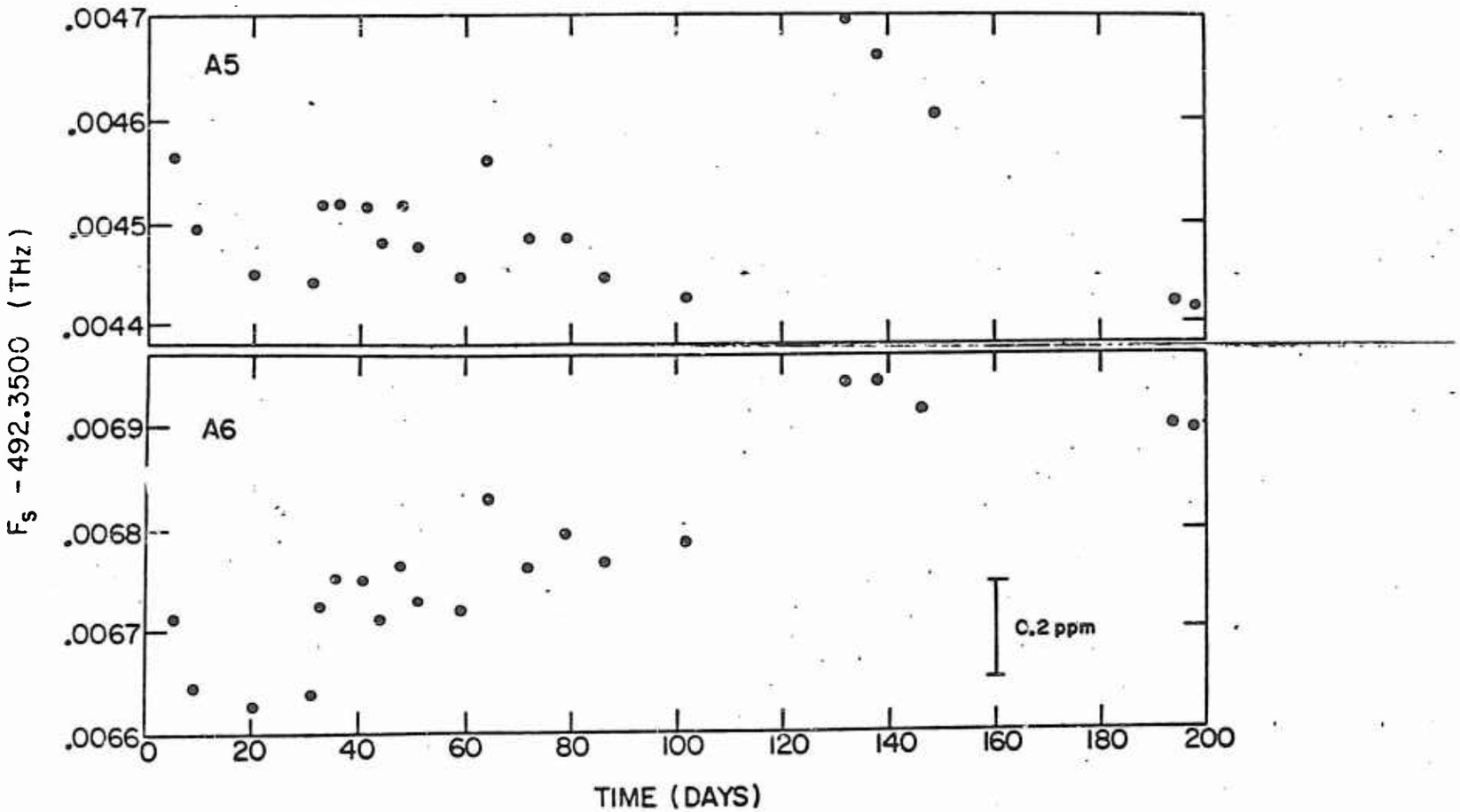
.0047
.0046
.0045
.0044
A5
.0069
.0068
.0067
.0066
A6
0.2 ppm
0
20
40
60
80
100
120
140
160
180
200
TIME (DAYS)
F_s - 492.3500 (THz)

Fig. 24

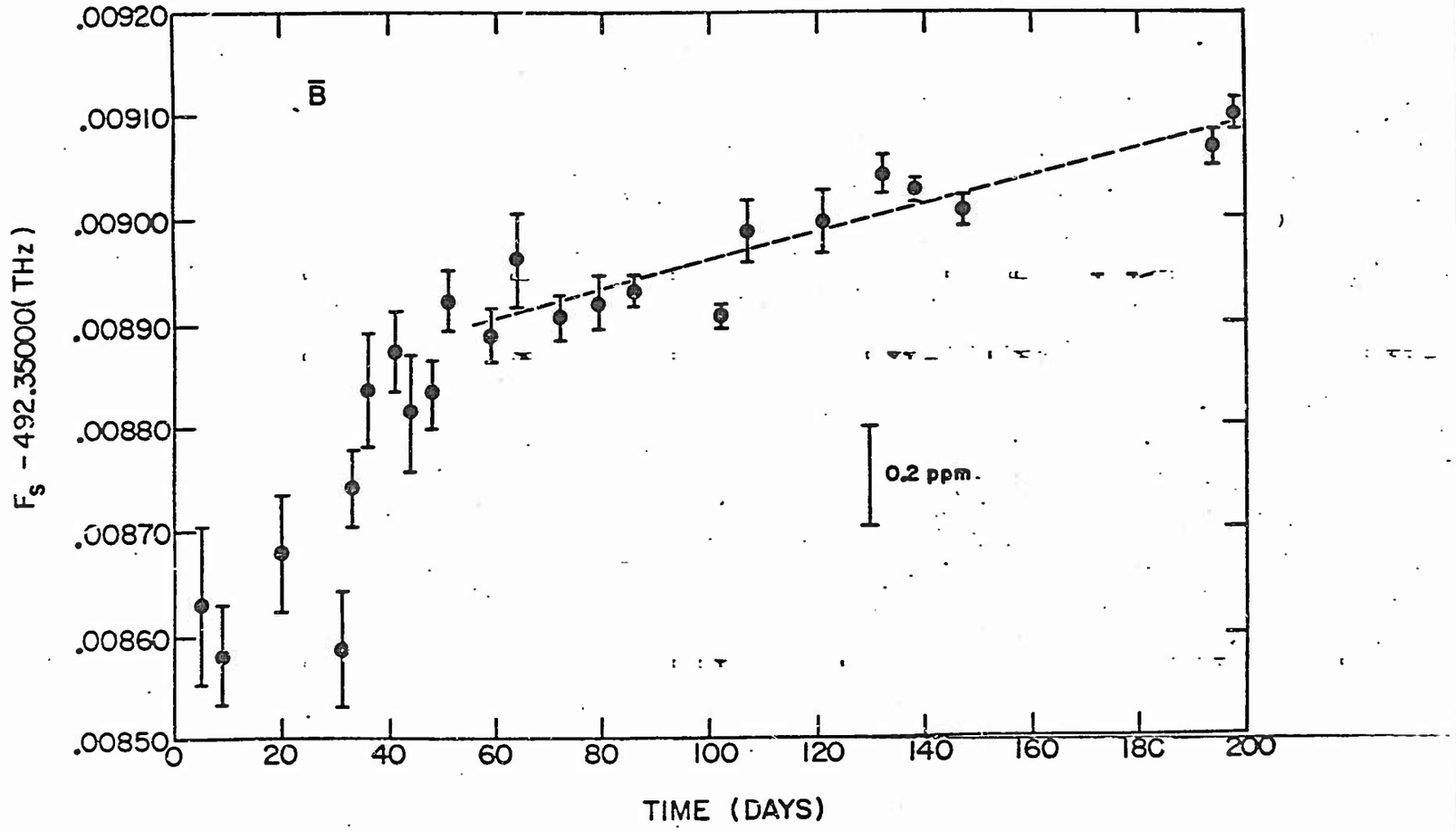
.00920
.00910
.00900
.00890
.00880
.00870
.00860
.00850
F_s - 492.35000 (THz)
B̄
0.2 ppm.
0
20
40
60
80
100
120
140
160
180
200
TIME (DAYS)

Fig. 25

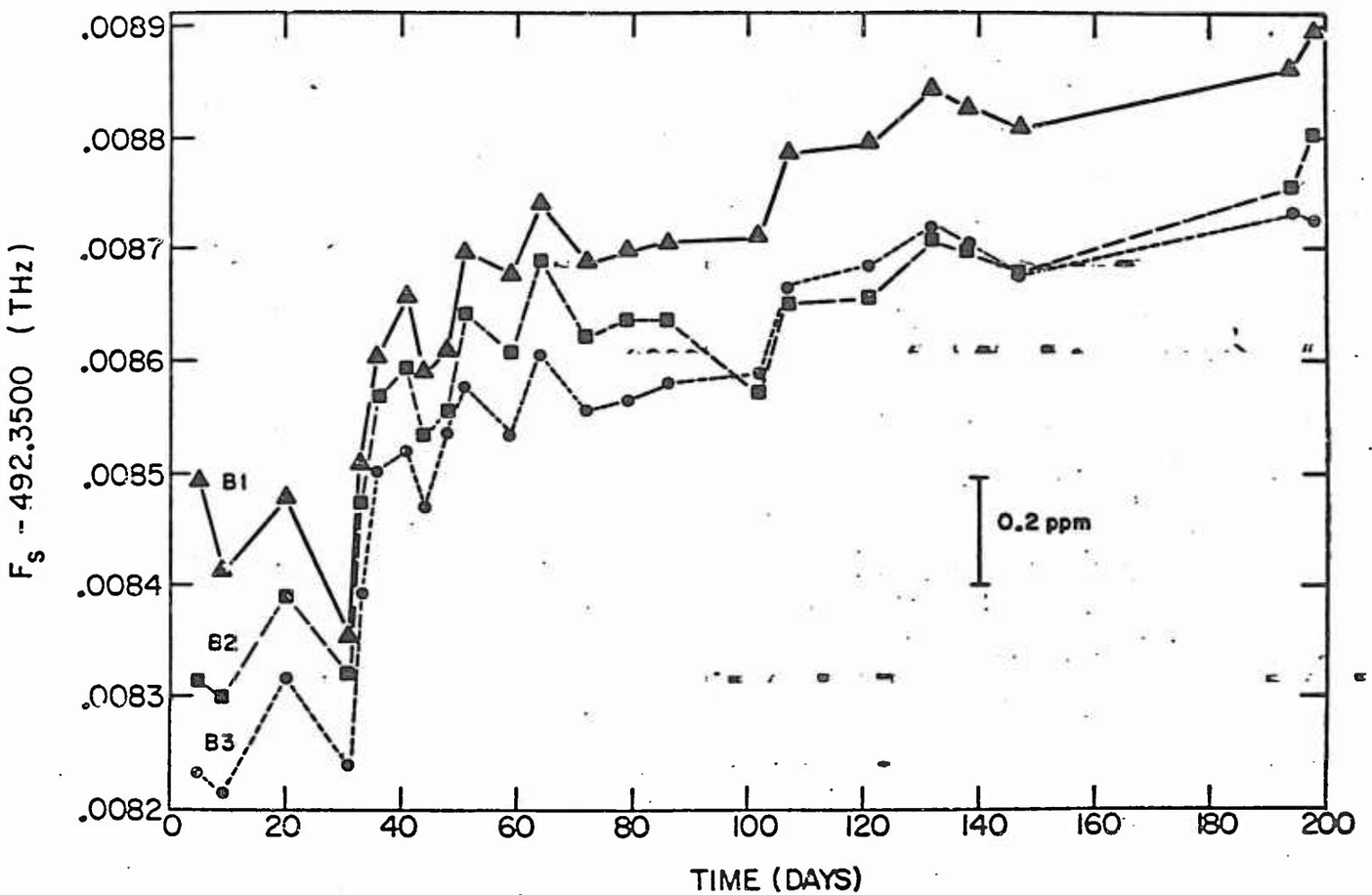
.0089
.0088
.0087
.0086
.0085
.0084
.0083
.0082
F_s - 492.3500 (THz)
B1
B2
B3
0.2 ppm
0
20
40
60
80
100
120
140
160
180
200
TIME (DAYS)

Fig. 26

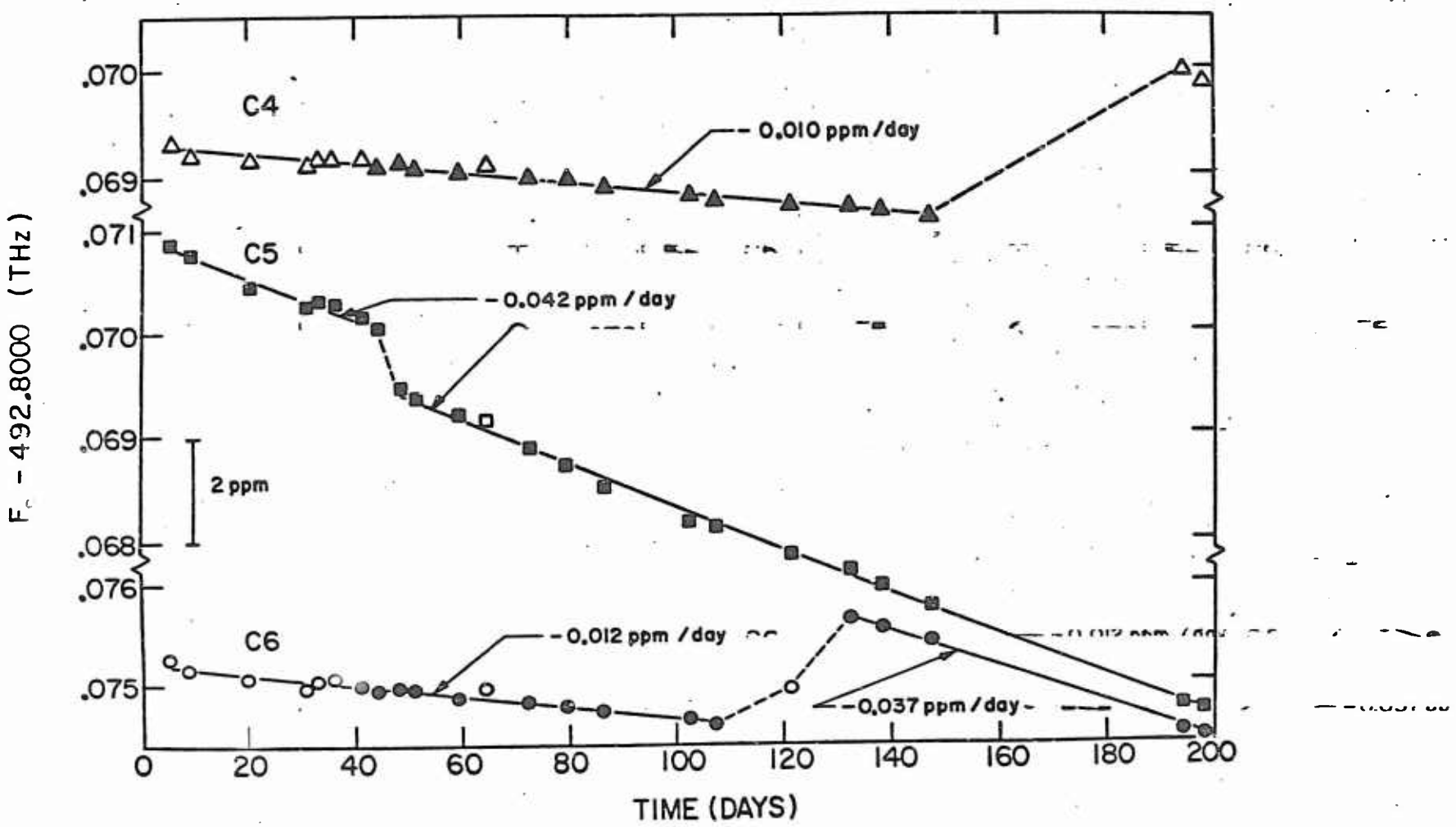
C4
0.010 ppm / day
C5
0.042 ppm / day
2 ppm
C6
0.012 ppm / day
0.037 ppm / day
.070
.069
.071
.070
.069
.068
.076
.075
0
20
40
60
80
100
120
140
160
180
200
TIME (DAYS)
F - 492.8000 (THz)

Fig. 27

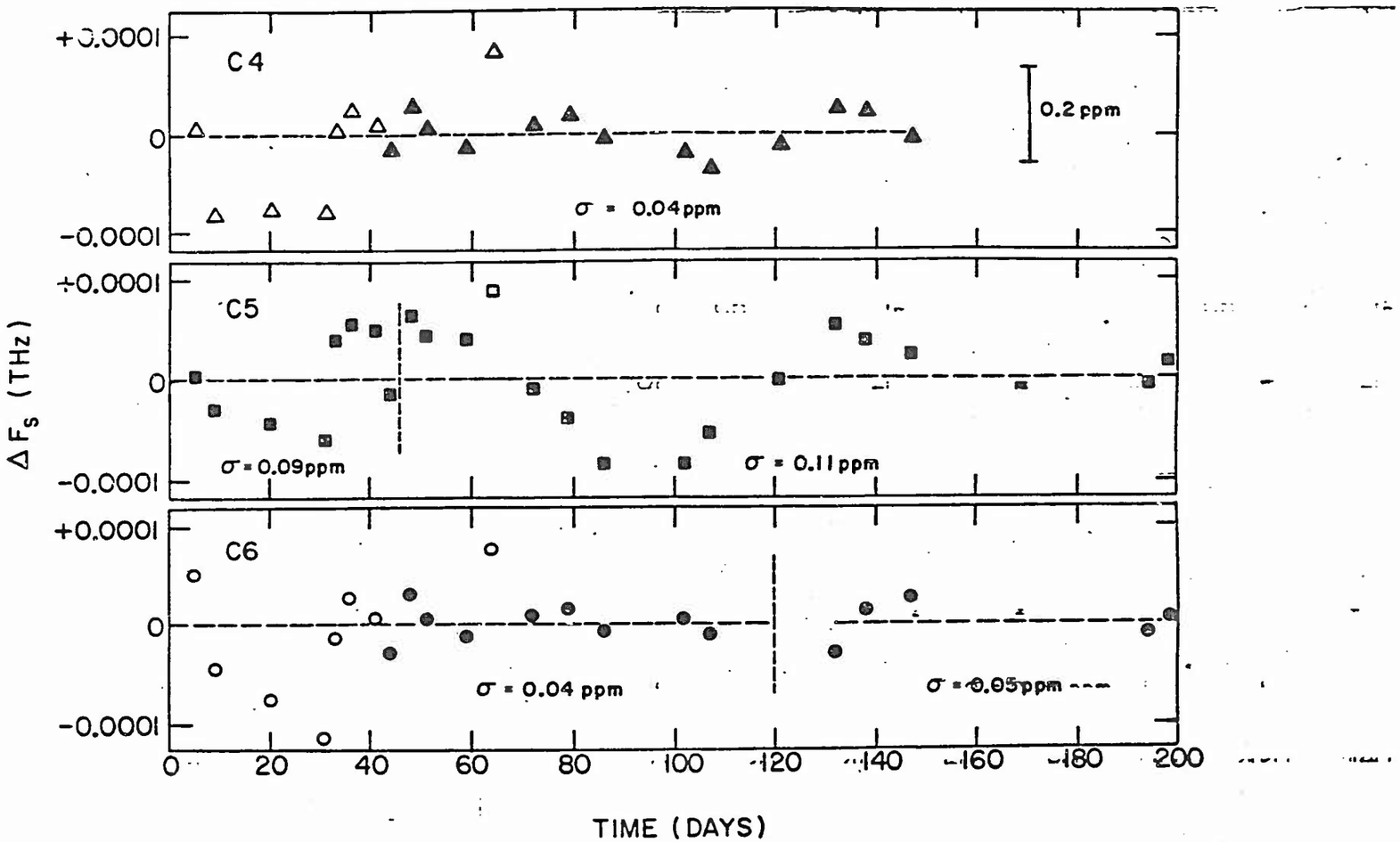
+0.0001
C4
0
-0.0001
0.2 ppm
σ = 0.04ppm
+0.0001
C5
0
-0.0001
σ = 0.09ppm
σ = 0.11ppm
+0.0001
C6
0
-0.0001
σ = 0.04 ppm
σ = 0.05ppm
ΔF_s (THz)
0
20
40
60
80
100
120
140
160
180
200
TIME (DAYS)

Fig. 28

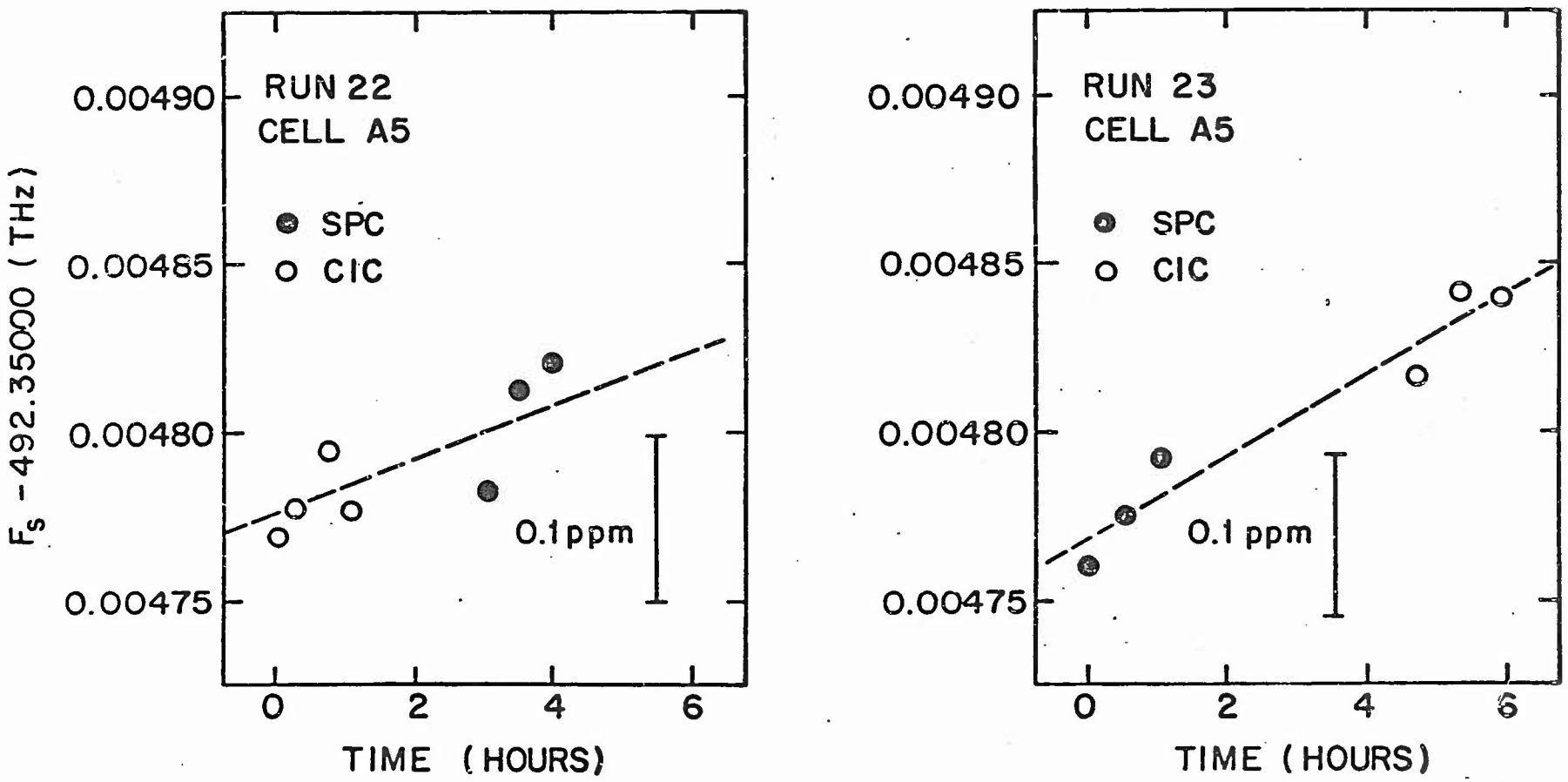
RUN 22
CELL A5
SPC
CIC
0.1 ppm
F_s - 492.35000 (THz)
0.00490
0.00485
0.00480
0.00475
0
2
4
6
TIME (HOURS)
RUN 23
CELL A5
SPC
CIC
0.1 ppm
0.00490
0.00485
0.00480
0.00475
0
2
4
6
TIME (HOURS)

Fig. 29,

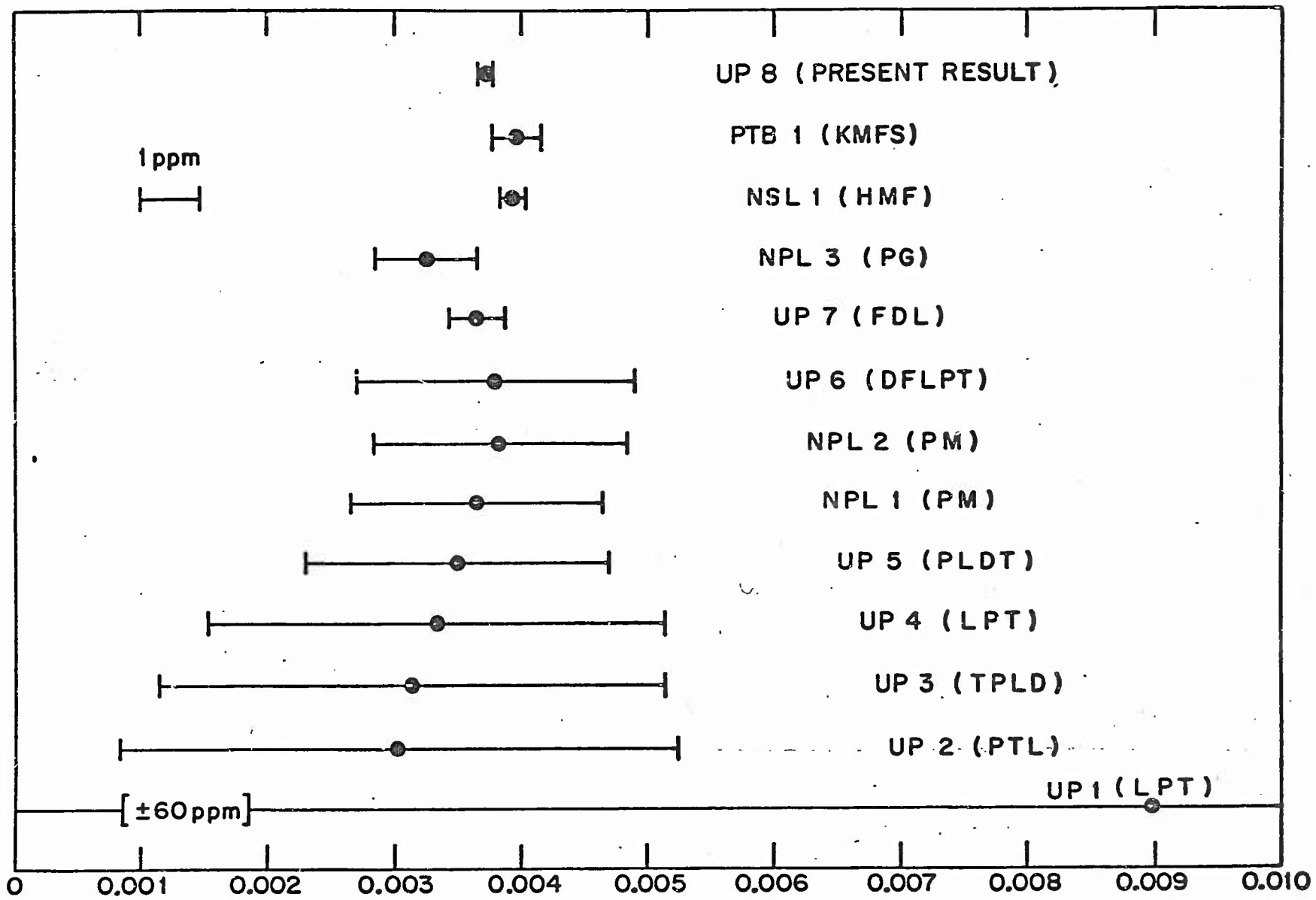

$(2e/h) - 483.590\ (MHz/\mu V_{NBS\ 69})$

Fig. 30,

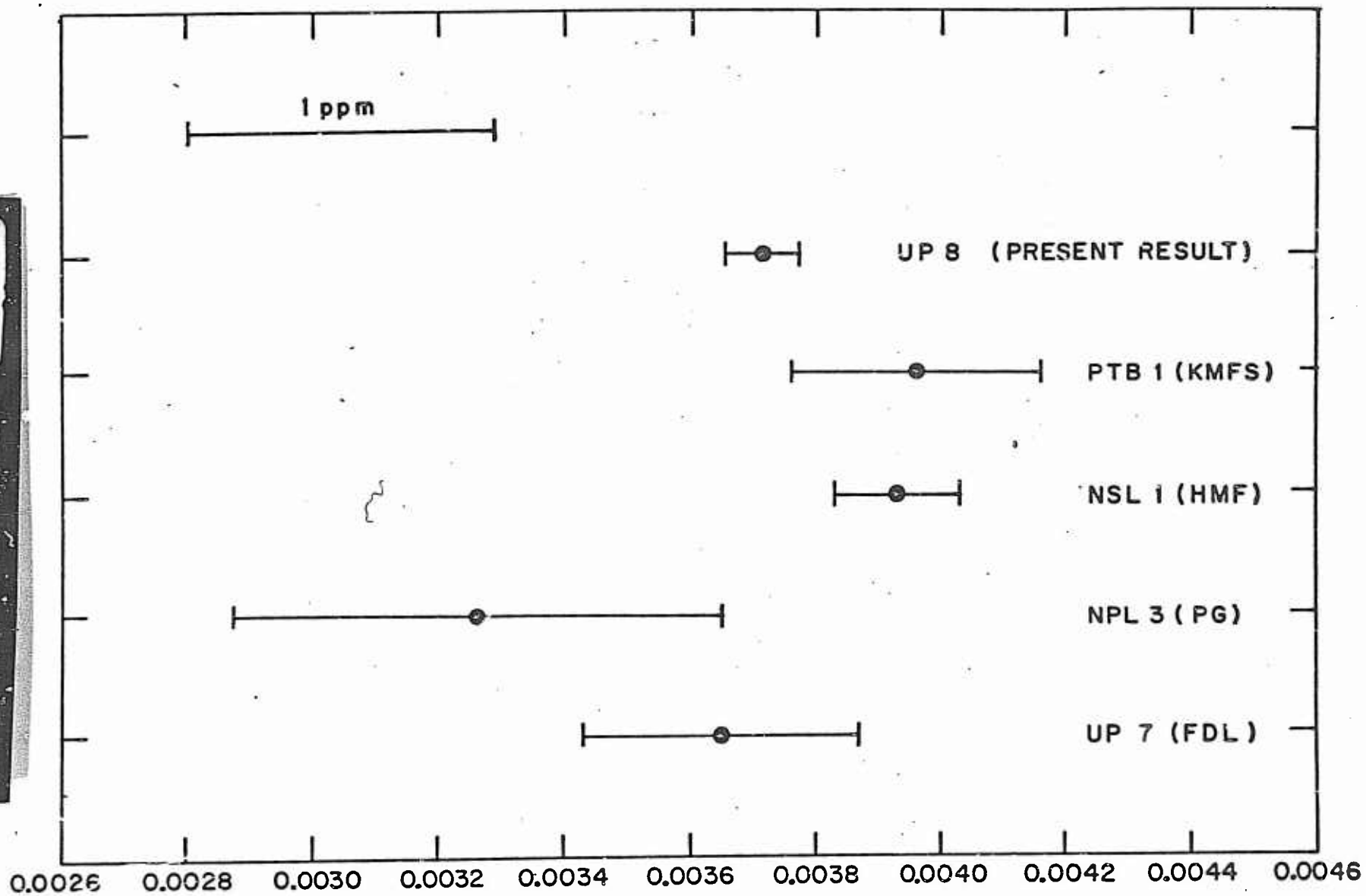
1 ppm
UP 8 (PRESENT RESULT)
PTB 1 (KMFS)
NSL 1 (HMF)
NPL 3 (PG)
UP 7 (FDL)
0.0026
0.0028
0.0030
0.0032
0.0034
0.0036
0.0038
0.0040
0.0042
0.0044
0.0046
(2e/h) - 483.590 (MHz/μV NBS 69)

Fig. 31,